

**The ecomorphological role of wings in migration performance and wing morphometric
growth rates in ectoparasite-reduced nests**

by

Lawrence Lam

A Thesis submitted to the Faculty of Graduate Studies of

The University of Manitoba

in partial fulfilment of the requirements of the degree of

MASTER OF SCIENCE

Department of Biological Sciences

University of Manitoba

Winnipeg

Copyright © 2017 Lawrence Lam

Abstract

Wings have an ecomorphological role in migration, but how morphology affects migration has not been demonstrated in a natural environment. Selection is expected to favour a high-speed wing profile, but ecological interactions during growth may interfere with wing development. Using purple martins (*Progne subis*) as a model species, the objectives of this thesis were to 1) determine whether wing morphology, migration timing, and/or environmental factors were useful predictors of spring migration performance, and 2) examine wing growth rates of nestlings under different nest-ectoparasite conditions. Departure timing and temperature, but not wing morphology, reliably predicted spring migration performance. Growth rates of nestlings varied between nests but overall wing morphology nearing fledging was similar among all nestlings. If differences in wing morphology at fledging arising from ecological interactions during growth are negligible, then migration performance is less dependent on morphological parameters and more dependent on migration timing.

Acknowledgments

The completion of this thesis could not have been possible without the aid of my thesis committee: my internal committee member, Dr. Darren Gillis, who provided valuable lessons in statistics; my external committee member, Dr. Terry Galloway, for his guidance throughout my thesis and teaching me how to identify bird ectoparasites; my thesis advisor, Dr. Kevin Fraser, who guided me throughout my thesis, provided support when I needed it, and helped me become better at conducting research. I also could not have completed my project without the help and support of my lab mates: Amanda Shave, Alisha Ritchie, Amélie Roberto-Charron, Nicole Kaminski, Kelsey Bell, Amanda Van-Loon, Reyd Smith, Sabina Mastrodonato, Neil Balchan, and Ellyne Geurts, and all volunteers that aided me in field work. I also thank members of the Biological Sciences Graduate Student Speaker's Group that have provided feedback in all presentations I have given.

A special thanks to research affiliates: Jason Fisher and James Ray for gathering data in Florida and Texas, respectively; purple martin landlords: Paul and Maxine Clifton, Mark and Donna MacDougal for their permission to deploy geolocators on purple martins in their backyards; Oak Hammock Marsh and Town & Country Campground for their permission to deploy geolocators on purple martins on their property; Dr. Wayne Knee for identifying the mites in my study. Finally, I thank the Department of Biological Sciences, Faculty of Science, and Faculty of Graduate Studies at the University of Manitoba for providing funding for my research.

Permits and Ethics Statement

This research was conducted in accordance with the recommendations of the Ornithological Council “Guidelines to the Use of Wild Birds in Research” and was approved by the University of Manitoba’s Animal Care Committee (Animal Care Protocol Number: F14-009/1 (AC10930)). The capture, handling, banding, and deployment of geolocators on purple martins (*Progne subis*) for this project was permitted by the Canadian Wildlife Service (Permit No. 10876 D) and adheres to the North American Banding Council’s Bander’s Code of Ethics and the Canadian Council on Animal Care.

Table of Contents

Abstract	i
Acknowledgments.....	ii
Permits and Ethics Statement	iii
Table of Contents	iv
List of Tables.....	vi
List of Figures	ix
Chapter 1: General Introduction.....	16
References	27
Chapter 2: Contrasting the influence of morphology, timing, and environmental conditions on the spring migration performance of a trans-hemispheric migrant	34
Abstract.....	34
2.1 Introduction	35
2.2 Methods	40
2.3 Results	49
2.4 Discussion.....	59
2.5 References	67
Chapter 3: Wing morphometric growth of a cavity-nesting bird in insecticide-treated nests	79
Abstract.....	79

3.1 Introduction	79
3.2 Methods	82
3.3 Results	88
3.4 Discussion.....	102
3.5 References	109
Chapter 4: Thesis Conclusion	116
References	118
Appendix A	119
Appendix B.....	130

List of Tables

Table 2.1. List of purple martin breeding colonies and the number of geolocators deployed and retrieved per location.	39
Table 2.2. Sample size and mean morphometric values (\pm SD) of purple martins by population, and sex. Significance ($P < \alpha=0.05$) between groups is denoted by the symbols above the estimates; groups with the same symbol within rows indicate significant differences between those two groups.....	50
Table 2.3. Summary of the linear regression model (equation 2.5). Estimates are standardized to a mean of 0 and standard deviation of 1.	53
Table 2.4. Summary of the linear mixed effect (LME) model (equation 2.7). Fixed effect estimates are standardized to a mean of 0 and standard deviation of 1.	55
Table 2.5. Summary of the generalized linear regression model (GLM) (equation 2.6). Estimates are standardized to a mean of 0 and standard deviation of 1.	56
Table 2.6. List of locations where stopovers were made along spring migration. Mean temperature, precipitation and normalized difference vegetation index (NDVI) (\pm SD) are shown for each location.	57
Table 2.7. Summary of the generalized linear mixed effect model (GLMM) (equation 2.8). Fixed effect estimates are standardized to a mean of 0 and standard deviation of 1.	58
Table 3.1. Total number of ectoparasites (by species) collected from each of the 12 nests, at all study sites, at the end of the breeding season, for each treatment group. The number of young per nest (clutch size) is also provided. Each nest is identified by a letter based on the assigned treatment group (Control, Sham-treated, Insecticide-Treated), followed by a	

numerical code to distinguish within-group. Nests C1, T1, and S1 were from Oak Hammock Marsh (50.17°N, 97.13°W), while the rest were from the Town and Country Campground (49.83°N, 96.98°W).89

Table 3.2. Summary output of the results for the linear mixed effect model for nestling body weight (3.3). The estimates, standard errors, and P values are provided for each fixed effect at each group level (control, sham-treated, and insecticide-treated), while the standard deviation is provided for the random effect (individual); all estimates were obtained using restricted maximum likelihood (REML). Estimates of the insecticide-treated and sham-treated groups are presented relative to the reference group (control); the parameter estimates for the intercept, age, and age² represent the estimates for the control group.93

Table 3.3. Summary output of the results for the linear mixed effect model for wing length (3.4). The estimates, standard errors, and P values are provided for each fixed effect at each group level (control, sham-treated, and insecticide-treated), while the standard deviation is provided for the random effect (individual); all estimates were obtained using restricted maximum likelihood (REML). Estimates of the insecticide-treated and sham-treated groups are presented relative to the reference group (control); the parameter estimates for the intercept and age represent the estimates for the control group.96

Table 3.4. Summary output of the results for the linear mixed effect model for wingtip pointedness (3.4). The estimates, standard errors, and P values are provided for each fixed effect at each group level (control, sham-treated, and insecticide-treated), while the standard deviation is provided for the random effect (individual); all estimates were obtained using restricted maximum likelihood (REML). Estimates of the insecticide-treated and sham-treated groups are presented relative to the reference group (control); the

parameter estimates for the intercept and age represent the estimates for the control group.

.....98

Table 3.5. Summary output of the results for the linear mixed effect model for aspect ratio (3.4).

The estimates, standard errors, and P values are provided for each fixed effect at each group level (control, sham-treated, and insecticide-treated), while the standard deviation is provided for the random effect (individual); all estimates were obtained using restricted maximum likelihood (REML). Estimates of the insecticide-treated and sham-treated groups are presented relative to the reference group (control); the parameter estimates for the intercept and age represent the estimates for the control group.100

List of Figures

Figure 2.1. Boxplots comparing measurements of aspect ratio (A), wingtip pointedness (B), wing length (C), and tarsus length (D) among four breeding populations of purple martins (Alberta Manitoba, Texas, and Florida). Significance between populations is denoted above each box.	51
Figure 2.2. Boxplot comparing measurements of aspect ratio (A), wingtip pointedness (B), wing length (C), and tarsus length (D) between male and female purple martins. Significance between populations is denoted above each box.	52
Figure 2.3. Migration performance of purple martins by departure date (A, D), aspect ratio (B, E), and wingtip pointedness (C, F). Departure date is shown in day of year format (1 January, 2016 = 1). A regression line (predicted by the models) and 95% confidence intervals are represented by the solid line and the shaded grey area, respectively.	54
Figure 2.4. Relationship between stopover duration and environmental variables: average minimum-temperature (A), precipitation (B), and normalized difference vegetation index (NDVI) (C). A negative binomial regression line (predicted by the model (2.8)) and the 95% CI are represented by the solid line and the shaded grey area, respectively.	59
Figure 3.1. Total number of ectoparasites found in each nest. Nests were given a unique identifier (Nest ID) and assigned one of three treatment groups: no treatment (control, black), sham-treated (red), or insecticide-treated (blue). Total ectoparasite loads per treatment group are provided in the figure above each bar; see Table 3.1 for the total number of each species per group. Nest S3 (not shown) was omitted from the analysis.	91

Figure 3.2. Changes in nestling body weight (g) from day 12 to day 22, across three treatment groups (control (black), sham-treated (red), insecticide-treated (blue)). The expected growth rate (predicted by the linear mixed effect model for nestling body weight (3.3)) is represented by the solid coloured lines, with the 95% confidence interval represented by the shaded area around each regression line. Weight was recorded once every three days and began when nestlings were at least 12 days old.....94

Figure 3.3. Changes in wing length (mm) from day 12 to day 22, across three treatment groups (control (black), sham-treated (red), insecticide-treated (blue)). The expected growth rate (predicted by the linear mixed effect model for wing length (3.4)) is represented by the solid coloured lines, with the 95% confidence interval represented by the shaded area around each regression line. Wing length was recorded once every three days and began when nestlings were at least 12 days old.97

Figure 3.4. Changes in wingtip pointedness from day 12 to day 22, across three treatment groups (control (black), sham-treated (red), insecticide-treated (blue)). The expected growth rate (predicted by the linear mixed effect model for wingtip pointedness (3.4)) is represented by the solid coloured lines, with the 95% confidence interval represented by the shaded area around each regression line. Metrics used to calculate wingtip pointedness were recorded once every three days and began when nestlings were at least 12 days old.99

Figure 3.5. Changes in aspect ratio from day 14 to day 22, across three treatment groups (control (black), sham-treated (red), insecticide-treated (blue)). The expected growth rate (predicted by the linear mixed effect model for aspect ratio (3.4)) is represented by the solid coloured lines, with the 95% confidence interval represented by the shaded area around each regression line. Metrics used to calculate aspect ratio were recorded once every three days

and began when nestlings were at least 12 days old, but aspect ratio could not be reliably determined for nestlings younger than 14 days. 101

Figure A1. Scatterplot matrix of the data used to examine wing morphometric differences among populations and sexes (Chapter 2). The diagonal plots depict the distribution of the variables in the data (from top-left to bottom-right: aspect ratio, wingtip pointedness, wing length (mm), and tarsus length (mm)). The lower, off-diagonal plots and the solid red line in these plots (loess smoother) depict the relationship between the different variables on the diagonal. The upper, off-diagonal boxes show the Pearson correlation coefficient between the two variables. 119

Figure A2. Diagnostic plot for linear model comparing wingtip pointedness between populations and sexes. The residuals versus fitted values plot (left) is used to assess for homogeneity of variance, and the q-q plot (right) is used to assess for normality in the residuals. Left: The random pattern in the residuals indicates that the model has met the assumption of homogeneity of variance. Right: as most of the observations fall onto a straight line, the model has met the assumption that the data is normally distributed. 120

Figure A3. Diagnostic plot for linear model comparing aspect ratio between populations and sexes. The residuals versus fitted values plot (left) is used to assess for homogeneity of variance, and the q-q plot (right) is used to assess for normality in the residuals. Left: The random pattern in the residuals indicates that the model has met the assumption of homogeneity of variance. Right: as most of the observations fall onto a straight line, the model has met the assumption that the data is normally distributed. 121

Figure A4. Diagnostic plot for linear model comparing wing length between populations and sexes. The residuals versus fitted values plot (left) is used to assess for homogeneity of

variance, and the q-q plot (right) is used to assess for normality in the residuals. Left: The random pattern in the residuals indicates that the model has met the assumption of homogeneity of variance. Right: as most of the observations fall onto a straight line, the model has met the assumption that the data is normally distributed. 122

Figure A5. Diagnostic plot for linear model comparing tarsus length between populations and sexes. The residuals versus fitted values plot (left) is used to assess for homogeneity of variance, and the q-q plot (right) is used to assess for normality in the residuals. Left: The random pattern in the residuals indicates that the model has met the assumption of homogeneity of variance. Right: as most of the observations fall onto a straight line, the model has met the assumption that the data is normally distributed. 123

Figure A6. Diagnostic plot for linear model for total spring migration speed. The residuals versus fitted values plot (left) is used to assess for homogeneity of variance, and the q-q plot (right) is used to assess for normality in the residuals. Left: The random pattern in the residuals indicates that the model has met the assumption of homogeneity of variance. Right: as most of the observations fall onto a straight line, the model has met the assumption that the data is normally distributed. 124

Figure A7. Diagnostic plot for linear mixed effects model for spring migration speed between stopovers. The residuals versus fitted values plot (left) is used to assess for homogeneity of variance, and the q-q plot (right) is used to assess for normality in the residuals. Left: The random pattern in the residuals indicates that the model has met the assumption of homogeneity of variance. Right: as most of the observations fall onto a straight line, the model has met the assumption that the data is normally distributed. 125

Figure A8. Semi-variogram of the standardized residuals from the linear mixed model for migration speed used to detect spatial autocorrelation. This figure displays the average distance between residual points plotted against the estimated values of the variogram. As birds migrate west, northwest, and north on spring migration, a variogram for each of these direction is shown (north = 0, west = 270, northwest = 315). The random patterns in the residuals in all three directions indicate that there is weak or no spatial autocorrelation present in the data. 126

Figure A9. Autocorrelation plot of the residuals from the migration speed linear mixed effects model, with departure date as a time component in the model. The correlations between residual points (y-axis) at lag intervals (x-axis) is used to detect temporal autocorrelation in the data. With the exception of two points (at lag interval 8 and 17, excluding lag 0), all the points do not show any significant correlations; there is weak or no temporal autocorrelation of the residuals present in the data. 127

Figure A10. Semi-variogram of the standardized residuals from the generalized linear mixed model for stopover duration used to detect spatial autocorrelation. This figure displays the average distance between residual points plotted against the estimated values of the variogram. As birds migrate west, northwest, and north on spring migration, a variogram for each of these direction is shown (north = 0, west = 270, northwest = 315). The random patterns in the residuals in all three directions indicate that there is weak or no spatial autocorrelation present in the data. 128

Figure A11. Autocorrelation plot of the residuals from the stopover duration generalized linear mixed effects model, with departure date as a time component in the model. The correlations between residual points (y-axis) at lag intervals (x-axis) is used to detect

temporal autocorrelation in the data. All the points (excluding lag 0) do not show any significant correlations; there is weak or no temporal autocorrelation of the residuals present in the data. 129

Figure B1. Scatterplot matrix of the data used to examine growth rates of purple martin nestlings (Chapter 3). The diagonal plots depict the distribution of the variables in the data (from top-left to bottom-right: nestling age (days), body weight (g), wing length (mm), wingtip pointedness, and aspect ratio). The colour of the points in the plots correspond to the 3 different groups in the study (control (black), sham-treated (red), and insecticide-treated (blue)). The lower, off-diagonal plots and the solid red line in these plots (loess smoother) depict the relationship between the different variables on the diagonal. The upper, off-diagonal boxes show the Pearson correlation coefficient between the two variables. 130

Figure B2. Diagnostic plots of the linear mixed model for changes in weight over time between the three treatment groups. The residuals versus fitted values plot (top left) is used to assess for homogeneity of variance, and the q-q plot (top right) is used to assess for normality in the residuals. The residuals vs. age (bottom left) and residuals vs. group (bottom right) depict variance in the residuals between ages and groups, respectively. 131

Figure B3. Autocorrelation plot of the residuals from the body weight linear mixed effects model, with age as the time component in the model. The correlations between residual points (y-axis) at lag intervals (x-axis) is used to detect temporal autocorrelation in the data. With the exception of two points (at lag intervals 11 and 12, excluding lag 0), all the points do not show any significant correlations; there is weak or no temporal autocorrelation of the residuals present in the data. 132

Figure B4. Diagnostic plots of the wing length linear mixed-effects model. The residuals versus fitted values plot (top left) is used to assess for homogeneity of variance, and the q-q plot (top right) is used to assess for normality in the residuals. The residuals vs. age (bottom left) and residuals vs. group (bottom right) depict variance in the residuals between ages and groups, respectively. A power variance structure and first-order autoregressive correlation structure were included in the model when calculating the residuals, to correct for unequal variance between ages and temporal autocorrelation, respectively..... 133

Figure B5. Autocorrelation plot of the residuals from the wing length linear mixed effects model, with age as the time component in the model, used to detect temporal autocorrelation. The correlations between residual points (y-axis) at lag intervals (x-axis) is used to detect temporal autocorrelation in the data. With the exception of two points (at lag intervals 1 and 4, excluding lag 0), all the points do not show any significant correlations; there is weak or no temporal autocorrelation of the residuals present in the data..... 134

Figure B6. Diagnostic plots of the wingtip pointedness linear mixed-effects model. The residuals versus fitted values plot (top left) is used to assess for homogeneity of variance, and the q-q plot (top right) is used to assess for normality in the residuals. The residuals vs. age (bottom left) and residuals vs. group (bottom right) depict variance in the residuals between ages and groups, respectively. A power variance structure was included in the model when calculating the residuals, to correct for unequal variance between ages. 135

Figure B7. Autocorrelation plot of the residuals from the wingtip pointedness linear mixed effects model, with age as the time component in the model, used to detect temporal autocorrelation. The correlations between residual points (y-axis) at lag intervals (x-axis) is used to detect temporal autocorrelation in the data. With the exception of two points (at lag

intervals 12 and 13, excluding lag 0), all the points do not show any significant correlations; there is weak or no temporal autocorrelation of the residuals present in the data..... 136

Figure B8. Diagnostic plots of the aspect ratio linear mixed-effects model. The residuals versus fitted values plot (top left) is used to assess for homogeneity of variance, and the q-q plot (top right) is used to assess for normality in the residuals. The residuals vs. age (bottom left) and residuals vs. group (bottom right) depict variance in the residuals between ages and groups, respectively. A power variance structure was included in the model when calculating the residuals, to correct for unequal variance between ages. 137

Figure B9. Autocorrelation plot of the residuals from the aspect ratio linear mixed effects model, with age as the time component in the model, used to detect temporal autocorrelation. The correlations between residual points (y-axis) at lag intervals (x-axis) is used to detect temporal autocorrelation in the data. With the exception of two points (at lag intervals 3 and 7, excluding lag 0), all the points do not show any significant correlations; there is weak or no temporal autocorrelation of the residuals present in the data..... 138

Chapter 1: General Introduction

The evolution and ecomorphology of wings in birds

Flight allows organisms to travel long distances, bypassing geographical barriers that would otherwise be limited, in land-based movement. However, the only extant animals capable of aerial locomotion (discounting gliding) are insects, birds, and bats.

The reason why flight is limited to so few species is due to the evolution of

morphological structures that have enabled flight in organisms (*i.e.*, wings), which have evolved differently in these three taxa. For birds, wings evolved from the fusion of the carpal and metacarpal bones (Feduccia 1999), which differs from insect wings, which evolved from outgrowths of the exoskeleton (Snodgrass 1997), and bat wings, which arose through and modifications to the phalanges (Altringham 2011). Furthermore, unlike bat wings, which are formed by the stretching of the thin membranous skin between the extended forelimb digits (Altringham 2011), the evolution of flight feathers has formed the basis of wing morphology, enabling flight in birds.

Through adaptive evolution, wing shape and size have evolved to become more specialized to fit the ecological niche of the bird. Forest-inhabiting songbirds, such as yellow warblers (*Setophaga petechia*), may have evolved elliptical wings, in order to navigate (fly) through forested areas (Savile 1957, Pennycuick 1975). Due to the shape of elliptical wings, greater forces of drag are created during flight, which is beneficial when birds need to perform turns while flying at low to moderate speeds, but the shape of these wings is poor for flying at high speeds. High-speed wings are described as being long and narrow, with long primary feathers relative to the secondary feathers (Pennycuick 1975, 2008). The aerodynamic properties of a high-speed wing profile decrease the amount of drag birds experience, allowing them to fly with less air resistance (Pennycuick 1975; 2008, Newton 2010), and are characteristic of swifts, swallows, falcons, and other fast-flying species. However, high-speed wings are not adapted for flying in forested habitats or for rapid take-off, as the geometry of these wings is poor at generating enough drag to perform aerial maneuvers at moderate to high-speeds and the amount of force generated to create lift would require more energy (Pennycuick 1975). Selection for a high-speed

wing is theorized to occur in species where the importance of speed is emphasized above all other aspects of flight. Many swallows feed on flying insects, which requires the use of a high-speed wing profile to overcome wind resistance to catch fast-moving prey (Strandberg and Alerstam 2007).

Wing morphology can be characterized and quantified using a variety of different measurements. The most common measurement of wing morphology is wing length. Wing length measures the distance from distal end of the carpal to the tip of the longest primary feather (Pyle 1997), and is generally used as a proxy for body and wing size, where longer wings indicate a larger body size and thus larger wings (Pyle 1997, Pennycuik 2008). Although wing length provides a quick and easy method of quantifying morphometric parameters related to size, the measurement does not explain much about the geometry of the wing. For more detailed measurements of wing geometry, measurements, such as wingtip pointedness and aspect ratio, serve as better indicators of wing morphology.

Wingtip pointedness (also known as wing pointedness or wing(tip) roundedness) is a measure of how pointed/rounded wings are (Lockwood *et al.* 1998). There are multiple methods to quantifying this parameter, such as Kipp's index (Lockwood *et al.* 1998), but all methods ultimately end up describing lengths of the primary and secondary flight feathers that form the basis of the wing shape to determine whether the wings are pointed or rounded. In more pointed wings, the primary feathers are longer than the secondary feathers, while in more rounded wings, the secondary flight feathers are longer or of equal length to the primary feathers. Due to the contrasting geometry of pointed and rounded wings, the aerodynamic properties associated with each morphology differ,

reflecting the adaptive function of the wing (Lockwood *et al.* 1998). Because primary flight feathers function in generating thrust during flight (forward momentum), pointed wings are more aerodynamically efficient for flight at high-speeds and are characteristic of fast-flying birds. In contrast, secondary flight feathers creating lift, allowing birds with rounded wings to take-off more rapidly and efficiently (Lockwood *et al.* 1998).

Aspect ratio is another measure of wing geometry, similar to wingtip pointedness, but also takes into account the size of the bird (Pennycuick 1975, Rayner 1990, Lockwood *et al.* 1998, Newton 2010). Aspect ratio is generally calculated as the ratio of the wingspan (squared) to the area of the wings. Higher values of aspect ratio indicate long and narrow wings, while lower values indicate short, more stubby wings. Birds with high aspect ratio wings, such as swallows, are able to fly at a greater speed because the smaller wing area relative to the wing span results in fewer wingtip vortices being generated in flight; wingtip vortices act as a form of drag, which forces birds to use more energy to overcome air resistance (Pennycuick 1975, Rayner 1990, Lockwood *et al.* 1998, Newton 2010). In contrast, birds with low aspect ratio wings, such as hawks, possess greater maneuverability because less energy is required to overcome wing inertia, but are not able to fly as fast as birds with higher aspect ratio wings (Pennycuick 1975, Rayner 1990, Lockwood *et al.* 1998, Newton 2010).

Migration as the driver of morphological evolution

Migration has been proposed as an important factor affecting wing morphology. Migration in a temperate-tropical system is the annual movement between the breeding and wintering grounds. The distances between breeding and wintering grounds vary among species and can also vary among populations of the same species (Newton 2010).

Migratory birds typically make two annual journeys: fall migration and spring migration. Despite the names, fall and spring migration may not always occur during the fall or spring seasons. Fall migration refers to the movement from the breeding grounds to the wintering grounds, preceding the breeding season. Spring migration is the returning movement from the wintering grounds to the breeding grounds, which occurs following the wintering period. Movements during migration typically follow a north-south axis, with the breeding grounds being higher in latitude than the wintering grounds, but east-west movements can also occur when birds need to migrate over-land to avoid crossing large bodies of water (Newton 2010).

Although only a small proportion of all extant birds are migratory (~18.5%; Rolland *et al.* 2014), the difference in wing morphology between migratory and non-migratory birds is noticeable. When examining wing morphology across many species, migratory birds typically possess wings that are adapted to high-speed flight, or sustained periods of flight, while non-migratory birds typically have wings adapted for other functions, such as rapid take-off or hovering (Lockwood *et al.* 1998). The difference in wing morphology is even present within-species. The Eurasian blackcap (*Sylvia atricapilla*), for example, is a partial migrant (*i.e.*, some populations of this species migrate, while others remain at the breeding ground) that has been found to have different wing morphometry between migratory and non-migratory birds (Pérez-Tris and Tellería 2001); migrants have wings that are characteristic of high-speed, long-distance flight.

One of the reasons for selection to favour morphological adaptations to high-speed flight in migratory birds is explained by optimal migration theory (Alerstam and Lindström 1990, Alerstam 1991, Hedenström 2008, Chernetsov 2012). According to

optimal migration theory, resources are limiting and diminish over time, causing competition for these resources at the destination (wintering grounds on fall migration and breeding grounds on spring migration). It is expected that selection favours an earlier arrival, as individuals that arrive at the destination before conspecifics and allospecifics sharing the same habitat will have greater access and less competition for high-quality resources (Kokko 1999). Although individuals may arrive earlier on migration by shifting their migration schedules so that they are able to depart earlier (Alerstam and Lindström 1990), the mechanisms controlling migration schedules are complex and may not be easily adjusted. There is strong support that migration timing in birds is largely controlled by circadian and circannual rhythms, with environmental conditions, such as photoperiod, acting as zeitgebers to synchronize the bird's internal biological clock to the fluctuating environmental conditions on migration (Gwinner 1989; 1990; 1996). Because biological rhythms follow a fixed timing, the onset of migration may be inflexible to change, preventing birds from departing earlier and thus arriving earlier.

Alternatively, birds may reduce the amount of time spent on migration by completing migration as fast as possible, achieving an earlier arrival without having to adjust the timing of their departure. However, limitations in wing morphology may govern migration speed, constrain migration routes, or force birds to use more energy throughout migration (Pennycuick 1969, Alerstam and Lindström 1990, Hedenström and Alerstam 1998, Hedenström 2008). For instance, transoceanic flights may be a shorter route for many land birds but crossing large bodies of water may not be possible if these birds lack the minimum morphological parameters (*e.g.*, low aspect ratio wings) required for sustained, long-distance flight (Åkesson and Hedenström 2007). Birds that travel

longer distances on migration (partially due to having higher-latitude breeding grounds) are hypothesized to have evolved wings that are adapted for a faster completion of migration in order to compete with conspecifics and allospecifics that share the same habitat (Alerstam and Lindström 1990, Alerstam 1993). However, wing morphology is only one of many factors that may influence migration performance. Endogenous factors, such as the timing of migration (Ellegren 1993, Fransson 1995), and environmental factors, such as temperature and precipitation (Marra *et al.* 1998, Drake *et al.* 2014), may additionally affect migration performance, but the combination of these effects on migration performance and whether one factor exerts a greater influence on migration over another has not been previously studied.

Parasitism and the constraints on wing development

Although selection for adaptive morphological characteristics may drive wing-morphometric variation among and within-species, ecological interactions may also interfere with the growth and development of wing morphology, further driving morphological variation. One of the most common forms of interference with growth and development is parasitism. Birds are exposed to numerous parasites throughout their life and the interaction between birds and parasites usually result in the latter benefitting, while the former are harmed (Hopla *et al.* 1994). Ectoparasites inhabit the host's body, feeding on the blood, skin, or feathers of the host (Rothschild and Clay 1957, Walter and Proctor 1999). Common ectoparasites encountered by birds include mites and ticks (Acari), lice (Phthiraptera), flies (Diptera), and fleas (Siphonaptera) (Clayton 1991).

While some ectoparasites may cause little to no effect on their host (Johnson and Albrecht 1993), others can have detrimental effects on the host, reducing host-fitness

(Lehmann 1993). Great abundance of ectoparasites can reduce reproductive success in adults (Richner and Tripet 1999), decrease fledging success of chicks (Richner *et al.* 1993, Richner and Heeb 1995), or cause their host to abandon the nest (Oppliger *et al.* 1994). Although it is generally not beneficial for ectoparasites to kill their host, high nest loads can (indirectly) lead to mortality in birds (Merino and Potti 1995). Ectoparasites can also negatively impact host fitness through indirect means. For instance, hosts may invest more energy into defense mechanisms against the effects of parasites (*e.g.*, increasing immune system), but this allocation of energy towards building immunocompetence reduces the amount of energy the hosts can put towards growth, resulting in delayed or stunted growth (Saino *et al.* 1998).

As host-parasite interactions have persisted for centuries, birds have evolved defenses against ectoparasites, such as grooming or a better immune response, reducing the negative effects of parasitism (Clayton 1991). However, in juveniles, defenses against ectoparasites are less developed than in adults (Christe *et al.* 1998), leaving them more vulnerable to the negative effects of parasitism. The effects of ectoparasites may reduce body size, growth, and body condition in nestlings (Brown and Brown 1986, Bize *et al.* 2003, Brommer *et al.* 2011). Due to the allometric relationship between wing and body size (Nudds 2007), a reduction in body size is expected to also reduce wing length, which has been demonstrated in previous studies (Brown and Brown 1986, Heeb *et al.* 2000, Bize *et al.* 2003). Although wing length can be used to make inferences about body size, fewer inferences can be made on wing geometry using wing length; there are no studies on wing morphometric growth patterns, thus, how ecological interactions affect wing morphology during growth and development is unclear.

Because growth and development occur when birds are still nestlings (*i.e.* more susceptible to parasitism), any ecological interactions that cause growth to be stunted, poor body condition, or maladaptive-morphological traits (*e.g.* small body size), may reduce the fitness and survival of the nestling after fledging. For birds to successfully fledge, wing morphology must meet the minimum aerodynamic requirements for flight (Pennycuick 2008). Although the requirements for fledging are largely dependent on wing size, as wings must be large enough to create enough force for take-off and carry the weight of the birds in order to fledge successfully, ultimately allowing birds to successfully forage, and depart and complete migration (Pennycuick 1975), wing geometry upon fledging should also fit the ecological niche of the bird (*e.g.*, low aspect ratio wings in forest songbirds). Thus, selection should favour the development of wing morphology that not only allows for successful fledging, but is also adaptive to the life of the bird.

Purple martin as a study species

Where populations of the same species are widely distributed geographically and ecological conditions of the habitat also vary between populations, variation in wing morphology is expected to arise due to selection for morphological characteristics for the ecological niche of the different populations (Winkler and Leisler 1992, Bock 1994). Purple martins are a cavity-nesting, migratory songbird with a wide distribution range, whose breeding range spans most of eastern North America (from Alberta to the eastern coast of the U.S.), extending from Florida to Alberta (Tarof and Brown 2013). Due to the wide distribution range of purple martins, migration routes and the timing of migration vary across latitudes, with southern populations migrating earlier than more northern

populations, and eastern populations taking more eastern routes (Fraser *et al.* 2013). During fall migration (starting in July or August depending on the breeding location), purple martins cross the Gulf of Mexico, arriving at the wintering grounds in South America. They return to the breeding site following spring migration, which may begin anytime between January and April depending on the breeding location (Fraser *et al.* unpub). Total migration distance ranges anywhere from 10,000 to 22,000 km, varying across the breeding range (Fraser *et al.* unpub).

Purple martins now breed almost exclusively in human-made nest cavities (nest boxes), which makes them easy to locate, capture and for scientific study. Purple martins also have high site fidelity at the breeding grounds (Stutchbury *et al.* 2009), returning to the same breeding colony every year after completing spring migration, which makes them useful for tracking on migration. At the breeding grounds, purple martins build nests in artificial structures using leaves, twigs, and occasionally mud (Allen and Nice 1952). Due to their use of artificial nest boxes, experimental manipulations of nest ectoparasites are easier to perform on purple martins than natural-cavity nesting species (Wesolowski and Stanska 2001).

Purple martins are diurnal aerial insectivores, feeding on insects on the wing (Tarof and Brown 2013), and use a fly-and-forage strategy on stopovers along migration, similar to other swallows (Strandberg and Alerstam 2007). Trajectories of populations of aerial insectivores are in steep decline since at least 1990 (Michel *et al.* 2016), with more northern populations facing the steepest decline, but the cause of this decline has yet to be determined (Nebel *et al.* 2010). Being a cavity-nesting, long-distance migratory songbird with a continent-wide distribution, purple martins are an excellent model organism to

examine the ecomorphology of wings on migration performance and changes in wing morphology throughout development.

Thesis objectives

In this thesis, I examined the wing morphology of purple martins in adults (Chapter 2) and juveniles (Chapter 3) to determine the ecomorphological role of the wings on migration and whether wing morphometric growth rates differ when reared in ectoparasite-reduced nests. I obtained measures of three wing morphological parameters (wing length, wingtip pointedness, and aspect ratio) to examine the degree of intraspecific variation in wing morphometry between several populations across the purple martin breeding range (Chapter 2). Using light-level geolocators to track the spring migration of purple martins from start-to-finish, I was able to quantify different parameters of spring migration, allowing me to determine whether wing morphology, the timing of spring migration, and/or environmental conditions en route predicted spring migration performance (Chapter 2). By treating nests with an insecticide to reduce nest ectoparasite loads, I monitored changes in nestling wing morphometry throughout the breeding season, and tested whether wing morphology and growth rates of nestlings raised in ectoparasite-reduced nests differed from nestlings raised in natural (untreated) nests (Chapter 3). Overall, I test long-standing hypotheses using more descriptive measures of wing morphology to determine whether variation in wing morphology is driven by selection for a faster migration or by ecological interactions constraining wing growth.

References

- Åkesson, S., and Hedenström, A. 2007. How migrants get there: migratory performance and orientation. *Bioscience*. **57**(2): 123–133.
- Alerstam, T., and Lindström, Å. 1990. Optimal Bird Migration: The Relative Importance of Time, Energy, and Safety. *In* Bird Migration. *Edited by* E. Gwinner. Springer Berlin Heidelberg, Berlin, Heidelberg. pp. 331–351.
- Alerstam, T. 1991. Bird flight and optimal migration. *Trends Ecol. Evol.* **6**(7): 210–215.
- Alerstam, T. 1993. Bird migration. Cambridge University Press, Cambridge, UK.
- Allen, R.W., and Nice, M.M. 1952. A study of the breeding biology of the purple martin (*Progne subis*). *Am. Midl. Nat.* **47**(3): 606–665.
- Altringham, J.D. 2011. Bats: from evolution to conservation, 2nd edition. Oxford University Press, New York, NY.
- Brommer, J.E., Pitala, N., Siitari, H., Klun, E., and Gustafsson, L. 2011. Body size and immune defense of nestling blue tits (*Cyanistes caeruleus*) in response to manipulation of ectoparasites and food supply. *Auk* **128**(3): 556–563.
- Chernetsov, N. 2012. Passerine migration. Springer Berlin Heidelberg, Berlin, Heidelberg.

- Christe, P., Møller, A.P., and Lope, F. de. 1998. Immunocompetence and nestling survival in the house martin: the tasty chick hypothesis. *Oikos*. **83**(1): 175–179.
- Christe, P., Richner, H., and Oppliger, A. 1996. Begging, food provisioning, and nestling competition in great tit broods infested with ectoparasites. *Behav. Ecol. Ecol* **7**(7): 127–131.
- Clayton, D.H. 1991. Coevolution of avian grooming and ectoparasite avoidance. *In* Bird-parasite interactions. *Edited by* Loye, J.E., and Zuk, M. Oxford University Press; Ornithology Series, 2.
- Cox, G.W. 1968. The role of competition in the evolution of migration. *Source Evol.* **22**(1): 180–192.
- Drake, A., Rock, C.A., Quinlan, S.P., Martin, M., Green, D.J. 2014. Wind speed during migration influences the survival, timing of breeding, and productivity of a Neotropical migrant, *Setophaga petechia*. *PLoS One*. **9**(5): e97152.
- Ellegren, H. 1993. Speed of migration and migratory flight lengths of passerine birds ringed during autumn migration in Sweden. *Ornis Scand.* **24**(3): 220–228.
- Feduccia, A. 1999. The origin and evolution of birds. Yale University Press.
- Fransson, T. 1995. Timing and speed of migration in north and west European populations of *Sylvia* warblers. *J. Avian Biol.* **26**(1): 39.

- Fraser, K.C., Stutchbury, B.J.M., Kramer, P., Silverio, C., Barrow, J., Newstead, D., Mickle, N., Shaheen, T., Mammenga, P., Applegate, K., Bridge, E., and Tautin, J. 2013. Consistent range-wide pattern in fall migration strategy of purple martin (*Progne subis*), despite different migration routes at the Gulf of Mexico. *Auk* **130**(2): 291–296.
- Gwinner, E. 1990. Bird migration. Springer Berlin Heidelberg, Berlin, Heidelberg.
- Gwinner, E. 1989. Photoperiod as a modifying and limiting factor in the expression of avian circannual rhythms. *J. Biol. Rhythms*. **4**(2): 125–138.
- Gwinner, E. 1996. Circadian and circannual programmes in avian migration. *J. Exp. Biol.* **199**(1): 39–48.
- Hedenström, A. 2008. Adaptations to migration in birds: behavioural strategies, morphology and scaling effects. *Philos. Trans. R. Soc. London B Biol. Sci.* **363**(1490): 287–299.
- Hedenström, A., and Ålerstam, T. 1998. How fast can birds migrate? *J. Avian Biol.* **29**(4): 424.
- Hopla, C.E., Durden, L.A., and Keirans, J.E. 1994. Ectoparasites and classification. *Rev. Sci. Tech.* **13**(4): 985–1017.

- Johnson, S.L., and Albrecht, D.J. 1993. Effects of haematophagous ectoparasites on nestling house wrens, *Troglodytes aedon*: who pays the cost of parasitism? *Oikos*. **66**(2): 255–262.
- Kokko, H. 1999. Competition for early arrival in migratory birds. *J. Anim. Ecol.* **68**(5): 940–950.
- Marra, P.P., Hobson, K.A., and Holmes, R.T. 1998. Linking winter and summer events in a migratory bird by using stable-carbon isotopes. *Science*. **282**(5395): 1884–1886.
- Merino, S., and Potti, J. 1995. Mites and blowflies decrease growth and survival in nestling pied flycatchers. *Oikos*. **19**(2): 107–113.
- Michel, N.L., Smith, A.C., Clark, R.G., Morrissey, C.A., and Hobson, K.A. 2016. Differences in spatial synchrony and interspecific concordance inform guild-level population trends for aerial insectivorous birds. *Ecography*. **39**(8): 774–786.
- Nebel, S., Mills, A., McCracken, J., and Taylor, P. 2010. Declines of aerial insectivores in North America follow a geographic gradient. *Avian Conserv.* **5**(2): 1.
- Newton, I. 2010. *The migration ecology of birds*. Burlington: Elsevier Science, Burlington.
- Nudds, R. 2007. Wing-bone length allometry in birds. *J. Avian Biol.* **38**(4): 515–519.

- Oppliger, A., Richner, H., and Christe, P. 1994. Effect of an ectoparasite on lay date, nest-site choice, desertion, and hatching success in the great tit (*Parus major*). *Behav. Ecol.* **5**(2): 130–134.
- Pennycuik, C.J. 1969. The mechanics of bird migration. *Ibis*. **111**(4): 525–556.
- Pennycuik, C.J. 1975. Mechanics of flight. *Avian Biol.* **5**: 1–75. London and New York.
- Pennycuik, C.J. 2008. Modelling the flying bird. Elsevier.
- Pérez-Tris, J., and Tellería, J.L. 2001. Age-related variation in wing shape of migratory and sedentary blackcaps *Sylvia atricapilla*. *J. Avian Biol.* **32**(3): 207–213.
- Rayner, J.M.V. 1990. The mechanics of flight and bird migration performance. *In* Bird migration. *Edited by* E. Gwinner. Springer Berlin Heidelberg, Berlin, Heidelberg. pp. 283–299.
- Richner, H., and Heeb, P. 1995. Are clutch and brood size patterns in birds shaped by ectoparasites? *Oikos*. **73**(3): 435–441.
- Richner, H., and Tripet, F. 1999. Ectoparasitism and the trade-off between current and future reproduction. *Oikos*. **86**: 535–538.
- Richner, H., Oppliger, A., and Christe, P. 1993. Effect of an ectoparasite on reproduction in great tits. *J. Anim. Ecol.* **62**: 703–710.

- Rolland, J., Jiguet, F., and Jønsson, K. 2014. Settling down of seasonal migrants promotes bird diversification. *R. Soc. B* **281**(1784): 1–9.
- Rothschild, M., and Clay, T. 1957. Fleas, flukes and cuckoos. A study of bird parasites. HarperCollins Publishers, Limited.
- Salewski, V., and Bruderer, B. 2007. The evolution of bird migration—a synthesis. *Naturwissenschaften* 94(4): 268–279.
- Savile, O. 1957. Adaptive evolution in the avian wing. *Evolution*. **11**(2): 212–224.
- Snodgrass, R.E. 1997. Principles of insect morphology. McGraw-Hill Book: London.
- Strandberg, R., and Alerstam, T. 2007. The strategy of fly-and-forage migration, illustrated for the osprey (*Pandion haliaetus*). *Behav. Ecol. Sociobiol.* **61**(12): 1865–1875.
- Stutchbury, B.J.M., Hill III, J.R., Kramer, P.M., Rush, S.A., and Tarof, S.A. 2009. Sex and age-specific annual survival in a neotropical migratory songbird, the purple martin (*Progne Subis*). *Auk*. **126**(2): 278–287.
- Tarof, S., and Brown, C.R. 2013. Purple martin (*Progne subis*). The birds of North America online (ed., A Poole). Ithaca, NY: Cornell Lab of Ornithology.
- Walter, D., and Proctor, H. 1999. Mites: ecology, evolution and behaviour. Sydney: UNSW Press.

Wesołowski, T., and Stańska, M. 2001. High ectoparasite loads in hole-nesting birds – a nestbox bias? *J. Avian Biol.* **32**(2): 281–285.

Winkler, H., and Leisler, B. 1992. On the ecomorphology of migrants. *Ibis.* **134**(s1): 21–28.

Chapter 2: Contrasting the influence of morphology, timing, and environmental conditions on the spring migration performance of a trans-hemispheric migrant

Abstract

Optimal migration theory predicts that birds are selected to minimize the amount of time spent on spring migration to arrive earlier and secure resources at the breeding grounds. Due to previous limitations in tracking small birds (<60g) on migration, few studies have examined factors influencing songbird migration performance, which includes speed of travel and stopover duration. Using miniaturized light-level geolocators, I tracked the spring migration of purple martins (*Progne subis*) to test whether wing morphology, migration timing, and/or environmental conditions en route predicted their migration performance. Measurements of aspect ratio and wingtip pointedness were poor predictors of migration performance, but birds that departed later from wintering sites travelled at faster migration speed on average and spent less time at stopovers than earlier departing conspecifics. Individuals also spent less time at stopovers when temperatures were lower. Intraspecific variation in wing morphology had a weak effect on spring migration performance, but departure date and temperature en route were stronger predictors of migration performance. Future studies aimed at understanding the impacts of climate change on performance and fitness should focus on factors impacting migration departure and stopover locations.

2.1 Introduction

Where fitness and/or survival advantages have favoured a quicker migration and/or earlier arrival, migratory birds may engage in a time-selected migration, where more energy is allocated to increase migration speed to minimize the duration of migration (Alerstam and Lindström 1990, Hedenström and Alerstam 1997). Migrants that follow this strategy on spring migration are expected to arrive earlier at the breeding grounds and benefit by having greater access to resources (such as territory and food), more time to secure territory, and are able to begin breeding earlier (Kokko 1999). However, migration performance is also dependent on morphological and ecological parameters, thus factors contributing to speed and/or energy efficiency may also contribute to arrival timing (Alerstam and Lindström 1990, Rayner 1990, Hedenström and Alerstam 1997, Chernetsov 2012). For this study, I focus on three factors that are suspected to influence migration performance of a trans-hemispheric migratory songbird: wing morphology, migration timing, and environmental conditions.

Wing morphology is an important component of flight (and migration) performance, as changes to wing shape and size will affect flight aerodynamics (Lockwood *et al.* 1998, Åkesson and Hedenström 2007, Pennycuick 2008, Newton 2010). High aspect ratio wings (*i.e.*, large wingspan relative to wing area) and pointed wingtips (longer primary remiges compared to secondary remiges) reduce wingtip vortices and induced-drag, allowing birds to fly faster and use less energy on flights (Rayner 1990, Yong and Moore 1994, Lockwood *et al.* 1998, Pennycuick 2008). Migratory birds must travel long distances on migration exceeding 1,000 km, so it is expected that selection has favoured wing characteristics that aid in completing migration faster (Lockwood *et al.*

1998, Åkesson and Hedenström 2007, Pennycuick 2008, Newton 2010). Several comparative studies support the hypothesis that wing morphology is adapted for long-distance flight in migratory birds, showing that morphological characteristics for high-speed flight are more evident in migratory birds than non-migratory birds (Marchetti *et al.* 1995, Lockwood *et al.* 1998). Wing morphology may also vary within-species (Rayner 1990). For example, birds that breed at more northern latitudes may have evolved morphological features that are adaptive for long-distance migration (Fiedler 2005, Hedenström 2008). There are strong influences of wing morphology on flight performance (Swaddle and Lockwood 2003, Bowlin and Wikelski 2008), and these effects are expected to carry over to influence the whole of migration (Yong and Moore 1994, Marchetti *et al.* 1995). The few studies that have examined the relationship between wing morphology and migration performance were only able to infer migration performance using theoretical models (Rayner 1990, Pennycuick 1969), range distributions (Yong and Moore 1994, Marchetti *et al.* 1995), or short-distance flight performance (Swaddle and Lockwood 2003, Alerstam *et al.* 2007, Bowlin and Wikelski 2008). It is therefore unknown whether wing morphology in migrants contributes importantly to migration performance from start-to-finish.

Migration timing is critical to breeding arrival date, as birds that depart late are expected to arrive late (Nilsson *et al.* 2013). Mistiming their breeding period to coincide with the period of maximum food availability may lead to lower reproductive success (Both *et al.* 2006). A late arrival can also shorten the breeding period, leaving late-birds less time to find and secure a suitable habitat thereby decreasing mating success (Møller 1994). However, birds that depart later on spring migration may avoid arriving late by

completing migration faster. Thus, late-departing migrants may be selected to complete migration as fast as possible, while early-departing migrants may have less pressure to complete migration as fast as possible and instead use alternative migration strategies to minimize energy expenditure on spring migration, such as an energy-selected migration (Hedenström and Ålerstam 1997).

As birds spend several days at various locations throughout migration, they experience daily changes in weather between and during stopovers. It is expected that birds change their behaviour on migration in response to shifts in weather and avoid migrating in unfavourable conditions such as rain, strong headwinds, or extreme temperatures (Lack 1960, Newton 2010), due to increased energetic costs, decreased visibility, increased rate of water loss, any combination of which could force them to make stopovers, delaying the progression of migration (Pennycuik 1969, Richardson 1978, 1990). Other environmental factors, such as habitat quality and food abundance, may also affect migration performance. It is assumed that when a bird makes a stopover, the decision to remain at the stopover or move to another location is dependent on the condition of the bird and the quality of the stopover (Chernetsov 2012). Birds that make stops at low-quality sites will spend more time foraging to refuel, increasing the amount of time spent on migration (Ålerstam and Lindström 1990, Ålerstam and Hedenström 1998, Åkesson and Hedenström 2007, Chernetsov 2012). Therefore, it is suspected that weather heavily influences stopover duration and thus migration performance. Weather affects timing of migration (Marra *et al.* 2005, Studds and Marra 2007), flight costs (Bowlin and Wikelski 2008), and migration strategies (Able 1973, Richardson 1990). However, these studies were limited to using weather data at single locations (*e.g.*, key

stopovers, breeding or capture/recapture sites), and not for journey-long migration. Spatial and temporal changes in weather throughout migration make it difficult to determine how migrants behave in response to these changes on migration. Knowledge of the time and location of individuals throughout migration is required to identify weather and environmental conditions experienced on migration accurately. Advancements in tracking devices have provided more precise methods of estimating migration routes (Bridge *et al.* 2011), providing a better understanding of routes and stopover locations, as well as weather conditions en route. Recent studies have taken advantage of these improvements to avian-tracking devices and found that some migratory songbirds adjust their migration speed or stopover duration in response to changes in weather conditions (Smith and McWilliams 2014, Schmaljohann *et al.* 2017, Van Loon *et al.* 2017). Environmental conditions, wing morphology, and migration timing are thus important factors when predicting migration performance and behaviour. How these factors interact to influence migration performance and whether one factor holds more importance in predicting migration performance has not been tested.

I directly tracked the spring migration of a long-distance migratory songbird, the purple martin (*Progne subis*), using light-level geolocators that provided information on the geographic location of the birds throughout migration. The wide breeding range of purple martins and large body-size relative to other songbirds (approx. 15 mm tarsus, 55 g (Behle 1968)) allowed me to conduct continent-wide, intraspecific comparisons and deploy larger geolocators that are capable of recording information on migration over several years, thus making purple martin an ideal model species in this study. I measured the aspect ratio, wingtip pointedness, wing length, and tarsus length of 47 purple martins

at seven study sites across North America (Table 2.1) to examine morphometric variation among different breeding populations and sexes. Using the information collected by the geolocators, I examined two variables of migration performance: migration speed and stopover duration.

Table 2.1. List of purple martin breeding colonies and the number of geolocators deployed and retrieved per location.

Colony location	Site coordinates	Geolocators deployed (2015)	Geolocators retrieved (2016)	Percentage retrieved
Alberta	52.68°N, 113.51°W	30	11	36.7%
	50.17°N, 97.13°W	8	1	12.5%
	49.82°N, 96.98°W	19	5	26.3%
Manitoba	49.78°N, 97.17°W	8	2	25.0%
	49.73°N, 97.13°W	21	8	38.1%
Texas	35.04°N, 101.93°W	14	5	35.7%
Florida	28.37°N, 81.59°W	30	4	13.3%

The aim of this study was to examine the extent of intraspecific morphological variation between several purple martin populations across the breeding range, and to test two hypotheses pertaining to time-selection migration. In the first hypothesis, I propose that if selection favours a faster completion of spring migration to arrive earlier at the breeding grounds, then birds with morphological characteristics that are better adapted to

high-speed, long-distance flights and birds that were more time-constrained on spring migration would complete spring migration in less time. Because higher aspect ratio wings and pointed wingtips are characteristics of a high-speed wing profile, I predicted that these morphologies are characteristics of more northern-latitude birds, which migrate longer distances (Lam *et al.* 2015), and that birds with these morphologies would complete migration in less time and use less energy resulting in shorter stopovers. Furthermore, birds that depart later on spring migration are thought to be more time-constrained, thus I predicted that later-departing birds would migrate at a faster speed and spend less time at stopovers. For the second hypothesis, I expect that environmental conditions en route would affect migration performance, such that migration performance is greater when environmental conditions are favourable for migration. I predicted that migration speed would be faster when birds departed in strong tailwinds and weak crosswinds, as high wind speeds moving in the same direction as the bird would increase their forward momentum and decrease energy expenditure, thereby extending the flight duration and distance. For stopover duration, I predicted that birds would spend more time at stopovers when (i) temperatures are lower because birds would need to spend more energy regulating their internal body temperature (Wikelski *et al.* 2003), (ii) there was a high amount of precipitation preventing birds from migrating (Richardson 1978), and the stopover-habitat quality was poor, which can result in birds spending more time at the stopover searching, foraging, and refueling (Alerstam and Lindström 1990).

2.2 Methods

This research was conducted in accordance with the recommendations of the Ornithological Council “Guidelines to the Use of Wild Birds in Research” and was

approved by the University of Manitoba's Animal Care Committee (Animal Care Protocol Number: F14-009/1 (AC10930)). The capture, handling, banding, and deployment of geolocators on purple martins (*Progne subis*) for this project was permitted by the Canadian Wildlife Service (Permit No. 10876 D) and adheres to the North American Banding Council's Bander's Code of Ethics and the Canadian Council on Animal Care.

Study sites

Purple martins were captured and banded during their breeding season in 2015 (between April and July) at four breeding colonies in Manitoba, and one colony each in Alberta, Florida, and Texas (Table 2.1). I used MK5 light-level geolocators (developed by Biotrack, Ltd.) to track the migration of each bird. Birds were fitted with a geolocator upon capture using a leg-loop harness method (Rappole and Tipton 1991) and released after measurements were recorded. Measurements for wing length, tarsus length, and wingtip pointedness were collected from 47 purple martins at four different populations: Alberta, Manitoba, Texas, and Florida (Table 2.1). I was unable to examine the effects of wing morphometries on migration performance of birds from Florida and Texas, as these measurements were not available for the birds that were recovered from these populations. I grouped purple martins from breeding populations in Alberta and Manitoba due to the similar migration routes and distances and chose to focus on these two locations when analyzing migration performance. This subset included 26 purple martin migration tracks: 10 birds from Alberta and 16 birds from Manitoba.

Obtaining measurements

Purple martins were captured at their breeding grounds upon entering the nest box. Individuals were sexed and aged based on plumage (Pyle 1997). Measurements for wing length (to the nearest 0.1 mm using a wing ruler), tarsus length (to the nearest 0.1 mm using calipers), wing span (to the nearest 0.1 mm using a 1-metre ruler), distance between the tips of the longest primary feather and longest secondary feather (to the nearest 0.1 mm using calipers) and the surface area of the wing (*i.e.*, wing area) (to the nearest .01 cm²) were recorded upon capture of the birds (Pyle 1997). These measurements were recorded after banding and fitting a geolocator on the bird; in some situations, I was unable to record certain measurements (*e.g.*, when a bird began to exhibit signs of stress and was released) resulting in missing data. Wing span was measured by extending both wings and measuring the distance between the tips of the longest primary feather on each wing (Pennycuick 2008). For aspect ratio, I calculated the area of both wings to obtain the total wing area of the bird (see Supplement 1). Aspect ratio (*AR*) was calculated using the formula (Pennycuick 2008):

$$AR = \frac{b^2}{S} \quad (2.1)$$

where *b* is the wing span and *S* is the wing area. Higher values of *AR* indicate longer and narrower wings, while lower values indicate shorter and stubbier wings. Wingtip pointedness (*I_k*) was calculated using the formula (Lockwood *et al.* 1998):

$$I_k = 100 \times \frac{\Delta S_1}{W} \quad (2.2)$$

where ΔS_1 is the distance between the tips of the longest primary feather and the longest secondary feather and W is the wing length. Higher values of I_k indicate more pointed wingtips, while lower values indicate more rounded wingtips.

Migration performance

Data obtained from geolocators were downloaded onto a computer and analyzed using BASTrak software. Light levels recorded by the geolocators were used to identify the time of sunset and sunrise. The length of time between sunrise and sunset was used to determine latitude, while the timing of local noon and midnight was used to determine longitude (Hill and Braun 2001). I used the spatial coordinates (recorded by the geolocators) of the birds recorded at midnight to identify their stationary locations throughout migration. Stopover and wintering periods were defined as two or more days where the distance between spatial coordinates of consecutive days were less than the error of the geolocators (~210 km latitude and 196 km longitude; Fraser *et al.* 2013); periods of flight, and the timing of departure/arrival from stopovers or winter roosts were defined as shifts in latitude and longitude that were greater than the error of the geolocators. Migration movements between stopovers ranged from 280km to 6480km. I used the data from the geolocators to determine spring migration routes, which allowed me to determine migration speed and stopover duration.

I examined migration speed and stopover duration as measures of migration performance. Migration speed (km per day) was defined as how fast migrants moved between stopovers. This was calculated by dividing the total distance travelled during migration by the total number of days spent flying. I defined stopover duration by counting number of days spent at each stopover along migration. The focus of this study

was on spring migration because purple martins tend to migrate during the fall equinox during fall migration, where estimates of latitude are unreliable.

Environmental variables

For each stopover, I used data from the nearest weather station that had historical data on the minimum temperature (°C) and amount of precipitation (mm) at each stopover, normalized difference vegetation index (NDVI), and wind speed (km/hr) at departure from each stopover. The average distance between the stopover and the nearest weather station was 135.4 (± 124.2) km (range: 2.4 – 561.04 km). Data on temperature and precipitation were collected for each day spent at a stopover and wind speed and direction were collected on the last day spent at a stopover. For each stopover, I calculated the mean temperature and precipitation for each stopover. As I was unable to determine the time of day of departure from the stopovers, I used the wind speed recorded at (or closest to) sunrise as a proxy for our analysis. Data on wind speed and wind direction were used to compute two wind components: crosswinds and tailwinds. These components were calculated using the following formulas (Åkesson and Hedenström 2000, Bowlin and Wikelski 2008):

$$V_{Crosswind} = \sin(\alpha) \cdot v_w \quad (2.3)$$

$$V_{Tailwind} = \cos(\alpha) \cdot v_w \quad (2.4)$$

α represents the angle (radians) between the direction of wind vector and the flight direction of bird at the moment of departure (*i.e.* at sunrise), and v_w is wind speed at departure (km/hour). Higher $V_{crosswind}$ reflect higher wind speeds moving perpendicular to the bird. For $V_{tailwind}$, positive values correspond to tailwinds while negative values

correspond to headwinds, and the strength of the tail/ head wind is determined by the magnitude of the value. Values of zero (for both $V_{\text{crosswind}}$ and V_{tailwind}) correspond to the absence of a strong wind vector during departure.

Normalized difference vegetation index (NDVI) is a measure of the amount of reflectance given off by live vegetation indicating the presence/amount of vegetation. NDVI has been used in other studies to determine migratory behaviour; Thorup *et al.* (2017) found that Palearctic-African species move between areas in the wintering range where vegetation is most abundant. Here, I used NDVI as a measure of stopover-habitat quality; stopovers with high NDVI values indicate more live vegetation, which represents better stopover habitat for aerial insectivores (*i.e.*, purple martins) because greater primary production is associated with greater insect abundance (Wolda 1978). To obtain measures of NDVI, I downloaded vegetation index maps from NASA Earth Observations (NEO; <https://neo.sci.gsfc.nasa.gov/>) containing the NDVI values in 16-day increments and processed the maps in ArcMap[™]. Data for all other weather variables were collected from Weather Underground (<http://www.wunderground.com>), an online historical weather database.

Statistical analyses

All analyses were performed in R studio (version 3.4.0) (R Development Core Team 2012). I compared four different morphometries (aspect ratio, wingtip pointedness, wing length, and tarsus length) among four different breeding populations (Alberta, Manitoba, Florida, and Texas) and sexes using two-way ANOVAs. All assumptions were assessed visually using Q-Q plots and residuals versus fitted plots to tests the assumptions of normality and homogeneity of variance, respectively (Fig. A1-4) (Quinn and Keough

2002). The packages “*car*” (Fox and Weisberg 2011) and “*plyr*” (Wickham 2011) were used in the two-way ANOVAs, and all figures were made using the package “*ggplot2*” (Wickham 2009).

I tested the hypothesis that total spring migration speed (from start-to-finish) was determined by wing morphology (aspect ratio and wingtip pointedness) and departure timing, using a linear model defined by the equation (format following Nakagawa and Schielzeth (2013)):

$$TSpeed_i = \beta_0 + \beta_1 \cdot Dep + \beta_2 \cdot AR + \beta_3 \cdot WTP + \varepsilon_i \quad (2.5)$$

where for each observation i (from 1 to 23), $TSpeed_i$ is the total speed travelled on spring migration; Dep , AR , and WTP are the continuous predictors representing departure, aspect ratio, and wingtip pointedness, respectively; β_0 is the intercept at the mean values of the predictors (the predictor variables were standardized to have a mean of 0 and standard deviation of 1); β_1 , β_2 , and β_3 are the coefficients for the departure, aspect ratio, and wingtip pointedness, respectively; and ε_i is the residual for the i^{th} observation (which follows a normal distribution with a mean of 0 and a variance of σ^2_ε).

A generalized linear model (GLM) with a zero-truncated Poisson (ZTP) distribution and a log link function was used to test the effects of wing morphometry and departure timing on total stopover duration. The GLM was performed using the R package “*VGAM*” (Yee 2015, Yee *et al.* 2015) and can be defined by the equation:

$$\log(TStop_i) = \beta_0 + \beta_1 \cdot Dep + \beta_2 \cdot AR + \beta_3 \cdot WTP + \varepsilon_i \quad (2.6)$$

where for each observation i (from 1 to 23), $\log(TStop_i)$ is the log number of total days spent at stopovers along spring migration; Dep , AR , and WTP are the continuous predictors representing departure, aspect ratio, and wingtip pointedness, respectively; β_0 is the intercept at the mean values of the predictors (the predictor variables were standardized to have a mean of 0 and standard deviation of 1); β_1 , β_2 , and β_3 are the coefficients for the departure, aspect ratio, and wingtip pointedness, respectively; and ε_i is the residual for the i^{th} observation (which follows a normal distribution with a mean of 0 and a variance of σ^2_ε). Assumptions of normality and homogeneity of variance were assessed visually using Q-Q plots and residual versus fitted plots, respectively, for the linear model (Fig. A5) using the R package “car” (Fox and Weisberg 2011). The dispersion parameter (ϕ) for the stopover duration GLM was 0.94, meeting the assumption of equidispersion (Zuur *et al.* 2009).

To test the hypothesis that purple martin migration speed was affected by wind speed and direction, I examined the effects the tailwind and crosswind components at departure had on the migration speed between stopovers using a linear mixed effects (LME) model, with individuals as a random effect, in the R package “nlme” (Pinheiro *et al.* 2017). The LME model can be defined by the equation:

$$SSpeed_i = \beta_0 + \beta_1 \cdot Tailwind + \beta_2 \cdot Crosswind + \alpha_j + \varepsilon_{ij} \quad (2.7)$$

where for each observation i (from 1 to 117), $SSpeed_i$ is the speed moving between stopovers; $Tailwind$, and $Crosswind$ are the continuous predictors representing tailwind and crosswind speed, respectively; β_0 is the intercept at the mean values of the predictors (the predictor variables were standardized to have a mean of 0 and standard deviation of 1); β_1 and β_2 are the coefficients for the tailwind and crosswind speed, respectively; α_j

(which follows a normal distribution with a mean of zero and variance of σ^2_α) is the random effect of individual j (from 1 to 26); and ε_{ij} is the residual for the i^{th} observation for individual j (which follows a normal distribution with a mean of 0 and a variance of σ^2_ε).

To test the hypothesis that the amount of time spent at stopovers was influenced by environmental conditions at the stopover, I examined the effects of the average minimum-temperature, average precipitation at the stopover, and NDVI using a generalized linear mixed effect model (GLMM) with a zero-truncated negative binomial (ZTNB) distribution and individuals as a random effect; the negative binomial distribution was used to deal with overdispersion of counts ($\phi = 1.92$) and was a better fit for the data than the zero-truncated Poisson (ZTP) distribution (likelihood-ratio test: $\chi^2 = 54.89$, $P < 0.01$). The GLMM can be defined by the equation:

$$\log(TStop_i) = \beta_0 + \beta_1 \cdot Temp + \beta_2 \cdot Precip + \beta_3 \cdot NDVI + \alpha_j + \varepsilon_{ij} \quad (2.8)$$

where for each observation i (from 1 to 117), $\log(TStop_i)$ is the log number of days spent at a single stopover; $Temp$, $Precip$, and $NDVI$ are the continuous predictors representing average minimum-temperature, average precipitation, and the NDVI, respectively; β_0 is the intercept at the mean values of the predictors (the predictor variables were standardized to have a mean of 0 and standard deviation of 1); β_1 , β_2 , and β_3 are the coefficients for the average minimum-temperature, average precipitation, and the NDVI, respectively; α_j (which follows a normal distribution with a mean of zero and variance of σ^2_α) is the random effect of individual j (from 1 to 26); and ε_{ij} is the residual for the i^{th} observation for individual j (which follows a normal distribution with a mean of 0 and a variance of σ^2_ε). The GLMM was performed using the “*glmmADMB*” R package

(Fournier *et al.* 2012, Skaug *et al.* 2013). Estimates for the fixed and random effects in the LME (2.7) and GLMM (2.8) used restricted maximum likelihood (REML) estimation. Assumptions of normality and homogeneity of variance were assessed visually using Q-Q plots and residuals of the model plotted against the fitted values of the model, respectively (Fig. A6). Spatial and temporal autocorrelation for the LME model and GLMM were also assessed visually using variograms and autocorrelation plots, respectively (Fig. A7-10), using the R packages “*sp*” (Pebesma and Bivand 2005, Bivand *et al.* 2013), and “*gstat*” (Pebesma 2004, Gräler *et al.* 2016).

2.3 Results

Purple martin morphometry

The four morphometrics examined (aspect ratio, wingtip pointedness, wing length, and tarsus length) were weakly correlated with one another (Fig. A1). Among the four populations in the study, wing length and tarsus length were significantly different (wing length: $F_{3,41} = 5.67$, $P < 0.01$; tarsus length: $F_{3,40} = 7.74$, $P < 0.01$), while aspect ratio and wingtip pointedness were not (aspect ratio: $F_{3,38} = 1.30$, $P = 0.29$; wingtip pointedness: $F_{3,41} = 2.11$, $P = 0.11$) (Table 2.2).

Table 2.2. Sample size and mean morphometric values (\pm SD) of purple martins by population, and sex. Significance ($P < \alpha=0.05$) between groups is denoted by the symbols above the estimates; groups with the same symbol within rows indicate significant differences between those two groups.

	<i>n</i>	Aspect ratio*	Wingtip pointedness	Wing length (mm)	Tarsus length (mm)
Population					
Alberta	10	7.7 \pm 0.5	47.5 \pm 1.4	148.8 \pm 2.5 [†]	15.6 \pm 0.02 [†]
Manitoba	16	7.4 \pm 0.6	46.1 \pm 2.3	146.4 \pm 3.6	15.7 \pm 1.3 [‡]
Texas	10	7.2 \pm 0.7	44.8 \pm 2.9	143.4 \pm 2.6 [†]	17.0 \pm 1.3 ^{†‡‡}
Florida	11	7.5 \pm 0.4	45.3 \pm 3.1	145.8 \pm 3.7	15.1 \pm 0.6 [‡]
Sex					
Male	19	7.5 \pm 0.6	46.4 \pm 2.9	148.0 \pm 3.6 [†]	15.8 \pm 1.1
Female	28	7.4 \pm 0.5	45.7 \pm 2.4	144.9 \pm 3.0 [†]	15.8 \pm 1.2

* Missing measurements of aspect ratio for three individuals from Manitoba (two females and one male).

Mean wing length of purple martins breeding in the Alberta population was 5.4 (\pm 1.8) mm longer compared to the Texas population, and tarsus length of purple martins from the Texas population was longer than the other three populations (Tukey's HSD *post-hoc* test: $P_{adjusted} < 0.01$) (Fig. 2.1). Between sexes, wing length was the only

measurement that was significantly different ($F_{1,41} = 9.47$, $P_{adjusted} < 0.01$) (Fig 2.2); mean wing lengths in male were $2.7 (\pm 0.9)$ mm longer than for female wings.

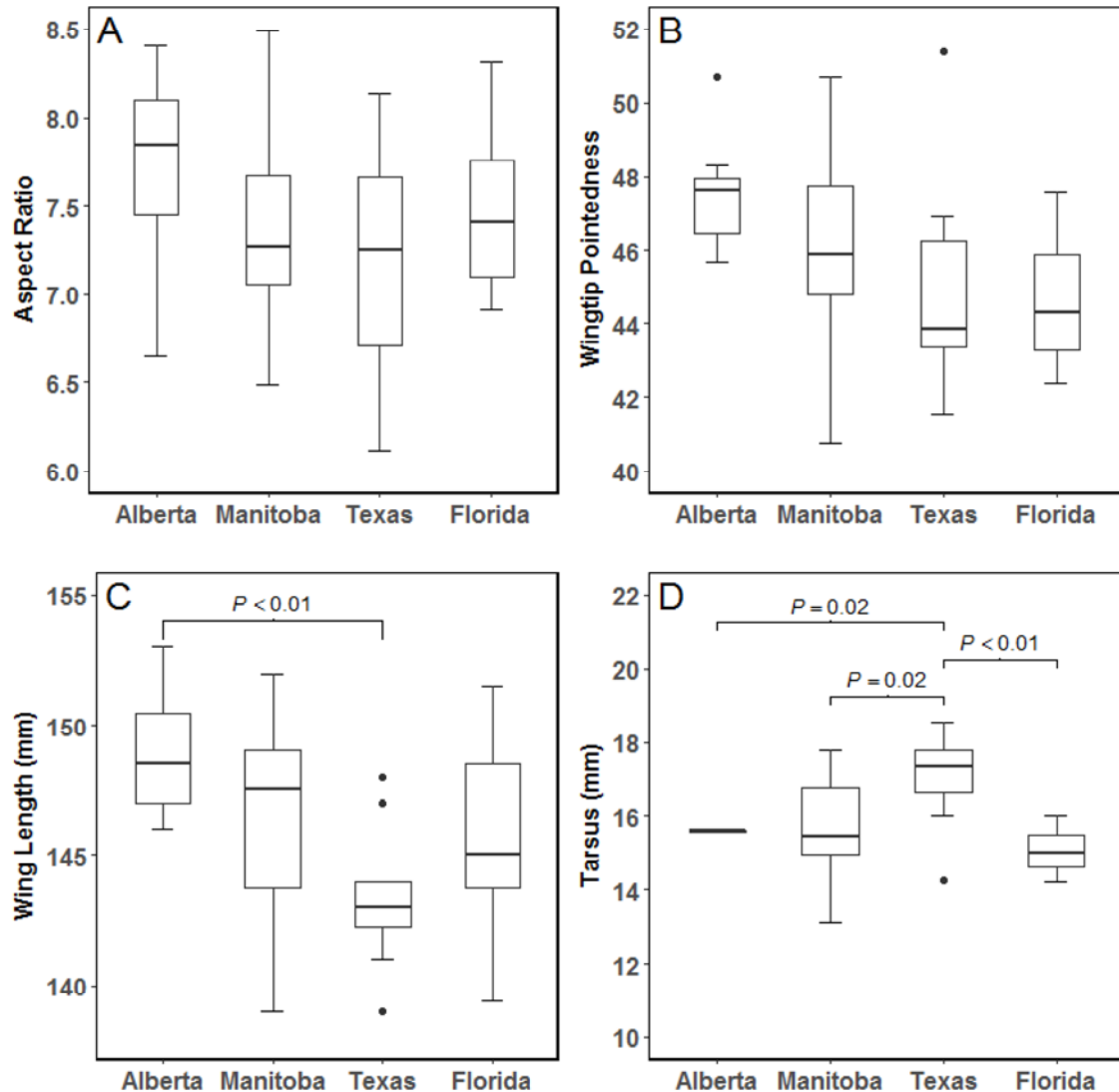


Figure 2.1. Boxplots comparing measurements of aspect ratio (A), wingtip pointedness (B), wing length (C), and tarsus length (D) among four breeding populations of purple martins (Alberta Manitoba, Texas, and Florida). Significance between populations is denoted above each box.

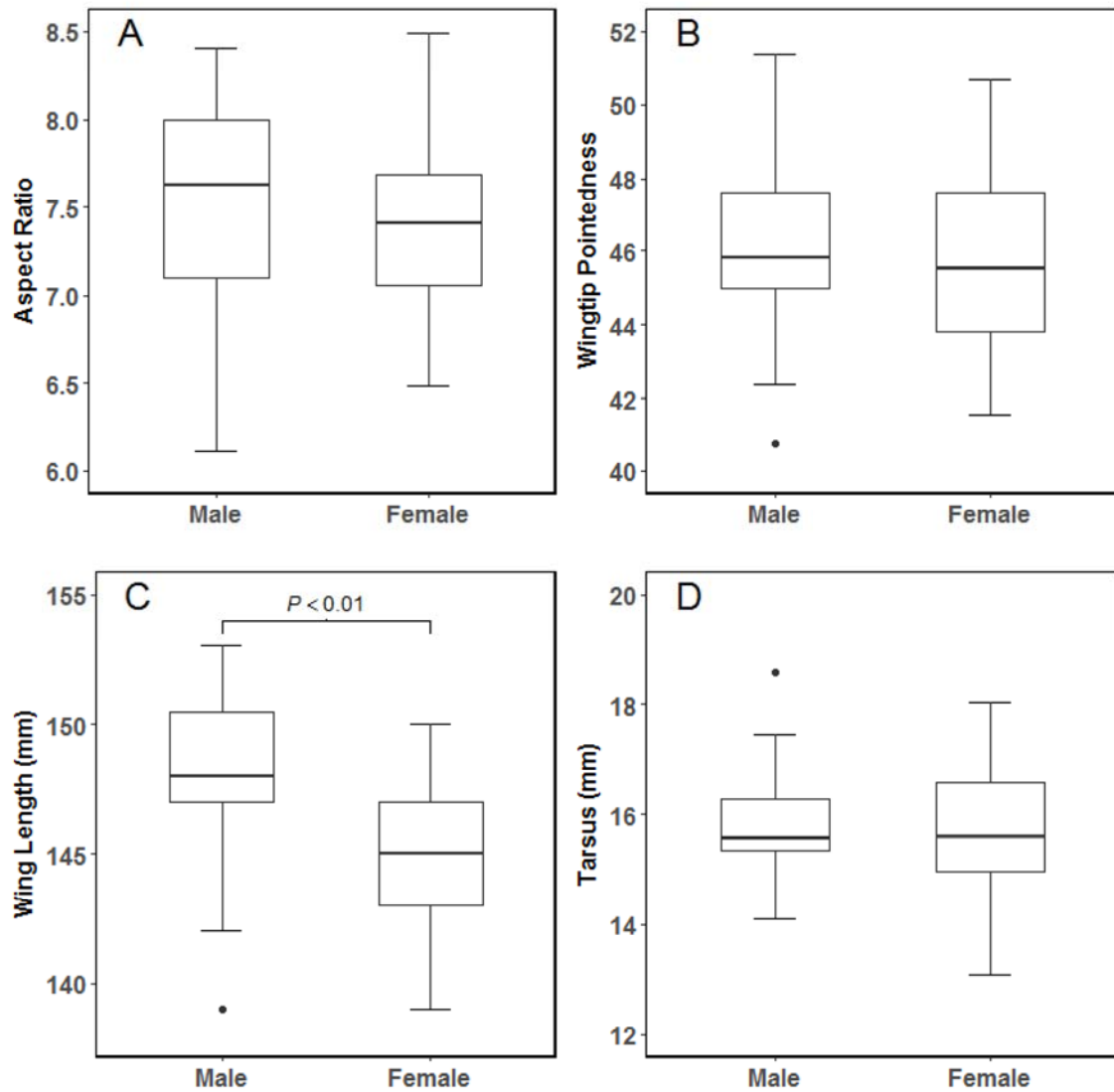


Figure 2.2. Boxplot comparing measurements of aspect ratio (A), wingtip pointedness (B), wing length (C), and tarsus length (D) between male and female purple martins. Significance between populations is denoted above each box.

Spring migration speed

Purple martins breeding at Alberta and Manitoba sites migrated at an average of 570.6 (± 121.5) km/day, travelling approximately 10,161 ($\pm 1,344$) km in 27 (± 7) days

from the last, known wintering site to the breeding grounds. Departure from the last, known wintering site and arrival at the breeding grounds varied among individuals, with departure dates ranging from 5 April to 8 May, 2016, and the date of arrival at the breeding site ranged from 8 May to 26 May, 2016; departure date and arrival date were positively correlated ($R^2 = 0.41$, $P < 0.01$). Migration speed was not significantly different between the Alberta and Manitoba populations ($F_{1,16} = 0.15$, $P = 0.7$) nor between sexes ($F_{1,16} = 3.86$, $P = 0.07$). Similarly, departure dates were not significantly different between the two populations ($F_{1,20} = 0.78$, $P = 0.39$) nor between sexes ($F_{1,20} < 0.01$, $P = 0.95$).

Neither wing morphometric variables (aspect ratio and wingtip pointedness) were significant predictors of spring migration speed (Table 2.3). However, departure date had a significant effect on migration speed ($P_{\text{departure}} = 0.01$), where the total speed travelled on spring migration was expected to increase by 7.52 km/day for each day that departure from the last wintering site was delayed (Fig. 2.3).

Table 2.3. Summary of the linear regression model (equation 2.5). Estimates are standardized to a mean of 0 and standard deviation of 1.

Parameter	Estimate	SE	<i>P</i>
Intercept	570.61	19.54	<0.01
Departure date	62.58	22.69	0.01
Aspect ratio	34.07	22.513	0.15
Wingtip pointedness	7.07	20.26	0.71

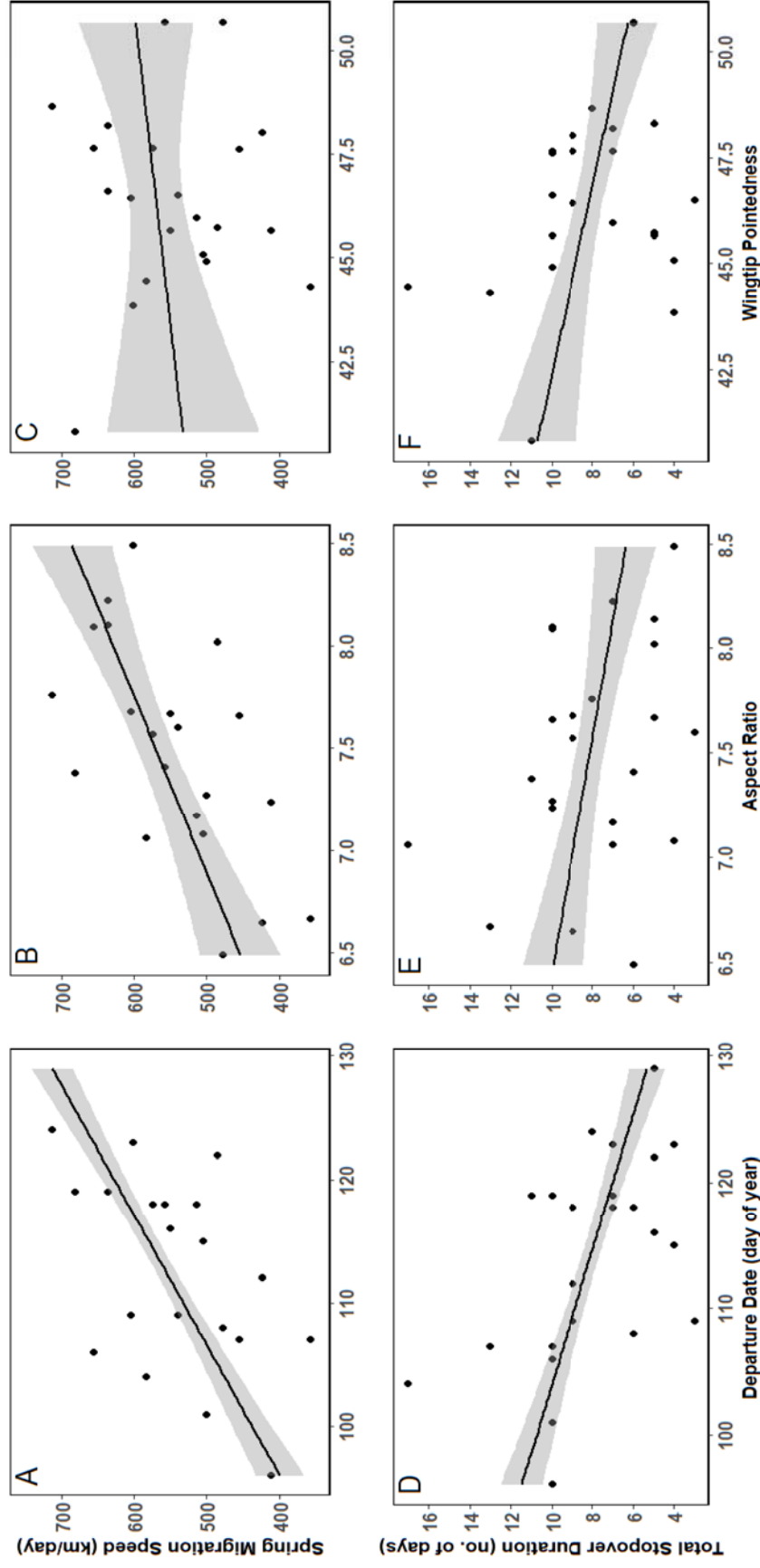


Figure 2.3. Migration performance of purple martins by departure date (A, D), aspect ratio (B, E), and wingtip pointedness (C, F).

Departure date is shown in day of year format (1 January, 2016 = 1). A regression line (predicted by the models) and 95% confidence intervals are represented by the solid line and the shaded grey area, respectively.

Of all (117) the stopovers examined, 32.5% of departures from stopovers occurred in the absence of a strong wind vector, while 18% of departures occurred in tailwinds, 26% in headwinds, and 24% in crosswinds. Wind speeds at departure ranged from 0 to 29.6km/hr; tailwinds ranged from 3.6 to 29.6km/hr, headwinds ranged from 3.6 to 27.8km/hr, and crosswinds ranged from 3.6 to 29.6km/hr. Neither the tailwind nor crosswind component at departure had a significant effect on the migration speed travelling between stopovers (Table 2.4).

Table 2.4. Summary of the linear mixed effect (LME) model (equation 2.7). Fixed effect estimates are standardized to a mean of 0 and standard deviation of 1.

Fixed effects			
Parameter	Estimate	SE	<i>P</i>
Intercept	576.95	27.11	<0.01
Tailwind	-37.48	27.24	0.17
Crosswind	3.17	27.24	0.91
Random effects			
Parameter	SD		
Individual	0.02		

Stopover duration

On spring migration, purple martins spent (on average) a total of 9 (± 4) days at stopovers while the total number of stopovers taken varied among individuals (3 to 9 stopovers). The total number of days spent at stopovers did not differ significantly between the two populations ($F_{1,20} < 0.01$, $P = 0.96$) or between sexes ($F_{1,20} = 0.32$, $P = 0.58$). The total number of stopovers taken on spring migration also did not differ

significantly between populations ($F_{1,20} = 0.02$, $P = 0.90$) or between sexes ($F_{1,20} = 0.08$, $P = 0.78$). The total stopover duration was positively correlated with the total duration of spring migration ($R^2 = 0.58$, $P < 0.01$), indicating birds spending more time at stopovers along spring migration also spent longer on spring migration.

Similar to the total spring migration speed, aspect ratio and wingtip pointedness were not significant predictors of the total stopover duration on spring migration (Table 2.5). Departure date, however, had a significant effect on stopover duration ($P_{\text{departure}} < 0.05$), where the total number of days spent at stopovers on spring migration was expected to decrease by 2.0% for each day that departure from the last wintering site was delayed (Fig. 2.3).

Table 2.5. Summary of the generalized linear regression model (GLM) (equation 2.6). Estimates are standardized to a mean of 0 and standard deviation of 1.

Parameter	Estimate	SE	<i>P</i>
Intercept	2.06	0.08	<0.01
Departure date	-0.16	0.08	0.05
Aspect ratio	-0.06	0.09	0.50
Wingtip pointedness	-0.10	0.08	0.18

A total of 117 stopovers were recorded and stopover duration varied among individuals, from one to seven days. However, 60% of all stopovers only lasted a single day, while stopovers lasting four or more days were less common (~10%). Most stopovers were made in the United States (38%), followed by Mexico (28%) and South America (28%), while only 5% of stopovers were made in Central America (Table 2.6).

Stopovers in the United States were cooler (temperature = 13°C (±5.7)) than the other regions on spring migration. More than half of the recorded stopovers did not experience any precipitation (59% or 69/117 stopovers), while approximately 5% of all stopovers recorded an average precipitation amount greater than 10mm.

Table 2.6. List of locations where stopovers were made along spring migration. Mean temperature, precipitation and normalized difference vegetation index (NDVI) (±SD) are shown for each location.

Location	Total stopovers made	Total stopover duration (days)	Temperature (°C)	Precipitation (mm)	NDVI*
USA	44	68	13.0 (±5.7)	4.89 (±10.51)	175.9 (±41.1)
Mexico	34	74	24.0 (±2.9)	0.38 (±1.34)	128.3 (±62.3)
Central America	6	7	23.0 (±2.7)	0.38 (±0.42)	164.2 (±27.3)
South America	33	64	24.0 (±2.9)	2.18 (±4.04)	194.7 (±50.2)

*NDVI values are calculated from ArcMapTM. Values range from 0 to 255, with higher values reflecting greater live vegetation.

The temperature at the stopover (averaged throughout the duration of a single stopover) was the only predictor variable in the model that had a significant effect on the number of days spent at a single stopover ($P_{\text{temperature}} = 0.04$); neither the average amount of precipitation at the stopover, nor the natural difference vegetation index (NDVI) had a significant effect on the stopover duration (Table 2.7). The number of days spent at a

single stopover was expected to increase by 3.9% for every 1°C increase in temperature at the stopover (Fig. 2.4).

Table 2.7. Summary of the generalized linear mixed effect model (GLMM) (equation 2.8). Fixed effect estimates are standardized to a mean of 0 and standard deviation of 1.

Fixed effects			
Parameter	Estimate	SE	<i>P</i>
Intercept	0.30	0.11	<0.01
Temperature	0.25	0.11	0.02
Precipitation	-0.02	0.10	0.85
NDVI	0.11	0.09	0.24
Random effect			
Parameter	SD		
Individual	0.27		

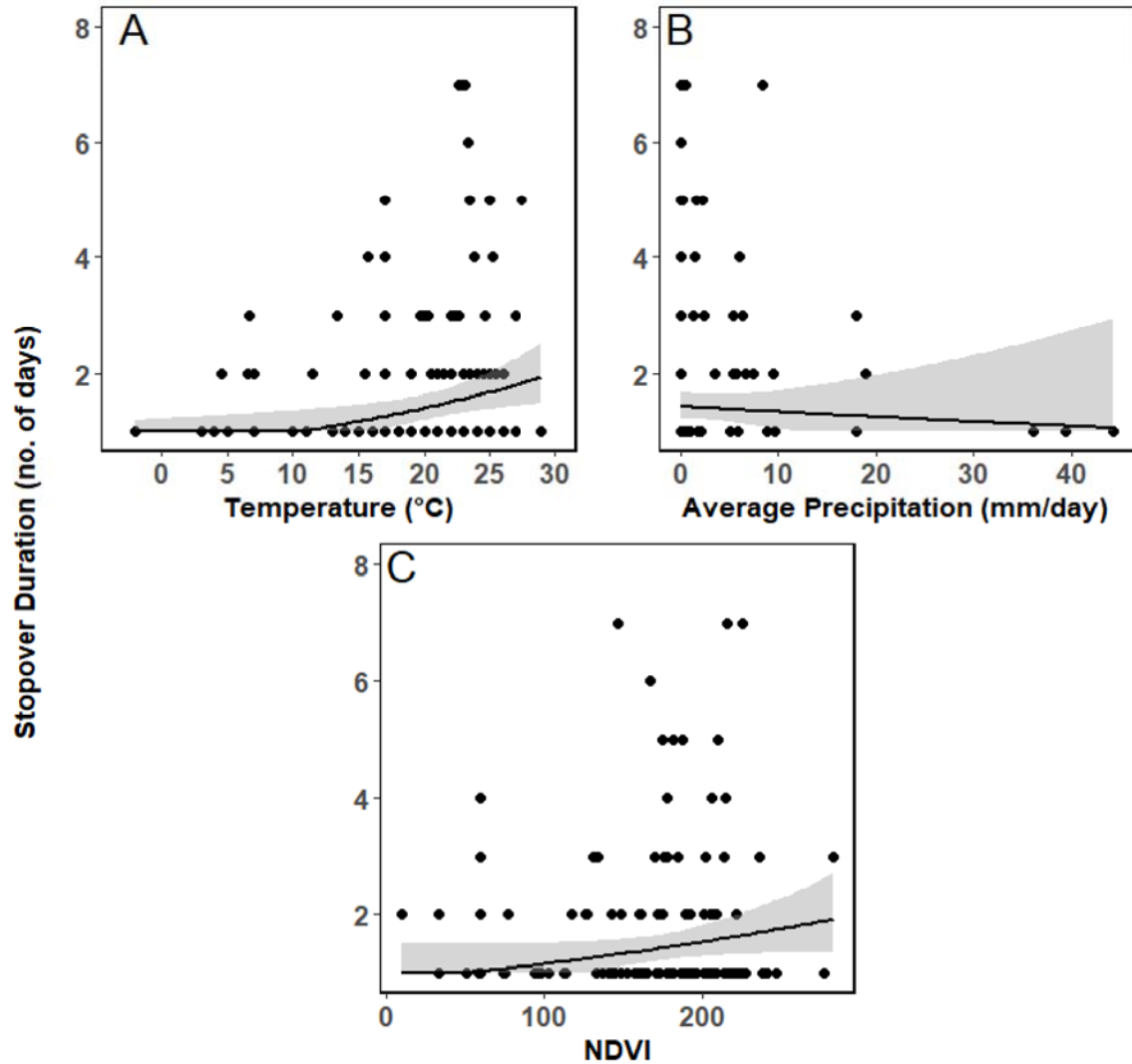


Figure 2.4. Relationship between stopover duration and environmental variables: average minimum-temperature (A), precipitation (B), and normalized difference vegetation index (NDVI) (C). A negative binomial regression line (predicted by the model (2.8)) and the 95% CI are represented by the solid line and the shaded grey area, respectively.

2.4 Discussion

I show that spring departure date was the greatest predictor of spring migration performance, where birds that departed later traveled at a greater speed and spent fewer

days at stopovers. Despite the variation in wing morphology, these factors were poor predictors of migration speed and stopover duration. Temperature was the only reliable environmental predictor of stopover duration, where birds had longer stopovers with higher temperatures. Birds generally did not avoid unfavourable wind conditions at departure. The results of this study support the time minimization hypothesis, and show for the first time how performance is impacted across all of spring migration by migration timing.

Morphometric variation

I found that neither aspect ratio nor wingtip pointedness varied significantly between populations or sexes. However, structural body size differed between populations and sexes, with purple martins from the Texas breeding population having shorter wings and longer tarsi than the northern-most breeding population, Alberta. These morphometric differences between Texas and Alberta contrast those found in Lam *et al.* (2015), who found that wing length did not differ across the purple martin latitude and tarsus length was shorter in purple martins from more southern breeding populations than those from more northern populations. However, the most northern breeding population examined in Lam *et al.* (2015) only included in three birds from Alberta, while my study, which included both Alberta and Manitoba breeding populations was a greater representation of more northern populations. Additionally, most (34%) of the data in Lam *et al.* (2015) were purple martins from Pennsylvania, which were not featured in my study. I suspect the differences in body morphology between populations are a result of different selection forces acting on the populations. The longer wings of Alberta purple martins may suggest selection for greater flight speed, while shorter wings of the Texas

birds may be favoured for higher aerial maneuverability (Alerstam and Lindström 1990). Among the four morphometrics, only wing length differed between males and females, with males having longer wings, matching results from past studies (Behle 1968, Lam *et al.* 2015), which may be a result of sexual selection (longer wings may be an indication of higher male quality or reduce flight costs when performing mating displays (Møller 1991)) or differences in foraging efficiency.

Contrary to my predictions, I did not find that wing morphology had a strong effect on migration speed nor total stopover duration. I suspect that because there was little variation in wing morphometry, neither aspect ratio nor wingtip pointedness proved useful in predicting migration performance. The low variation in wing morphometry within and between populations does not support the hypothesis that longer-distance migrants have higher aspect ratio wings and pointed wingtips. I hypothesize that northern and southern populations have similar morphologies due to selection favouring the same morphology (*e.g.*, high aspect ratio wings) but selective forces (*i.e.*, purpose/function) differing between populations. In the example of aspect ratio, birds with high aspect ratio wings are more adept at flying faster, which may benefit northern population birds that travel longer distances on migration, but for southern population birds, this morphology may be a product of selection for more efficient foraging at the breeding grounds rather than faster migration. Despite wing morphology not showing a strong influence on migration performance in our study and in some previous studies (Lam *et al.* 2015), I do not imply that wing morphology is unrelated to migration performance, as this study focused on intraspecific comparisons of migration. Recent studies have shown vast differences in migration distance in several species (Vágási *et al.* 2016, Møller *et al.*

2017), suggesting the effects of wing morphology on migration are more evident when comparing migration performance between species rather than within species.

Departure timing on migration performance

The timing of spring migration (specifically the onset of spring migration) plays an important role in determining migration speed and stopover duration. Purple martins that departed later during spring migration were found to have completed migration by travelling at a greater average speed and spending fewer days at stopovers, suggesting that late-departing migrants follow a time-selection strategy. Similar findings have been documented in studies on trans-Saharan songbirds, such as garden warblers (*Sylvia borin*), where the date of capture (marking the date of departure) was positively correlated with the (estimated) migration speed (Ellegren 1993, Fransson 1995).

The underlying mechanisms that dictate departure timing and the onset of spring migration in birds are implied to be endogenously controlled by circadian and circannual rhythms, such that differences in inherent timing between conspecifics results in variation in departure dates (Gwinner 1989; 1990; 1996). Endogenous control of migration schedules implies that timing is fixed, such that individuals that depart earlier than conspecifics will arrive earlier. My finding that departure date from the wintering grounds was positively correlated with the arrival date at the breeding grounds supports the hypothesis that migration timing is endogenously controlled by circadian/circannual rhythms. Although endogenous control over migration may seem unfavourable for migrants that cue for a later departure, in this study, a completion of spring migration in a shorter amount of time may be an adaptive strategy for late migrants to compete with conspecifics/allospecifics that arrive earlier for habitat. Differences in the timing of

departure on spring migration within-species has been shown in garden warblers, where individuals that experience longer photoperiods begin gonadal development and subsequently depart on spring migration earlier (Gwinner 1989). Therefore, a late start on spring migration may be the result of inherent timing, programmed for a later departure, but selection may favour the use of a time-selected strategy in migrants that are genetically programmed to depart late, to prevent arriving late. Because previous studies have primarily focused on the relationship between departure and arrival times, events on migration that may affect departure timing could only be postulated; I bridge this gap by showing that migration performance can vary with departure timing, which may consequently affect arrival timing.

Although the results of this study suggest late-departing birds follow a time-selection strategy, I did not have the data to examine the consequences of time-selected migrants. Optimal migration theory posits that time-selected birds minimize the time spent on migration but are less conservative on energy use (Hedenström and Ålerstam 1997), depleting fat stores faster, which can result in poor body condition upon arrival. Marra *et al.* (1998) found that American redstarts that arrived late at the breeding grounds had lower body conditions than conspecifics that arrived earlier. Arrival at the breeding site in poor body condition may leave birds vulnerable to predation (Ålerstam and Lindström 1990), delay breeding, or decrease clutch size (Bêty *et al.* 2003). Future studies should consider examining events proceeding spring migration to determine whether following a time-selection strategy affects the fitness of the bird and/or their reproductive fitness.

Environmental conditions en route

I found that wind speed/direction at departure was a poor predictor of spring migration speed. Contrary to previous studies (Able 1973, Lietchi and Bruderer 1998, Åkesson and Hedenström 2000, Erni *et al.* 2002, Bowlin and Wikelski 2008), I did not find that migrants favoured a specific wind vector at departure, implying that purple martins may not selectively depart in favourable wind conditions. However, the recorded wind speed and direction used in this study were collected at ground level and thus may not reflect the same wind conditions experienced by migrants flying at higher altitudes. Altitude is likely an integral component in determining migration flight speed as several atmospheric factors vary by altitude, such as atmospheric pressure and temperature, which can impact energy expenditure and flight aerodynamics (Richardson 1990, Åkesson and Hedenström 2007, Alerstam *et al.* 2011). It is possible that purple martins do not rely on wind vectors when making decisions to depart because they are able to adjust their flight altitudes to match favourable flight conditions, similar to other birds (Richardson 1990, Bowlin *et al.* 2015). Alerstam *et al.* (2011) found that unlike noctuid moths, migratory birds were not restricted by wind vectors on migration, which the authors postulate is due to birds possessing physiological adaptations for flying at higher altitudes allowing them to adjust their flight altitude to obtain a favourable migration condition. Migration altitudes of purple martins are currently not well understood, but knowledge of flight and migration altitude may allow us to obtain a better estimate of the wind conditions martins experience during migration.

Temperature was the only environmental factor that was found to affect stopover duration. I suspect the positive relationship between temperature and stopover duration

was related to stopover/departure decisions based on the energetic costs of remaining at stopovers. At lower temperatures, birds must spend energy to maintain their body temperature, forcing them to deplete their fat stores, which may lead to insufficient fat stores for migration (Butler and Woakes 1990, Piersma *et al.* 1999, Newton 2010). Wikelski *et al.* (2003) found that New World thrushes (*Catharus* spp.) that remained at a stopover under cool spring conditions ($\sim 10^{\circ}\text{C}$) spent more energy than birds on migration flights, demonstrating that under some conditions migration may be less costly than remaining at stopovers. It may also be more beneficial for birds to migrate during lower temperatures to reduce water loss associated with migrating during higher temperatures (Carmi *et al.* 1992). Therefore, birds may have spent less time at cooler stopovers because (1) it is detrimental to remain at cooler stopovers, and/or (2) the benefits of departing in lower temperatures are greater than the costs associated with migrating during lower temperatures.

Despite precipitation having prominent effects on migration in numerous studies (Marra *et al.* 2005, Saino *et al.* 2007, Studds and Marra 2007; 2011), I did not find that the average amount of precipitation recorded at the stopover was a reliable predictor of stopover duration. I suspect the effect of amount of precipitation on stopover duration was not significant due to the few occurrences of precipitation being greater than 10 mm. Since the environmental data I collected were from the same year, the low occurrence of precipitation may have been a result of a dry migration season in 2016; a multi-year study that includes years with higher rainfall (and greater ranges of temperatures) may reveal a stronger pattern in stopover duration. NDVI, as a proxy for habitat quality, similarly had little to no effect on stopover duration, which was unexpected because optimal migration

theory states that birds are able to forage faster in higher-quality habitats (*i.e.*, higher insect abundance), reducing the amount of time spent refueling at a stopover. A similar finding in purple martins was reported by Van Loon *et al.* (2017), where habitat quality was a poor predictor of stopover duration at the Yucatan Peninsula during fall migration. Overall, this study suggests some environmental factors such as NDVI and precipitation have for a weak effect on stopover duration, while others (*e.g.*, temperature) have a stronger effect.

Conclusion

This study is the first to field-test long-standing hypotheses of optimal migration theory related to the influence of wing morphology on migration performance. I found that migration performance may be related to departure timing but not wing morphology (aspect ratio and wing-tip pointedness), which suggests morphological parameters have a weaker influence on migration performance than the timing of migration. My data support the hypothesis that late-departing migrants follow a time-selected migration strategy, but this is not the only migration strategy birds may follow (Alerstam and Lindström 1990, Hedenström and Alerstam 1997). An energy-selected migration strategy, for example, states migrants prioritize the minimization of energy expenditure throughout migration, to arrive at the destination with a better body condition, which may be favoured over a time-selected strategy when costs of completing migration as fast as possible (*e.g.*, greater energy expenditure) exceed the benefits of a faster migration (Alerstam and Lindström 1990, Hedenström and Alerstam 1997). Energy-selected migration is suggested to be more common during fall migration than spring migration because resource availability at the wintering grounds (the destination of fall migration) is

not as limited as resources at the breeding grounds, reducing competition for an earlier arrival (Nilsson *et al.* 2013).

I also present the first study to examine the environmental conditions at every stopover made on a 10,000 km migration from South America to Canada of a long-distance migratory songbird. My finding that temperature was positively correlated with stopover duration suggests environmental conditions impact stopover decisions on migration, and implies increases in global temperatures predicted by climate change (Intergovernmental Panel on Climate Change 2014) may result in birds spending more time at stopovers and consequently extending the amount of time spent on spring migration. The mechanisms behind migration timing are poorly understood but several studies, including my own, indicate that timing plays a pivotal role in determining how migrants perform on spring migration. I recommend future research should focus determining the factors that influence departure date and the relative role of innate versus environmental effects on timing to better understand the implications of climate change on migratory songbirds.

2.5 References

- Able, K.P. 1973. The role of weather variables and flight direction in determining the magnitude of nocturnal bird migration. *Ecology* **54**(5): 1031–1041.
- Åkesson, S., and Hedenström, A. 2000. Wind selectivity of migratory flight departures in birds. *Behav. Ecol. Sociobiol.* **47**(3): 140–144.

- Åkesson, S., and Hedenström, A. 2007. How migrants get there: Migratory performance and orientation. *Bioscience*. **57**(2): 123–133.
- Alerstam, T., and Lindström, Å. 1990. Optimal Bird Migration: The Relative Importance of Time, Energy, and Safety. *In* Bird Migration. *Edited by* E. Gwinner. Springer Berlin Heidelberg, Berlin, Heidelberg. pp. 331–351.
- Alerstam, T., Chapman, J.W., Bäckman, J., Smith, A.D., Karlsson, H., Nilsson, C., Reynolds, D.R., Klaassen, R.H.G., and Hill, J.K. 2011. Convergent patterns of long-distance nocturnal migration in noctuid moths and passerine birds. *Proc. R. Soc. London B Biol. Sci.*
- Alerstam, T., and Hedenström, A. 1998. The development of bird migration theory. *J. Avian Biol.* **29**(4): 343–369.
- Alerstam, T., Rosén, M., Bäckman, J., Ericson, P.G.P., and Hellgren, O. 2007. Flight speeds among bird species: allometric and phylogenetic effects. *PLoS Biol.* **5**(8): e197.
- Allen, R.W., and Nice, M.M. 1952. A study of the breeding biology of the purple martin (*Progne subis*). *Am. Midl. Nat.* **47**(3): 606–665.
- Behle, W.H. 1968. A new race of the purple martin from Utah. *Condor*. **70**(2): 166–169.

- Bêty, J., Gauthier, G., and Giroux, J.-F. 2003. Body condition, migration, and timing of reproduction in snow geese: a test of the condition-dependent model of optimal clutch size. *Am. Nat.* **162**(1): 110–121.
- Bivand, R.S., Pebesma, E.J., Gomez-Rubio, V. and Pebesma, E.J., 2008. *Applied spatial data analysis with R*. Springer, New York, NY.
- Both, C., Bouwhuis, S., Lessells, C.M., and Visser, M.E. 2006. Climate change and population declines in a long-distance migratory bird. *Nature*. **441**(7089): 81–83.
- Bowlin, M.S., and Wikelski, M. 2008. Pointed wings, low wing loading and calm air reduce migratory flight costs in songbirds. *PLoS one*. **3**(5): e2154.
- Bowlin, M.S., Enstrom, D.A., Murphy, B.J., Plaza, E., Jurich, P., and Cochran, J. 2015. Unexplained altitude changes in a migrating thrush: long-flight altitude data from radio-telemetry. *Auk*. **132**(4): 808–816.
- Bridge, E.S., Thorup, K., Bowlin, M.S., Chilson, P.B., Diehl, R.H., Fléron, R.W., Hartl, P.H., Kays, R., Kelly, J.F., Robinson, W.D., and Wikelski, M. 2011. Technology on the move: recent and forthcoming innovations for tracking migratory birds. *Bioscience*. **61**(9): 689–698.
- Butler, P.J., and Woakes, A.J. 1990. The physiology of bird flight. *In* *Bird migration*. Edited by E. Gwinner. Springer Berlin Heidelberg, Berlin, Heidelberg. pp. 300–318.

- Carmi, N., Pinshow, B., Porter, W.P., and Jaeger, J. 1992. Water and energy limitations on flight duration in small migrating birds. *Auk*. **109**(2): 268–276.
- Chernetsov, N. 2012. Passerine migration. Springer Berlin Heidelberg, Berlin, Heidelberg.
- Ellegren, H. 1993. Speed of migration and migratory flight lengths of passerine birds ringed during autumn migration in Sweden. *Ornis Scand.* **24**(3): 220–228.
- Erni, B., Liechti, F., and Bruderer, B. 2002. Stopover strategies in passerine bird migration: a simulation study. *J. Theor. Biol.* **219**(4): 479–493.
- Fiedler, W. 2005. Ecomorphology of the external flight apparatus of blackcaps (*Sylvia atricapilla*) with different migration behavior. *Ann. N. Y. Acad. Sci.* **1046**(1): 253–263.
- Fournier, D.A., Skaug, H.J., Ancheta, J., Ianelli, J., Magnusson, A., Maunder, M.N., Nielsen, A., and Sibert, J. 2012. AD model builder: using automatic differentiation for statistical inference of highly parameterized complex nonlinear models. *Optim. Methods Softw.* **27**(2): 233–249.
- Fox, J., and Weisberg, S. 2011. *An R Companion to Applied Regression*, Second Edition. Thousand Oaks, Calif.: SAGE Publications
- Fransson, T. 1995. Timing and speed of migration in North and West European populations of *Sylvia* warblers. *J. Avian Biol.* **26**(1): 39.

- Fraser, K.C., Silverio, C., Kramer, P., Mickle, N., Aepli, R., and Stutchbury, B.J.M. 2013. A trans-hemispheric migratory songbird does not advance spring schedules or increase migration rate in response to record-setting temperatures at breeding sites. *PLoS one*. **8**(5): e64587.
- Gräler, B., Pebesma, E., and Heuvelink, G. 2016. Spatio-temporal interpolation using gstat. *R Journal*. **8**(1): 204-218.
- Gwinner, E. 1989. Photoperiod as a modifying and limiting factor in the expression of avian circannual rhythms. *J. Biol. Rhythms* **4**(2): 125–138.
- Gwinner, E. 1990. *Bird Migration*. Springer Berlin Heidelberg, Berlin, Heidelberg.
- Gwinner, E. 1996. Circadian and circannual programmes in avian migration. *J. Exp. Biol.* **199**(1): 39–48.
- Hedenström, A., and Ålerstam, T. 1997. Optimum fuel loads in migratory birds: distinguishing between time and energy minimization. *J. Theor. Biol.* **189**(3): 227–234.
- Hedenström, A. 2008. Adaptations to migration in birds: behavioural strategies, morphology and scaling effects. *Philos. Trans. R. Soc. London B Biol. Sci.* **363**(1490): 287–299.

- Hill, R., and Braun, M. 2001. Geolocation by light level. *In* Electronic tagging and tracking in marine fisheries. *Edited by* J.R. Sibert and J.L Nielsen. Springer, Dordrecht. pp. 315–330.
- Intergovernmental Panel on Climate Change, 2014. Climate Change 2014—impacts, adaptation and vulnerability: regional aspects. Cambridge University Press.
- Kokko, H. 1999. Competition for early arrival in migratory birds. *J. Anim. Ecol.* **68**(5): 940–950.
- Lam, L., McKinnon, E.A., Ray, J.D., Pearman, M., Hvenegaard, G.T., Mejeur, J., Moscar, L., Pearson, M., Applegate, K., Mammenga, P., Tautin, J., and Fraser, K.C. 2015. The influence of morphological variation on migration performance in a trans-hemispheric migratory songbird. *Anim. Migr.* **2**(1): 86–95.
- Liechti, F., and Bruderer, B. 1998. The relevance of wind for optimal migration theory. *J. Avian Biol.* **29**(4): 561.
- Lockwood, R., Swaddle, J.P., and Rayner, J.M. V. 1998. Avian wingtip shape reconsidered: wingtip shape indices and morphological adaptations to migration. *J. Avian Biol.* **29**(3): 273–292.
- Marchetti, K., Price, T., and Richman, A. 1995. Correlates of wing morphology with foraging behaviour and migration distance in the genus *Phylloscopus*. *J. Avian Biol.* **26**(3): 177–181.

- Marra, P.P., Francis, C.M., Mulvihill, R.S., and Moore, F.R. 2005. The influence of climate on the timing and rate of spring bird migration. *Oecologia*. **142**(2): 307–315.
- Marra, P.P., Hobson, K.A., and Holmes, R.T. 1998. Linking winter and summer events in a migratory bird by using stable-carbon isotopes. *Science*. **282**(5395): 1884–1886.
- Møller, A.P. 1991. Influence of wing and tail morphology on the duration of song flight in skylarks. *Behav. Ecol. Sociobiol.* **28**(5): 309–314.
- Møller, A.P. 1994. Phenotype-dependent arrival time and its consequences in a migratory bird. *Behav. Ecol. Sociobiol.* **35**(2): 115–122.
- Møller, A.P., Rubolini, D., and Saino, N. 2017. Morphological constraints on changing avian migration phenology. *J. Evol. Biol.* **30**(6): 1177–1184.
- Nakagawa, S., and Schielzeth, H. 2013. A general and simple method for obtaining R^2 from generalized linear mixed-effects models. *Methods Ecol. Evol.* **4**(2): 133–142.
- Newton, I. 2010. The migration ecology of birds. Burlington: Elsevier Science, Burlington.
- Nilsson, C., Klaassen, R.H.G., and Alerstam, T. 2013. Differences in speed and duration of bird migration between spring and autumn. *Am. Nat.* **181**(6): 837–845.

- Pebesma, E.J., 2004. Multivariable geostatistics in S: the gstat package. *Computers & geosciences*. **30**(7): 683-691.
- Pebesma, E.J., and Bivand, R.S. 2005. Classes and methods for spatial data in R. *R news*. **5**(2): 9-13.
- Pennycuik, C.J. 1969. The mechanics of bird migration. *Ibis*. **111**(4): 525–556.
- Pennycuik, C.J. 2008. *Modelling the flying bird*. Elsevier.
- Piersma, T., Dietz, M., Dekinga, A., and Nebel, S. 1999. Reversible size-changes in stomachs of shorebirds: when, to what extent, and why. *Acta Ornithol.* **34**(2): 175–181.
- Pinheiro, J., Bates, D., DebRoy, S., and Sarkar, D. 2017. nlme: linear and nonlinear mixed effects models. R package version 3.1-131.
- Pyle, P. 1997. *Identification guide to North American birds. Part I*. Braun-Brumfield Inc., Bolinas, California.
- Quinn, G.P., and Keough, M.J. 2002. *Experimental design and data analysis for biologists*. Cambridge University Press.
- Rappole, J.H., and Tipton, A.R. 1991. New harness design for attachment of radio transmitters to small passerines. *J. Field Ornithol.* **62**: 335–337.

- Rayner, J.M. V. 1990. The mechanics of flight and bird migration performance. *In* Bird migration. Springer Berlin Heidelberg, Berlin, Heidelberg. pp. 283–299.
- Richardson, W.J. 1978. Timing and amount of bird migration in relation to weather: a review. *Oikos*. **30**(2): 224–272.
- Richardson, W.J. 1990. Timing of bird migration in relation to weather: updated review. *In* Bird migration. Springer Berlin Heidelberg, Berlin, Heidelberg. pp. 78–101.
- Saino, N., Rubolini, D., Jonzén, N., Ergon, T., Montemaggiori, A., Stenseth, N., and Spina, F. 2007. Temperature and rainfall anomalies in Africa predict timing of spring migration in trans-Saharan migratory birds. *Clim. Res.* **35**(1–2): 123–134.
- Schmaljohann, H., Lisovski, S., and Bairlein, F. 2017. Flexible reaction norms to environmental variables along the migration route and the significance of stopover duration for total speed of migration in a songbird migrant. *Front. Zool.* **14**(17): 1–16.
- Skaug, H., Fournier, D., Nielsen, A., and Magnusson, A. 2013. Generalized linear mixed models using AD model builder. R package version 0.7, 2013.
- Smith, A.D., and McWilliams, S.R. 2014. What to do when stopping over: behavioral decisions of a migrating songbird during stopover are dictated by initial change in their body condition and mediated by key environmental conditions. *Behav. Ecol.* **25**(6): 1423–1435.

- Studds, C.E., and Marra, P.P. 2007. Linking fluctuations in rainfall to nonbreeding season performance in a long-distance migratory bird, *Setophaga ruticilla*. *Clim. Res.* **35**(1–2): 115–122.
- Studds, C.E., and Marra, P.P. 2011. Rainfall-induced changes in food availability modify the spring departure programme of a migratory bird. *Proc. R. Soc. London B Biol. Sci.*
- Swaddle, J.P., and Lockwood, R. 2003. Wingtip shape and flight performance in the European Starling *Sturnus vulgaris*. *Ibis.* **145**(3): 457–464.
- Tarof, S., and Brown, C.R. 2013. Purple martin (*Progne subis*). The birds of North America online (ed. A Poole). Ithaca, NY: Cornell Lab of Ornithology.
- Thorup, K., Tøttrup, A.P., Willemoes, M., Klaassen, R.H.G., Strandberg, R., Vega, M.L., Dasari, H.P., Araújo, M.B., Wikelski, M., and Rahbek, C. 2017. Resource tracking within and across continents in long-distance bird migrants. *Sci. Adv.* **3**(1): e1601360.
- Vágási, C.I., Pap, P.L., Vincze, O., Osváth, G., Erritzøe, J., and Møller, A.P. 2016. Morphological adaptations to migration in birds. *Evol. Biol.* **43**(1): 48–59.
- Van Loon, A., Ray, J.D., Savage, A., Mejeur, J., Moscar, L., Pearson, M., Pearman, M., Hvenegaard, G.T., Mickle, N., Applegate, K., and Fraser, K.C. 2017. Migratory

- stopover timing is predicted by breeding latitude, not habitat quality, in a long-distance migratory songbird. *J. Ornithol.* **158**(3): 745–752.
- Wickham, H. 2009. *ggplot2: Elegant graphics for data analysis*. Springer-Verlag, New York.
- Wickham, H. 2011. The split-apply-combine strategy for data analysis. *journal of statistical software*. **40**(1): 1-29.
- Wikelski, M., Tarlow, E.M., Raim, A., Diehl, R.H., Larkin, R.P., and Visser, G.H. 2003. Avian metabolism: costs of migration in free-flying songbirds. *Nature*. **423**(6941): 704.
- Wolda, H. 1978. Seasonal fluctuations in rainfall, food and abundance of tropical insects. *J. Anim. Ecol.* **47**(2): 369.
- Yee, T.W. 2015. *Vector generalized linear and additive models*. Springer, New York.
- Yee, T.W., Stoklosa, J., and Huggins, R.M. 2015. The VGAM package for capture–recapture data using the conditional likelihood. *J. Statist. Soft.* **65**(5): 1-33.
- Yong, W., and Moore, F.R. 1994. Flight morphology, energetic condition, and the stopover biology of migrating thrushes flight morphology, energetic condition, and the stopover biology of migrating thrushes. *Auk*. **111**(3): 683–692.

Zuur, A., Ieno, E.N., Walker, N., Saveliev, A.A., and Smith, G.M. 2009. Mixed effects models and extensions in ecology with R. Springer Science & Business Media.

Chapter 3: Wing morphometric growth of a cavity-nesting bird in insecticide-treated nests

Abstract

Nestling birds are thought to be vulnerable to parasitism due to having poor defense mechanisms against parasites. Previous studies have demonstrated that ectoparasites can negatively affect host structural growth, but these studies did not examine growth of wing shape and size, which can influence timing of fledging and flight performance. I experimentally manipulated nest conditions to reduce ectoparasite loads and examined whether wing morphometric growth rates of nestling purple martins (*Progne subis*) differed among nests. I found that nests contained varying intensities of mites, lice, and fleas, but ectoparasite loads did not differ among treatment groups. However, nestlings that were treated with an insecticide exhibited different morphometric growth rates than nestlings without any treatment (control). Variation in wing morphometry among all nestlings was highest during earlier stages of development, but morphometry nearing fledging was similar, suggesting that birds may accelerate wing growth and development to meet morphological requirements to fledge. This study suggests wing development and overall wing morphology is an important component in determining whether nestlings will be able to fledge.

3.1 Introduction

Growth and development of the wings is important for nestlings to fledge successfully, survive, and (ultimately) breed. Abnormal growth may delay fledging, result in reduced fitness and/or survivability, and (for long-distance migratory birds) impede flight performance or prevent the completion of migration. Although structural

development of the wings is largely determined by genetic factors (Saunders 1948, Singh *et al.* 1991), ecological interactions, such as bird-parasite interactions, can also affect wing growth (Kunz and Ekman 2000). Birds are host to a variety of parasites.

Endoparasites, such as nematodes and tapeworms, live within the body of a host organism (*e.g.*, birds) and can infect their host with diseases, which can result in reducing host fitness and survival (Ewald 1983). Ectoparasites, in contrast, are found external to their host, inhabiting the skin and/or outgrowths of the skin (hair, feathers) (Hopla *et al.* 1994), but can have similar effects on the host as endoparasites (Chapman and George 1991, Saino *et al.* 1998, Christe *et al.* 2000). Natural selection has favoured the development of host-defenses, such as greater immune response or grooming (Clayton 1991), to reduce or at least mitigate the negative effect effects caused by parasites. However, hosts are unable to defend against ectoparasites when the intensity of ectoparasites is overwhelming, resulting in poor body condition and reduced fitness/survival, which may carry over to their offspring (Tschirren *et al.* 2007). Furthermore, it is expected that juvenile birds are more susceptible to the detrimental effects from ectoparasites than adults, as young birds have yet to develop sufficient defenses against ectoparasites (Christe *et al.* 1998). The exposure to high ectoparasite loads in the nest may weaken the nestlings, causing growth and development to slow down and constrain development of wing morphology adapted for long-distance migration.

Nest cavities provide a favourable microclimate for many ectoparasites (*e.g.*, fleas), making cavity-nesting birds susceptible to parasitism. Purple martins (*Progne subis*), for example, have evolved to rely heavily on human-made structures for nesting and raising offspring during the breeding season (Allen and Nice 1952). The reliance on human-made

structures exposes purple martins to many different nest ectoparasites species, and poor maintenance of these structures can cause a buildup of ectoparasites in the nest over time. The effects of ectoparasites on the fitness of cavity-nesting birds has been extensively studied (Johnson and Albrecht 1993, Heeb *et al.* 2000, Harriman *et al.* 2013), but few studies have documented changes throughout nestling development, limiting our understanding of how ectoparasitism impacts host growth rates. Furthermore, our knowledge of the growth and development of wing size and shape is severely lacking; growth patterns of more detailed wing morphometries (*i.e.*, not just wing length) can be important in providing insight on changes in other properties of the wing throughout growth, such as growth of the retrices.

The objective of this study was to examine whether nestlings reared in ectoparasite-free nests exhibited different wing morphometric growth rates than nestlings reared in a natural environment (control nestlings). To test my objective, I conducted an experiment on purple martins, where nestlings and their nest cavity were treated with an insecticide to reduce parasitism throughout the nestling's growth period. I took measurements of wing length, wingtip pointedness, and aspect ratio once every three days to record changes in wing morphometry throughout growth. I also examined changes in weight over time, as a measure of body condition. Purple martin nests were collected after all nestlings had fledged and placed into Berlese-Tullgren funnels to extract ectoparasites from each nest. Ectoparasites from the nests were then identified through a dissecting microscope. I hypothesized that nestlings reared in ectoparasite-free nests would experience faster growth rates resulting in longer wings, more pointed wingtips, and higher aspect ratio wings than control nestlings, as well as weighing more due to being parasitized less. I

compared the total ectoparasite load between nests to determine whether ectoparasite loads differed among nests. I predicted that treated nests would have lower ectoparasite loads than treated nests due to the effects of the insecticide limiting colonization of ectoparasites.

3.2 Methods

This research was conducted in accordance with the recommendations of the Ornithological Council “Guidelines to the Use of Wild Birds in Research” and was approved by the University of Manitoba’s Animal Care Committee (Animal Care Protocol Number: F14-009/1 (AC10930)). The capture, handling, and banding of nestling purple martins (*Progne subis*) for this project was permitted by the Canadian Wildlife Service (Permit No. 10876 D) and adheres to the North American Banding Council’s Bander’s Code of Ethics and the Canadian Council on Animal Care. The application of the insecticide on the birds and the nests were approved by the University of Manitoba’s Animal Care Committee.

Study sites and breeding colony

The experiment was carried out at two locations in Manitoba, Canada: Oak Hammock Marsh (50.17°N, 97.13°W) and Town and Country Campground (49.83°N, 96.98°W) from 22 June, 2016 to 28 July, 2016. I used one purple martin house at the former site, and two purple martin houses at the latter site. All purple martin houses were the same multi-compartment, wooden model with four compartments (nest cavities) on each side (16 nest cavities total). I performed nest checks (*i.e.*, monitor the nest by recording information on the number and status of the eggs and nestlings) at each site once every three to four days, beginning 5 May, 2016 and predicted the hatch date of the

eggs using a purple martin prognosticator (a laminated wheel used to estimate key events (e.g., hatch date) in the purple martin breeding period (Hill 1999)). Nestlings were aged using purple martin aging photographs (Purple Martin Conservation Association (PMCA); <http://www.purplemartin.org>). Hatch dates of the nestlings in my study ranged from 20 June, 2016 to 7 July, 2016 and clutch sizes ranged from 3 to 6 nestlings per brood.

Experimental design

After a full clutch was laid, I randomly selected three active nest cavities per house (with the exception of one house where I selected six nests) and assigned each cavity one of three possible treatments: 1) an insecticide treatment (insecticide-treated), 2) a sham treatment (sham-treated), or 3) no treatment (control). A total of four nests were assigned to each group with a maximum of four nestlings per nest being randomly selected as subjects in the experiment. All nestlings were banded with a federal bird band at day 12 (*i.e.*, 12 days after hatching) (Hill III 2002) as a way to identify each individual in the study.

In the insecticide-treated group, nests were sprayed using a hand-pumped sprayer containing a solution of Durvet Permethrin 10% (solution diluted to 0.1%; 1 part permethrin, 99 parts distilled water) to reduce nest ectoparasite loads. Permethrin is a synthetic pyrethroid, which is extracted from chrysanthemum plants that are toxic to many arthropods but has low toxicity to birds (WHO 1990). I administered the insecticide to all sides of the nest cavities and to the nest surface, but I was unable to spray the bottom of the nests due to the nests being adhered to the bottom by mud. The treatment was not applied to the outside walls of the nest cavity, to prevent runoff of the insecticide

from affecting lower cavities that were also part of the study. Eggs and/or nestlings were temporarily removed from the nest during the spraying process, and placed in a basket lined with grass and leaves collected around the study site. Nests were only sprayed once throughout the study because the effects of permethrin can last over four-weeks in the absence of sunlight (Collison *et al.* 1981, WHO 1990), which provided nestlings enough time to complete growth and fledge. I applied the same solution of permethrin (Durvet Permethrin 10% (diluted to 0.1%)) to all young in the nest within two days after hatching by preening the body, wings, legs, and head (avoiding the eyes and beak) with a cotton swab dipped in the solution. Similar to the nest treatment, I did not administer the insecticide to the nestlings more than once.

The methods used to administer the treatment to nests and nestlings in the insecticide-treated group were replicated in the sham group, but replacing permethrin with water. The sham treatment was applied to determine whether the effects on nestlings were attributed to the insecticide or the methods used to apply the treatment (*e.g.*, increased moisture from spraying the solution into the nest cavity). In the control group, I did not administer any treatments to the nest or the nestlings but continued to monitor the status of the colony through nest checks.

Measurements

Measurements for weight (to the nearest 0.1 g using a Pesola[®] spring scale), wing length (to the nearest 0.1 mm using a wing ruler), wing span (to the nearest 0.1 mm using a 1-metre ruler), distance between the tips of the longest primary feather and longest secondary feather (*i.e.*, wingtip index) (to the nearest 0.1 mm using calipers) and the surface area of the wing (*i.e.*, wing area) (to the nearest .01 cm²) were taken once every

three days after the initial banding. I did not collect measurements of nestlings that were younger than 12 days because feathers would not have begun to form prior to this age (Allen and Nice 1952), nor did I collect measurements of nestlings older than 22 to avoid inducing early fledging. I followed the methods outlined in Pyle (1997) to obtain measurements of wing length. Wing span was measured by extending both wings and measuring the distance between the tips of the longest primary feather on each wing (Pennycuick 2008). I calculated wing area of both wings to obtain the total wing area for each nestling (see Supplement 1). Aspect ratio (AR) was calculated using the formula (Pennycuick 2008):

$$AR = \frac{b^2}{S} \quad (3.1)$$

where b is the wing span and S is the wing area. Higher values of AR indicate longer and narrower wings, while lower values indicate shorter and stubbier wings. Wingtip pointedness (I_k) was calculated using the formula (Lockwood *et al.* 1998):

$$I_k = 100 \times \frac{\Delta S_1}{W} \quad (3.2)$$

where ΔS_1 is the distance between the tips of the longest primary feather and the longest secondary feather and W is the wing length. Higher values of I_k indicate more pointed wingtips, while lower values indicate more rounded wingtips.

On days where poor weather conditions prevented handling of nestlings (*e.g.*, storms, strong winds), measurements were taken the following day, when weather conditions permitted the handling of birds. Tarsus length was also measured (to the nearest 0.1 mm using calipers) at the time of capture, but I found inconsistent methods of taking this measurement between handlers, thus I could not use tarsus length as a measure

of body size in my study. I was also unable to determine aspect ratio of 13 day old or younger nestlings due to errors in wing area photographs.

Ectoparasite collection and identification

Purple martin nests were collected between 11 and 20 October, 2016, placed into paper bags, and were immediately transferred into Berlese-Tullgren funnels upon arriving at the lab (see Supplement 2). All materials collected from the funnels were kept in jars, preserved in 70% ethanol and stored in a refrigerator at 5°C.

Nest material collected by the Berlese-Tullgren funnels were then filtered using a 90-micron testing sieve and the contents were emptied onto a petri dish with a numbered and lettered grid. Dishes were filled with 95% ethanol and placed under a dissecting microscope, where I found and separated purple martin ectoparasites from the debris collected by the Berlese-Tullgren funnels. All ectoparasites were mounted on microscope slides (following the methods outlined in Richards 1964), sexed and identified to species (Holland 1985; Lewis and Galloway 2001). Voucher specimens of each species found in this study can be found in the Wallis/Roughley Museum in Winnipeg, Manitoba.

Data set and analyses

Forty-six purple martin nestlings were used in this study; 15 insecticide-treated, 15 sham-treated, and 16 control (untreated) nestlings. Wing length was the only measurement I was able to obtain on all occasions (*i.e.*, no missing data), but measurement errors and unusable wing area photographs prevented me from calculating wingtip pointedness or aspect ratio at three different ages for each nestling. One aberrant nest in the sham group (S3 in Table 3.1) had a high number of fleas compared to other sham nests and was not included in all analyses to prevent skewing of the results. Thus, a

total of 42 nestlings (15 insecticide-treated, 11 sham-treated, and 16 control) in 11 nests (4 insecticide-treated, 3 sham-treated, and 4 control nests) were included in all analyses.

To determine whether nest loads differed among treatment groups, I used a generalized linear model, with a negative binomial (NB) distribution. The negative binomial distribution was used to deal with overdispersion of counts in the data ($\phi = 4.17$) and was a better fit than the Poisson distribution (likelihood-ratio test: $\chi^2 = 14.32$, $P < 0.01$).

I examined growth rates of weight, wing length, wingtip pointedness, and aspect ratio of each nestling and compared growth rates between the three treatment groups (treated, sham, and control nestlings) using linear mixed-effect models (LME); all analyses were performed in R using the package “*nlme*” (Pinheiro *et al.* 2017). Measurements were collected from each individual on multiple occasions (*i.e.*, longitudinal data), so I incorporated individuals as a random effect. Thus, my models consisted of a morphometric response variable (weight, wing length, wingtip pointedness, or aspect ratio), age (centered to have a mean of 0) and treatment group as the fixed effects, and individual as a random effect. The random effect was not tested, as it was included in the models by design. Estimates for the fixed and random effects were estimated using restricted maximum likelihood (REML) estimation (Zuur *et al.* 2009). Likelihood ratio tests were performed to test the significance of each fixed factor for each full model. Assumptions of normality, heterogeneity of variance, and temporal autocorrelation were assessed visually using Q-Q plots, residual versus fitted plots, and ACF plots, respectively (Fig. B2-9) (Quinn and Keough 2002, Zuur *et al.* 2009).

3.3 Results

Ectoparasite identification

Among all nests in the study, 92% (11 out of 12) of the nests had ectoparasites found in them. In all nests collected, two species of parasitic mites (*Dermanyssus prognephilus*, *Ornithonyssus sylvarum*) one species of facultative parasite mite (*Androlaelaps casalis*), one species of flea (*Ceratophyllus idius*), and one species of chewing louse (*Myrsidea dissimilis*) were found and identified; no other parasitic species were found in the Berlese-Tullgren funnels. Fleas and mites were the most prevalent taxa of ectoparasites in the study (present in 10 out of 12 nests), while presence of lice was rare (present in only 4 nests) (Table 3.1). Adult fleas were more commonly found in the nests, comprising 79% (48 out of 62) of all fleas collected in the Berlese-Tullgren funnels, while 21% (13 out of 62) of the fleas found were still in the larval stage. However, one nest in the sham group (S3 in Table 3.1) was found to have 26 fleas (24 adult, 2 juvenile), which was excluded from the analyses. Nest loads did not differ among the three groups (likelihood ratio test: $P = 0.79$) (Fig. 3.1).

Table 3.1. Total number of ectoparasites (by species) collected from each of the 12 nests, at all study sites, at the end of the breeding season, for each treatment group. The number of young per nest (clutch size) is also provided. Each nest is identified by a letter based on the assigned treatment group (Control, Sham-treated, Insecticide-Treated), followed by a numerical code to distinguish within-group. Nests C1, T1, and S1 were from Oak Hammock Marsh (50.17°N, 97.13°W), while the rest were from the Town and Country Campground (49.83°N, 96.98°W).

Parasite	Control				Sham-treated				Insecticide-treated			
	C1	C2	C3	C4	S1	S2	S3*	S4	T1	T2	T3	T4
Clutch size	5	5	6	6	4	5	5	3	4	3	6	4
Flea (Siphonaptera)												
<i>Ceratophyllus idius</i>	2	1	1	10	1	0	26	4	3	7	0	7
Lice (Phthiraptera)												
<i>Myrsidea dissimilis</i>	0	0	0	0	2	0	0	3	0	3	0	2
Mite (Mesostigmata)												
<i>Dermanyssus prognephilus</i>	1	1	0	0	2	1	0	1	5	0	0	0
<i>Ornithonyssus sylvarium</i>	0	1	0	0	2	0	0	0	0	0	0	0
<i>Androlaelaps casalis</i>	0	2	0	2	2	0	3	3	0	3	0	2
Total load per nest	3	5	1	12	9	1	29	11	8	13	0	11
Total load per group		21				50				32		

*Nest excluded from analyses due to an abnormally high number of fleas compared to other nests of the same group.

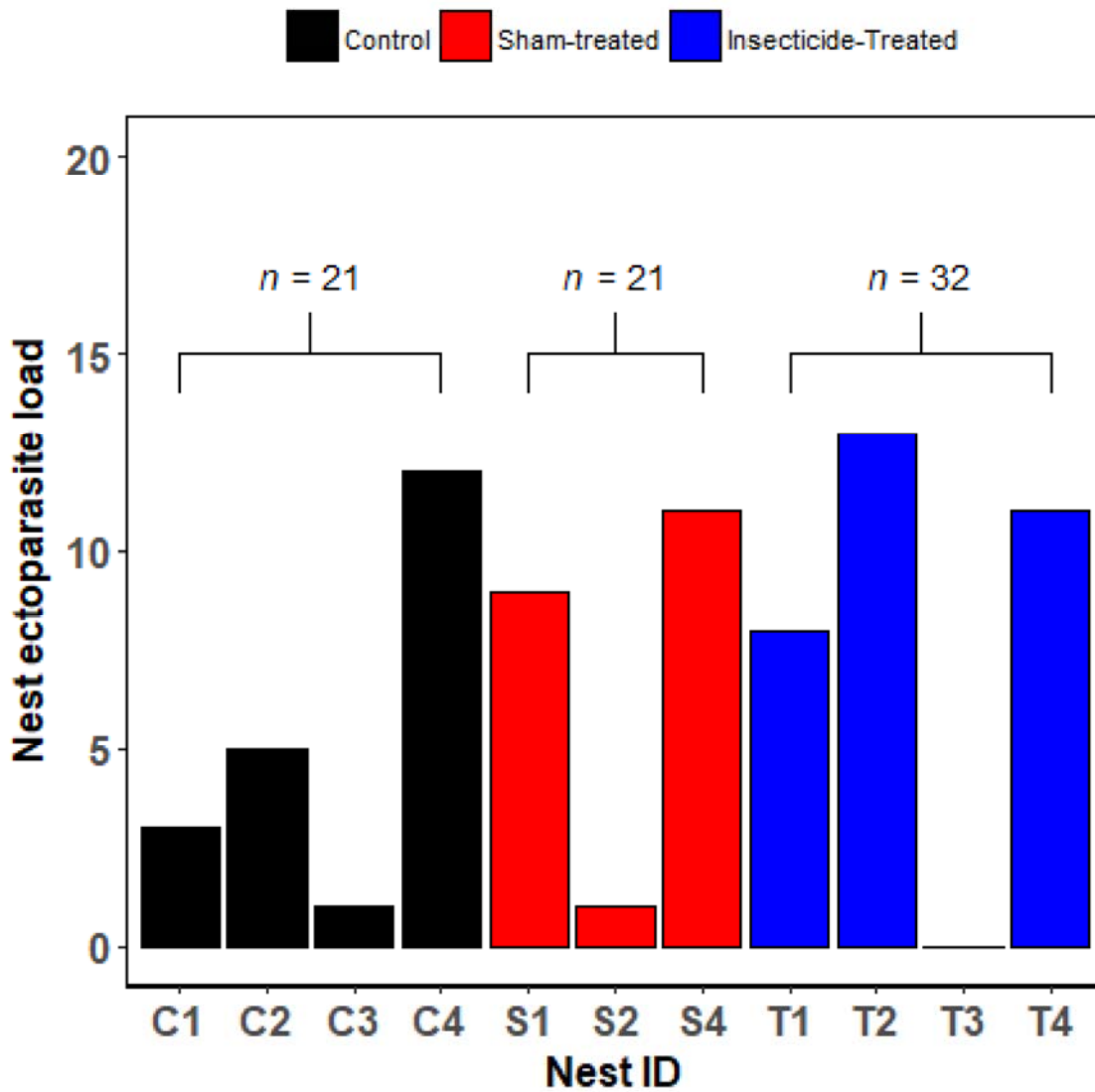


Figure 3.1. Total number of ectoparasites found in each nest. Nests were given a unique identifier (Nest ID) and assigned one of three treatment groups: no treatment (control, black), sham-treated (red), or insecticide-treated (blue). Total ectoparasite loads per treatment group are provided in the figure above each bar; see Table 3.1 for the total number of each species per group. Nest S3 (not shown) was omitted from the analysis.

Changes in weight

Changes in nestling weights were best described using a quadratic growth curve (Fig. 3.2), which can be defined by the equation (format following Nakagawa and Schielzeth (2013)):

$$W_i = \beta_0 + \beta_{1,k} \cdot \text{Group}_k + \beta_2 \cdot \text{Age} + \beta_3 \cdot \text{Age}^2 + \beta_{4,k} \cdot \text{Group}_k \cdot \text{Age} + \beta_{5,k} \cdot \text{Group}_k \cdot \text{Age}^2 + \alpha_j + \varepsilon_i \quad (3.3)$$

where for each observation i (from 1 to 126), W_i is the nestling's body weight (g); Group_k is a factor with 3 levels ($k = \{1, 2\}$, representing the treatment groups: control, sham-treated ($k = 1$), and insecticide-treated ($k = 2$)); Age and Age^2 are continuous predictors; $\text{Group}_k \cdot \text{Age}$ is the interaction between group k and age (*i.e.*, the group and age of individual j); $\text{Group}_k \cdot \text{Age}^2$ is the interaction between group k and age²; β_0 is the intercept at the mean age that body weight was measured (day 17) for the reference group (control); $\beta_{1,k}$ is the coefficient for the treatment group ($\beta_{1,k} = 0$ for the reference group); β_2 and β_3 are the linear and quadratic coefficients for age and age² of the reference group, respectively; $\beta_{4,k}$ and $\beta_{5,k}$ are the linear and quadratic coefficients, respectively, when the treatment group is not the reference group (*i.e.*, $\beta_{4,k}$ and $\beta_{5,k} = 0$ for the reference group); α_j (which follows a normal distribution with a mean of zero and variance of σ^2_α) is the random effect of individual j (from 1 to 42); and ε_i is the residual for the i^{th} observation (which follows a normal distribution with a mean of zero and a variance of σ^2_ε).

The fixed factors (*Group*, *Age*, and *Age*²) all had a significant effect on body weight (*Group*: $\chi^2 = 35.18$, $P < 0.01$; *Age*: $\chi^2 = 24.45$, $P < 0.01$; *Age*²: $\chi^2 = 21.17$, $P < 0.01$). The mean body weight of nestlings did not differ from the control group, but differences among groups occurred in the linear term, and not in the quadratic term (Table 3.2).

Table 3.2. Summary output of the results for the linear mixed effect model for nestling body weight (3.3). The estimates, standard errors, and *P* values are provided for each fixed effect at each group level (control, sham-treated, and insecticide-treated), while the standard deviation is provided for the random effect (individual); all estimates were obtained using restricted maximum likelihood (REML). Estimates of the insecticide-treated and sham-treated groups are presented relative to the reference group (control); the parameter estimates for the intercept, age, and age² represent the estimates for the control group.

Fixed effects			
Parameter	Estimate	SE	<i>P</i>
Intercept	58.11	0.87	< 0.01
Sham-treated	2.22	1.46	0.10
Insecticide-treated	-2.65	1.59	0.13
Age	0.59	0.17	< 0.01
Sham-treated	-1.40	0.27	< 0.01
Insecticide-treated	-0.88	0.28	< 0.01
Age ²	-0.21	0.05	< 0.01
Sham-treated	0.15	0.11	0.16
Insecticide-treated	-0.04	0.11	0.73
Random effect			
Parameter	SD		
Individual	2.74		

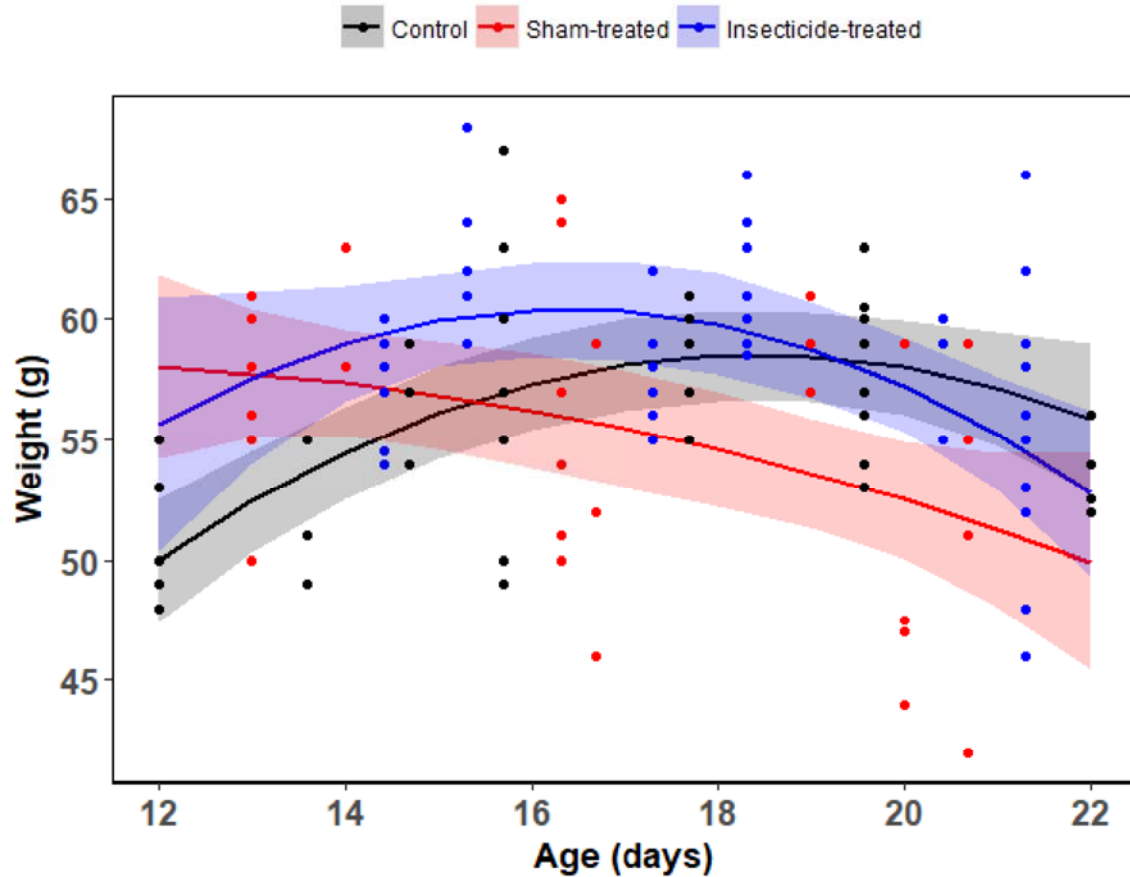


Figure 3.2. Changes in nestling body weight (g) from day 12 to day 22, across three treatment groups (control (black), sham-treated (red), insecticide-treated (blue)). The expected growth rate (predicted by the linear mixed effect model for nestling body weight (3.3)) is represented by the solid coloured lines, with the 95% confidence interval represented by the shaded area around each regression line. Weight was recorded once every three days and began when nestlings were at least 12 days old.

Wing morphometric growth

The three wing morphometric variables (wing length, wingtip pointedness, and aspect ratio) were not correlated with one another (Fig. B1). However, changes in these three

morphometries over time were best described by a linear trend (Fig. 3.3 – 3.5), defined by the equation:

$$Y_i = \beta_0 + \beta_{1,k} \cdot Group_k + \beta_2 \cdot Age + \beta_{3,k} \cdot Group_k \cdot Age + \alpha_j + \varepsilon_i \quad (3.4)$$

where for each observation i , Y_i is the value of one of the three morphometries (wing length, wingtip pointedness, or aspect ratio); $Group_k$ is a factor with 3 levels ($k = \{1,2\}$, representing the treatment groups: control, sham-treated ($k = 1$), and insecticide-treated ($k = 2$)); Age is a continuous predictor; $Group_k \cdot Age$ is the interaction between group k and age (*i.e.*, the group and age of individual j); β_0 is the intercept at the mean age that the measurements were taken (day 17 for wing length and wingtip pointedness, day 18 for aspect ratio) for the reference group (control); $\beta_{1,k}$ is the coefficient for the treatment group ($\beta_{1,k} = 0$ for the reference group); β_2 is the linear coefficient for age of the reference group; $\beta_{3,k}$ is the linear coefficient when the treatment group is not the reference group (*i.e.*, $\beta_{3,k} = 0$ for the reference group); α_j (which follows a normal distribution with a mean of zero and variance of σ_a^2) is the random effect of individual j (from 1 to 42); and ε_i is the residual for the i^{th} observation (which follows a normal distribution with a mean of zero and a variance of σ_ε^2). Due to missing data and/or outliers, the number of observations (i) varied between models ($i_{wing\ length} = 126$, $i_{wingtip\ pointedness} = 125$, $i_{aspect\ ratio} = 105$).

Wing length

Both fixed factors (*Group*, and *Age*) had a significant effect on wing length (*Group*: $\chi^2 = 19.32$, $P < 0.01$; *Age*: $\chi^2 = 324.84$, $P < 0.01$). The mean wing length of the insecticide-treated nestlings, but not the sham-treated nestlings, differed from the control group; the mean wing length of insecticide-treated nestlings at the mean age (day 17) was significantly shorter than the control nestlings (Table 3.3). Although wing length increased linearly for all three treatment

groups (Fig. 3.3), both the insecticide-treated and sham-treated groups had significantly faster growth rates than the control group (Table 3.3).

Table 3.3. Summary output of the results for the linear mixed effect model for wing length (3.4). The estimates, standard errors, and *P* values are provided for each fixed effect at each group level (control, sham-treated, and insecticide-treated), while the standard deviation is provided for the random effect (individual); all estimates were obtained using restricted maximum likelihood (REML). Estimates of the insecticide-treated and sham-treated groups are presented relative to the reference group (control); the parameter estimates for the intercept and age represent the estimates for the control group.

Fixed effects			
Parameter	Estimate	SE	<i>P</i>
Intercept	81.29	0.98	< 0.01
Sham-treated	-0.50	1.54	0.75
Insecticide-treated	-4.72	1.42	< 0.01
Age	4.41	0.16	< 0.01
Sham-treated	0.58	0.25	0.02
Insecticide-treated	0.63	0.24	0.01
Random effect			
Parameter	SD		
Individual	3.50		

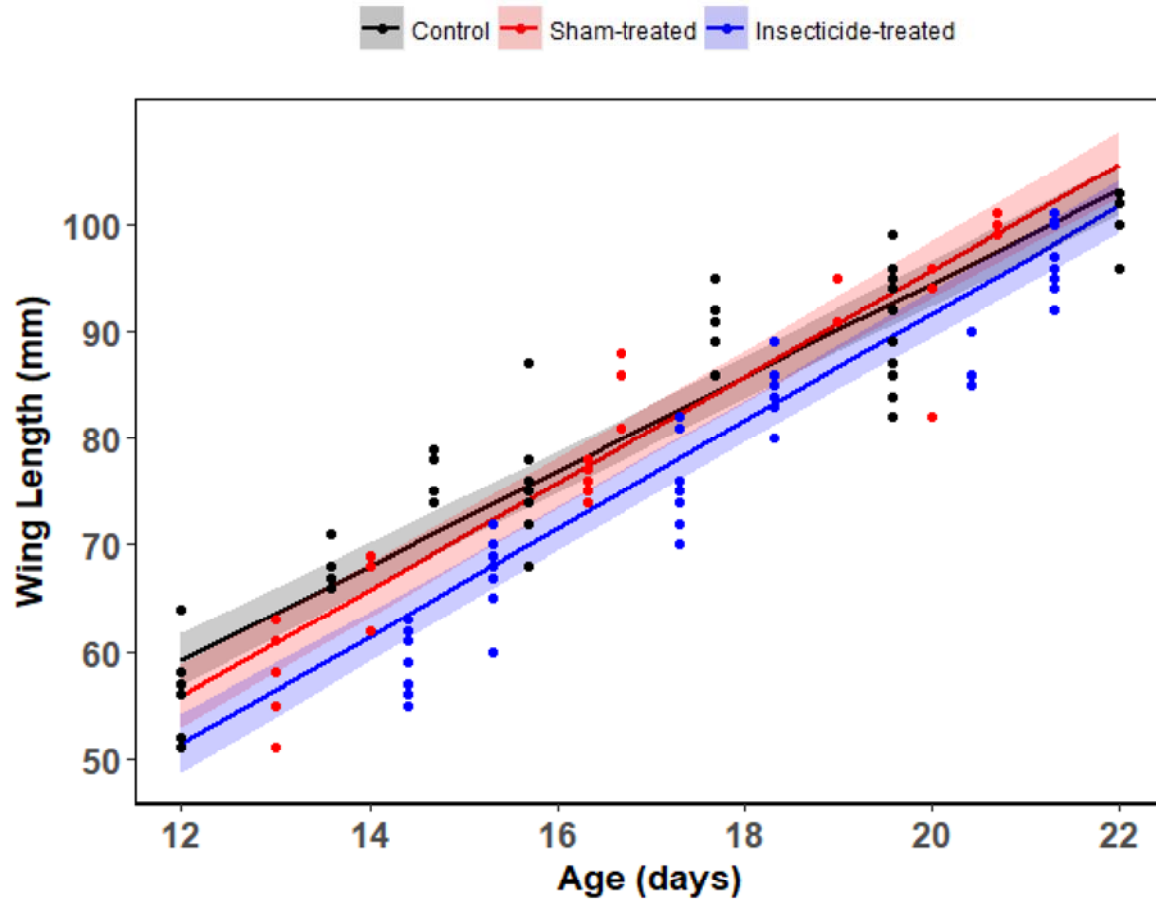


Figure 3.3. Changes in wing length (mm) from day 12 to day 22, across three treatment groups (control (black), sham-treated (red), insecticide-treated (blue)). The expected growth rate (predicted by the linear mixed effect model for wing length (3.4)) is represented by the solid coloured lines, with the 95% confidence interval represented by the shaded area around each regression line. Wing length was recorded once every three days and began when nestlings were at least 12 days old.

Wingtip pointedness

The fixed factor *Age* had a significant effect on wingtip pointedness ($\chi^2 = 12.72$, $P = 0.01$), but *Group* was not a significant predictor of wingtip pointedness ($\chi^2 = 7.34$, $P = 0.12$). The

mean wingtip pointedness of the sham-treated nestlings, but not the insecticide-treated nestlings, differed from the control group; the mean wingtip pointedness value of sham-treated nestlings at the mean age (day 17) was significantly higher than the control nestlings (Table 3.4). Although the change in wingtip pointedness was best described using age as a linear term (Fig. 3.4), there were no group differences in the linear term (Table 3.4).

Table 3.4. Summary output of the results for the linear mixed effect model for wingtip pointedness (3.4). The estimates, standard errors, and *P* values are provided for each fixed effect at each group level (control, sham-treated, and insecticide-treated), while the standard deviation is provided for the random effect (individual); all estimates were obtained using restricted maximum likelihood (REML). Estimates of the insecticide-treated and sham-treated groups are presented relative to the reference group (control); the parameter estimates for the intercept and age represent the estimates for the control group.

Fixed effects			
Parameter	Estimate	SE	<i>P</i>
Intercept	23.56	0.40	< 0.01
Sham-treated	1.48	0.63	0.02
Insecticide-treated	1.00	0.58	0.09
Age	0.35	0.12	< 0.01
Sham-treated	-0.16	0.19	0.41
Insecticide-treated	-0.12	0.19	0.53
Random effect			
Parameter	SD		
Individual	0.70		

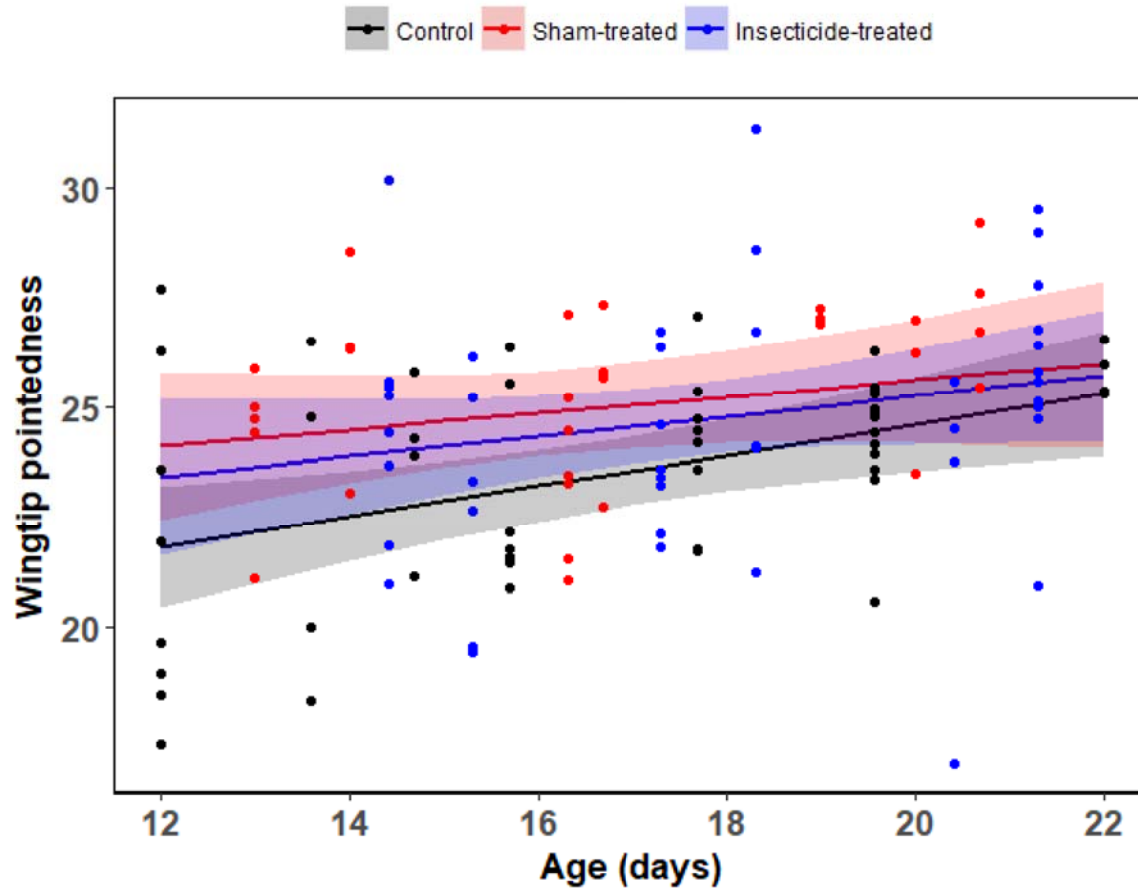


Figure 3.4. Changes in wingtip pointedness from day 12 to day 22, across three treatment groups (control (black), sham-treated (red), insecticide-treated (blue)). The expected growth rate (predicted by the linear mixed effect model for wingtip pointedness (3.4)) is represented by the solid coloured lines, with the 95% confidence interval represented by the shaded area around each regression line. Metrics used to calculate wingtip pointedness were recorded once every three days and began when nestlings were at least 12 days old.

Aspect ratio

Similar to the wing length model, both factors (*Group*, and *Age*) had a significant effect on aspect ratio (*Group*: $\chi^2 = 28.10$, $P < 0.01$; *Age*: $\chi^2 = 25.58$, $P < 0.01$). The mean aspect ratio

values of the sham-treated and insecticide-treated nestlings were significantly lower than the control group (Table 3.5). Unlike the other wing morphometries, aspect ratio decreased over time (Fig. 3.5), but the insecticide-treated nestlings, and not the sham-treated nestlings, had a significantly slower decrease in aspect ratio (Table 3.5).

Table 3.5. Summary output of the results for the linear mixed effect model for aspect ratio (3.4). The estimates, standard errors, and *P* values are provided for each fixed effect at each group level (control, sham-treated, and insecticide-treated), while the standard deviation is provided for the random effect (individual); all estimates were obtained using restricted maximum likelihood (REML). Estimates of the insecticide-treated and sham-treated groups are presented relative to the reference group (control); the parameter estimates for the intercept and age represent the estimates for the control group.

Fixed effects			
Parameter	Estimate	SE	<i>P</i>
Intercept	5.94	0.05	< 0.01
Sham-treated	-0.19	0.08	0.03
Insecticide-treated	-0.30	0.07	< 0.01
Age	-0.09	0.02	< 0.01
Sham-treated	0.05	0.02	0.06
Insecticide-treated	0.08	0.02	< 0.01
Random effect			
Parameter	SD		
Individual			

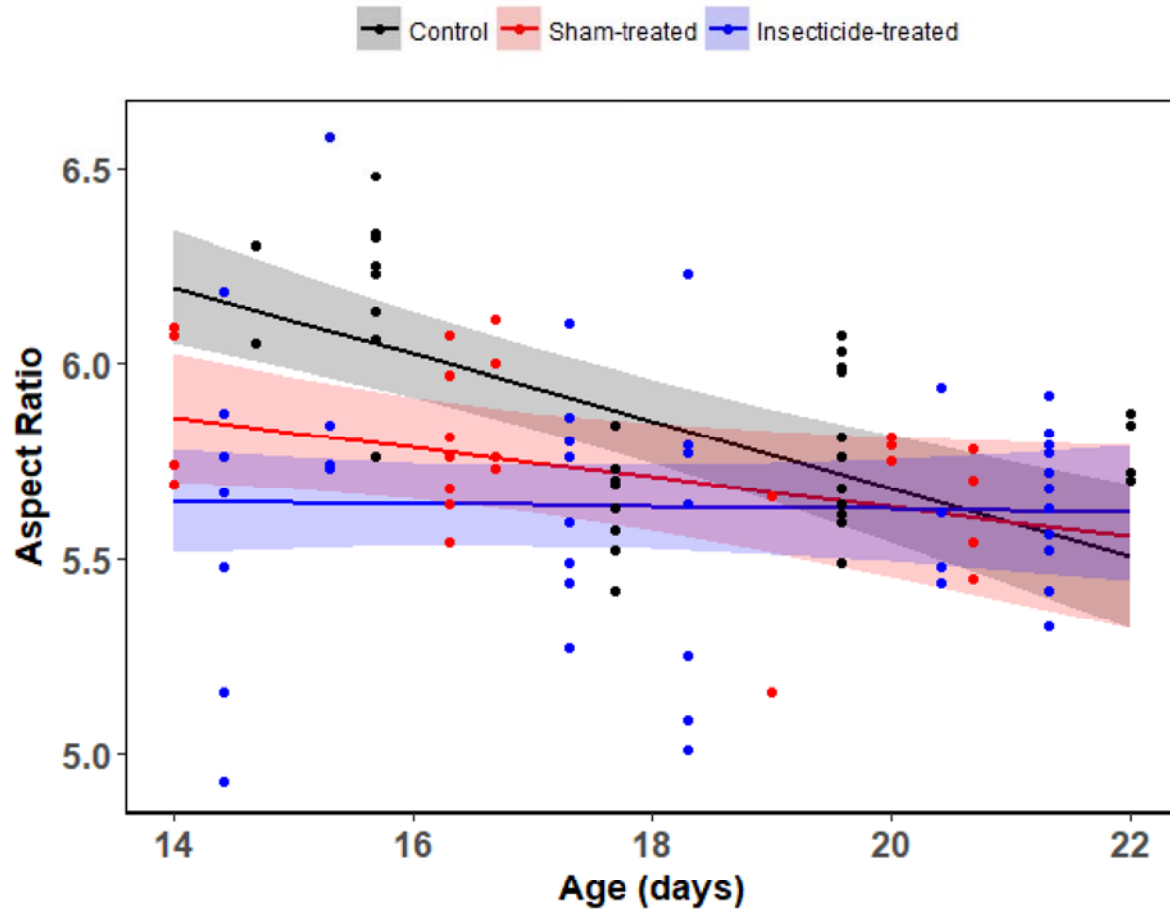


Figure 3.5. Changes in aspect ratio from day 14 to day 22, across three treatment groups (control (black), sham-treated (red), insecticide-treated (blue)). The expected growth rate (predicted by the linear mixed effect model for aspect ratio (3.4)) is represented by the solid coloured lines, with the 95% confidence interval represented by the shaded area around each regression line. Metrics used to calculate aspect ratio were recorded once every three days and began when nestlings were at least 12 days old, but aspect ratio could not be reliably determined for nestlings younger than 14 days.

3.4 Discussion

By experimentally manipulating nest conditions to reduce parasitism in nest boxes, I found that wing morphometry of nestlings reared in insecticide-treated nests differed from nestlings reared in natural nest boxes (*i.e.*, untreated nests). Although I did not find any differences in nest ectoparasite loads between the different treatment groups, control nestlings had longer and higher aspect ratio wings at an earlier age compared to insecticide-treated nestlings. However, due to varying growth rates across treatment groups, control and insecticide-treated nestlings had similar wing morphometry nearing the fledging age (approx. 27 days (Allen and Nice 1952)). This study suggests purple martins exhibit greater variation in wing morphometry earlier as nestlings, but have similar wing morphometry nearing fledge.

Nest ectoparasites

Among the nests that were collected, fleas (*Ceratophyllus idius*) were the most abundant ectoparasite found in the 12 nests, while lice were rare. Fleas spend a large portion of their life cycle in the host's nest, with the larval stage feeding on the detritus in the nest and the adults feeding on the blood of the hosts (Rothschild and Clay 1957, Marshall 1981), which may explain their abundance in the nests. Conversely, most lice (*e.g.*, chewing lice (Phthiraptera)) complete their life cycle on the skin/feathers of the host, thus are rarely found in the nest material (Crompton 1997); my finding of lice in the nests may have been a result of them falling off the hosts, siblings, or the parents prior to fledging. The majority of the fleas were adults, despite the nests being collected weeks after the nestlings fledged. Adult fleas disperse shortly after their hosts leave the nest, while larvae remain in the deserted nest to complete larval development and the teneral adults remain in the cocoons until next spring (Humphries 1968, Tripet and Richner 1997). The abundance of adult fleas relative to the number of larvae in the nests may have been a

result of anthropogenic disturbances triggering the emergence of fleas from the cocoons. Fleas pupate in response to rises in temperatures as well as mechanical disturbances (Humphries 1968), which may have been triggered by the heat source of the Berlese-Tullgren funnels and movement of the nest during the collection process.

Despite treating nests with an insecticide to prevent or reduce the presence of ectoparasites in the nest, ectoparasite loads did not differ among the three treatment groups. The nests built by the adult purple martins were composed of vegetation bound tightly together by mud that prevented the insecticide from being distributed throughout the nest material, thus, ectoparasites inhabiting the stratum between the top and bottom of the nests may have been unaffected by the insecticide. Pyrethroid-based insecticides have long-lasting residuals and are not easily washed off, especially in the absence of sunlight (Collison *et al.* 1981, WHO 1990), but nest materials that are brought into the nest or old nest material that is taken out by the adult purple martins after fumigation (*e.g.*, mud) may have reduced the effects of the insecticide. Additionally, some ectoparasites, such as mites and fleas, may have been introduced into the nests after fumigation (Marshall 1981, Proctor and Owens 2000) by using adult purple martins as a vector of transport, or transferred directly from an adjacent nest cavity. The exact date at which the host purple martin departed on fall migration (*i.e.*, left the breeding site) is unknown, but the period between the onset of fall migration and the time at which the nests were collected may have influenced the results. That is, ectoparasite loads may have changed after the purple martin breeding season, and thus the observed ectoparasite loads may not reflect the intensity of ectoparasites during the nestling's growth period. Collecting live ectoparasites from the nestlings and parents using methods such as dust ruffling, as well as using methods that can collect both live and dead parasites from the nest materials, such as nest washing (Clayton and Walther 1997),

would be beneficial and recommended for future studies aiming to estimate ectoparasite abundance and intensity in nests.

Overall, ectoparasite loads in this study were low relative to other studies using Berlese-Tullgren funnels (Merino and Potti 1995, Merilä and Allander 1995, Pacejka et al. 1998), where nests would on average contain over 100 parasitic species. There are no records of ectoparasite loads at the sites used in this study, so the low ectoparasite loads may indicate that ectoparasite abundances were low during the time that the study took place or that nests at these locations do not have high ectoparasite loads year-round. Moreover, there are no records that the nest cavities were cleaned prior to the start of the experiment nor are there any records that the nest cavities are maintained every year. Continual examination of ectoparasite loads at these study sites would allow us to determine whether the low ectoparasite loads are a result of an anomalous year for ectoparasites.

Differences in weight over time

The change in weight was best described as a quadratic curve, where weight increased starting at day 12 but began to decrease around day 17, similar to results from previous studies (Tarof and Brown 2013). The reduction in body weight before fledging may reflect weight recession (Edson 1930), which is weight loss associated with evaporative water loss from feathers (Ricklefs 1968), or fasting to decrease wing loading allowing individuals to fledge (Sprague and Breuner 2010).

Although the rate of change in body weight varied between nestlings in the study, the initial weight (at day 12) of control nestlings differed from sham-treated nestlings, but not from insecticide-treated nestlings. However, there was a greater overlap of weight among all nestlings in the study at day 22; that is, there was no strong evidence for any differences in body weight

among groups. Body weight is affected by the quantity and quality of the food received by the nestlings, as well as the rate at which nestlings were fed (*i.e.*, parental effort). Periods where food was more abundant could improve foraging success and efficiency, allowing the parents to feed their young more frequently throughout the day resulting in heavier nestlings (Naef-Daenzer and Keller 1999, Tremblay *et al.* 2003). Conversely, when food is scarce, nestlings would be fed less frequently throughout the day, resulting in a lower body mass. For aerial insectivores like purple martins, the amount of prey (food) throughout the breeding season tends to fluctuate but the abundance of aerial insects tends to peak during early July and decline mid to late July (Grüebler and Naef-Daenzer 2008, Dunn *et al.* 2011, Bastien *et al.* 2013). In my study, weights for control nestlings were taken from 14 July to 28 July, 2016, while insecticide-treated and sham-treated nestlings had measurements taken from 5 July to 19 July, 2016. If food was less abundant in the later period of the purple martin breeding season during the year of this study, then control nestlings may have weighed less than other nestlings in the study at day 12. Additionally, more individuals in the nest (*i.e.*, siblings) may increase competition for food, affecting the weight of the nestlings. In a study on barn swallows (*Hirundo rustica*), nestlings from larger broods received less food per visit by the parents and ultimately weighed less than nestlings from smaller broods (Saino *et al.* 1997). In my study, I was unable to account for clutch size due to clutch size being confounded with treatment group (*i.e.*, there were no control nests with less than 5 nestling).

Morphometric growth rates

Control nestlings possessed longer wings at a younger age than all other nestlings in the study, but grew at a slower rate. However, all nestlings in the study exhibited similar wing lengths at day 22, suggesting that all nestlings may fledge with a similar wing length. In order for

birds to fledge successfully, wings must meet physical requirements for flight (*e.g.*, being able to generate enough lift and thrust) (Pennycuik 1975). Wings must be long enough for an individual to generate enough thrust to propel themselves forward in flight (Pennycuik 1975; 2008). Nestlings with shorter wings at an earlier age may allocate more energy towards growth, causing an accelerated growth rate in wing length to meet the requirements for fledging (Saino *et al.* 1998). However, spending more energy/resources on body growth may result in less energy available for development of other important traits, such as an immune system against diseases (Szép and Møller 1999). Trade-offs between body growth and immune system development has been observed in barn swallows (*Hirundo rustica*; Saino *et al.* 1998), sand martins (*Riparia riparia*; Szép and Møller 1999), and magpies (*Pica pica*; Soler *et al.* 2003).

I found that all nestlings had similar values and growth rates of wingtip pointedness. This study marks the first time that changes in wingtip pointedness have been monitored in nestlings throughout development. Although wingtip pointedness does not have an ecomorphological function in flight at this stage of development (as nestlings are unable to fly), the novel discovery that wingtip pointedness increased over time provides insight on feather growth and development during the nestling stage. An increase in wingtip pointedness suggests the primary feathers grow at a faster rate than the secondary feathers (*i.e.*, wings become more pointed), while a decrease suggests faster growth of the secondary feathers relative to the primary feathers (*i.e.*, wings become more rounded) and no change in wingtip pointedness may indicate equal growth rates of the primary and secondary feathers. Thus, my study suggests the primary feathers grow at a faster rate than the secondary feathers, resulting in pointed wingtips upon fledging.

Control nestlings had the highest aspect ratio wings among all nestlings in the study at age 14, but exhibited the steepest rate of decline in aspect ratio. Aspect ratio is a ratio of

wingspan to wing area, so changes in aspect ratio over time may be used to infer changes in wingspan relative to wing area. The decreasing trend in aspect ratio for control and sham-treated nestlings suggest wing area increases at a faster rate than wingspan resulting in lower aspect ratio wings upon fledging. Although a higher aspect ratio is preferred for long-distance migrants (a higher aspect ratio reduces wingtip vortices allowing birds to sustain flight over longer distances), a lower aspect ratio may be required for nestlings to fledge; lower aspect ratio wing have a higher surface area allowing birds to generate enough force (lift) to take off from the nest (Pennycuick 1975; 2008). Only nestlings that were treated with the insecticide did not show a linear change in aspect ratio, retaining the same aspect ratio throughout development. As aspect ratio could not be calculated before day 14, it is possible that insecticide-treated nestlings also exhibited a decrease in aspect ratio, similar to the other nestlings, but this decrease may have occurred earlier in development (*i.e.*, before day 14).

Despite ectoparasite loads being similar among the nests in the study, other forms of parasitism, specifically internal parasites, may have influenced individual growth rates. Endoparasites (*i.e.*, organisms that parasitize their host from within the body) are commonly reported in birds and purple martins are no exception. One of the most common endoparasite found in purple martins is *Haemoproteus prognei* (Davidar and Morton 1993; 2006, Wagner and Morton 1997), a haematozoan suspected to be transmitted by hippoboscids flies (Bennett 1960). Davidar and Morton (1993) found *H. prognei* was less prevalent in second year birds than after-second year birds, which they posit was because infections of *H. prognei* are more virulent in younger birds than older birds, perhaps due to a weaker/less developed immune system in younger birds (Christe *et al.* 1998). Thus, despite *H. prognei* being one of the most reported endoparasite found in purple martins, I do not suspect that this parasitic species was present in

the nestlings during the time of the study. Moreover, autopsies have revealed the presence of nematodes (*e.g.*, *Diplotrriaena obtusa*) and trematodes (*e.g.*, *Plagiorchis maculosus*) in the stomach of purple martins (Webster 1959), but the effects of these parasites on their host has yet been reported. Nonetheless, most examinations of endoparasites in swallows and other songbirds focus on adults; future research should consider the effects of endoparasites on nestlings to determine whether endoparasites affect nestling growth.

Conclusion

Wing morphology is an important intrinsic property for flight, so stunted or abnormal growth may lead to underdeveloped wings, reducing flight efficiency. It is therefore important to consider how wing shape and size changes in nestlings, to identify whether intraspecific variation in wing morphology can be attributed to differences in growth as nestlings. Previous studies examined growth patterns of wing length in other species, but I present the first study to observe changes in wingtip pointedness and aspect ratio from the onset of feather development to fledging. Although wings do not serve much function for nestlings as they do for adults, wing morphometry is important for birds to fledge (Pennycuick 1975). If individuals do not meet morphological requirements for fledging, they may remain in the nest to continue growth until they meet the requirements, delaying fledging as a consequence, which may affect migration performance (Sprague and Breuner 2010).

Purple martins, like other cavity-nesting migratory birds, may reuse previously occupied nests the following year (Tarof and Brown 2013). Poor maintenance of purple martin houses can result in a buildup of ectoparasites causing martins to avoid nesting in these houses or rear offspring in heavily parasitized nests (Hill 1994). As this study demonstrates, the application of a pyrethroid-based insecticide may not fully prevent ectoparasites from inhabiting a nest, even after

the host leaves. Although there was a lack of support that ectoparasite loads affect nestling wing growth, the presence and abundance of ectoparasites in the nest may affect nestling behaviour (*e.g.*, increased stress, lower immune system defense) that could impact future life-history traits. It is therefore important to continue studying the interaction between parasites and their nestling hosts to better understand how ecological interactions in the nest can impact birds after fledging.

3.5 References

- Allen, R.W., and Nice, M.M. 1952. A study of the breeding biology of the purple martin (*Progne subis*). *Am. Midl. Nat.* **47**(3): 606–665.
- Bastien, S., Paquette, R., Garant, D., Pelletier, F., and Lisle, M.B. 2013. Seasonal patterns in tree swallow prey (Diptera) abundance are affected by agricultural intensification. *Ecol. Appl.* **23**(1): 122–133.
- Bennett, G.F. 1960. On some ornithophilic blood-sucking Diptera in Algonquin Park, Ontario, Canada. *Can. J. Zool.* **38**(2): 377–389.
- Bennett, G.F., and Whitworth, T. 1991. Studies on the life history of some species of *Protocalliphora* (Diptera: Calliphoridae). *Can. J. Zool.* **69**(8): 2048–2058.
- Bennett, G.F., and Whitworth, T. 1992. Host, nest, and ecological relationships of species of *Protocalliphora* (Diptera: Calliphoridae). *Can. J. Zool.* **70**(1): 51–61.
- Chapman, B.R. and George, J.E., 1991. The effects of ectoparasites on cliff swallow growth and survival. *In* Bird-parasite interactions. *Edited by* Loye, J.E., and Zuk, M. Oxford Univ. Press, Oxford. pp. 69-92.

- Christe, P., Møller, A.P., and Lope, F. de. 1998. Immunocompetence and nestling survival in the house martin: the tasty chick hypothesis. *Oikos*. **83**(1): 175–179.
- Christe, P., Møller, A.P., Saino, N., and De Lope, F. 2000. Genetic and environmental components of phenotypic variation in immune response and body size of a colonial bird, *Delichon urbica* (the house martin). *Heredity*. **85**(1): 75–83.
- Clayton, D. H. 1991. Coevolution of avian grooming and ectoparasite avoidance. *In* Bird-parasite interactions. *Edited by* J. E. Loye, & M. Zuk (Eds.) Oxford University Press; Ornithology Series, 2. pp. 258-289.
- Clayton, D.H, and Walther, B.A. 1997. Collection and quantification of arthropod parasites of birds. *In* Host-parasite evolution: general principles and avian models. Oxford Univ. Press, Oxford. pp. 419–440.
- Collison, C.H., Danka, R.G., and Kennell, D.R. 1981. An evaluation of permethrin, carbaryl, and amitraz for the control of northern fowl mites on caged chickens. *Poult. Sci.* **60**(8): 1812–1817.
- Coutant, A. 1915. The habits, life history, and structure of a blood-sucking muscid larva (*Protocalliphora azurea*). *J. Parasitol.* **1**(3): 135–150.
- Crompton, D. 1997. Birds as habitat for parasites. *In* Host–parasite evolution: general principles and avian models. Oxford University Press. pp. 252–270.
- Davidar, P., and Morton, E.S. 1993. Living with parasites: prevalence of a blood parasite and its effect on survivorship in the purple martin. *Auk*. **110**(1): 109–116.

- Davidar, P., and Morton, E.S. 2006. Are multiple infections more severe for purple martins (*Progne subis*) than single infections? *Auk*. **123**(1): 141–147.
- De Steven, D. 1980. Clutch size, breeding success, and parental survival in tree swallow (*Iridoprocne bicolor*). *Evolution* (N. Y). **34**(2): 278–291.
- Dunn, P.O., Winkler, D.W., Whittingham, L.A., Hannon, S.J., and Robertson, R.J. 2011. A test of the mismatch hypothesis: How is timing of reproduction related to food abundance in an aerial insectivore? *Ecology* **92**(2): 450–461.
- Edson, J. 1930. Recession in weight of nestling birds. *Condor*. **32**(3): 137–141.
- Ewald, P.W. 1983. Host-parasite relations, vectors, and the evolution of disease severity. *Annual Review of Ecology and Systematics*. **14**(1): 465–485.
- Grüebler, M.U., and Naef-Daenzer, B. 2008. Fitness consequences of pre- and post-fledging timing decisions in a double-brooded passerine. *Ecology*. **89**(10): 2736–2745.
- Harriman, V.B., Dawson, R.D., Clark, R.G., Fairhurst, G.D., and Bortolotti, G.R. 2013. Effects of ectoparasites on seasonal variation in quality of nestling tree swallows (*Tachycineta bicolor*). *Can. J. Zool.* **92**(2): 87–96.
- Heeb, P., Kölliker, M., and Richner, H. 2000. Bird-ectoparasite interactions, nest humidity, and ectoparasite community structure. *Ecology*. **81**(4): 958–968.
- Hill III, J.R., 1994. What's bugging your birds? An introduction to the ectoparasites of purple martins. *Purple Martin Update*. **5**:1-7.

- Hill JR. 1999. How to use the baby photos and prognosticator to determine if your martin nestlings have fledged. *Purple Martin Update*. **9**(1): 2-4.
- Hill, III, J.R. 2002. Banding purple martins. *Purple Martin Update*. **11**(3): 2-7.
- Hopla, C.E., Durden, L.A., and Keirans, J.E. 1994. Ectoparasites and classification. *Rev. Sci. Tech.* **13**(4): 985-1017.
- Humphries, D. 1968. The host-finding behaviour of the hen flea, *Ceratophyllus gallinae* (Schrank) (Siphonaptera). *Parasitology*. **58**(2): 403-414.
- Johnson, S.L., and Albrecht, D.J. 1993. Effects of haematophagous ectoparasites on nestling house wrens, *Troglodytes aedon*: who pays the cost of parasitism? *Oikos* **66**(2): 255-262.
- Kunz, C., and Ekman, J. 2000. Genetic and environmental components of growth in nestling blue tits (*Parus caeruleus*). *J. Evol. Biol.* **13**(2): 199-212.
- Lockwood, R., Swaddle, J.P., and Rayner, J.M. V. 1998. Avian wingtip shape reconsidered: wingtip shape indices and morphological adaptations to migration. *J. Avian Biol.* **29**(3): 273-292.
- Marshall, A.G. 1981. The ecology of ectoparasitic insects. Academic Press, London, NY.
- Merilä, J., and Allander, K. 2010. Do great tits (*Parus major*) prefer ectoparasite-free roost sites? an experiment. *Ethology*. **99**(1-2): 53-60.
- Merino, S., and Potti, J. 1995. Mites and blowflies decrease growth and survival in nestling pied flycatchers. *Oikos*. **19**(2): 107-113.

- Moyer, B.R., Drown, D.M., Clayton, D.H., Moyer, B.R., Drown, D.M., and Clayton, D.H. 2002. Low humidity reduces ectoparasite pressure: implications for host life history evolution. *Oikos*. **97**(2): 223–228.
- Naef-Daenzer, B., and Keller, L.F. 1999. The foraging performance of great and blue tits (*Parus major* and *P. caeruleus*) in relation to caterpillar development, and its consequences for nestling growth and fledging weight. *J. Anim. Ecol.* **68**(4): 708–718.
- Pacejka, A.J., Gratton, C.M., and Thompson, C.F. 1998. Do potentially virulent mites affect house wren (*Troglodytes aedon*) reproductive success? *Ecology*. **79**(5): 1797–1806.
- Pennycuik, C.J. 1969. The mechanics of bird migration. *Ibis*. **111**(4): 525–556.
- Pinheiro, J., Bates, D., DebRoy, S., Sarkar, D., Heisterkamp, S., Van Willigen, B. and Maintainer, R., 2017. Package ‘nlme’. Linear and nonlinear mixed effects models, version. pp. 3-1.
- Proctor, H., and Owens, I. 2000. Mites and birds: diversity, parasitism and coevolution. *Trends Ecol. Evol.* **15**(9): 358–364.
- Pyle, P. 1997. Identification guide to North American birds. Part I. Braun-Brumfield Inc., Bolinas, California.
- Quinn, G.P., and Keough, M.J. 2002. Experimental design and data analysis for biologists. Cambridge University Press.

- Richards, W.R. 1964. A short method for making balsam mounts of aphids and scale insects. *Can. Entomol.* **96**(7): 963–966.
- Richner, H., and Heeb, P. 1995. Are clutch and brood size patterns in birds shaped by ectoparasites? *Oikos*. **73**(3): 435–441.
- Ricklefs, R. 1968. Weight recession in nestling birds. *Auk* **85**(1): 30–35.
- Saino, N., Calza, S., and Møller, A.P. 1998. Effects of a dipteran ectoparasite on immune response and growth trade-offs in barn swallow, *Hirundo rustica*, nestlings. *Oikos*. **81**(2): 217–228.
- Saino, N., Calza, S., and Møller, A.P. 1998. Effects of a dipteran ectoparasite on immune response and growth trade-offs in barn swallow, *Hirundo rustica*, nestlings. *Oikos* **81**(2): 217–228.
- Saunders, J.W. 1948. The proximo-distal sequence of origin of the parts of the chick wing and the role of the ectoderm. *J. Exp. Zool.* **108**(3): 363–403.
- Shek, D.T.L., and Ma, C.M.S. 2011. Longitudinal data analyses using linear mixed models in SPSS: concepts, procedures and illustrations. *Scientific World Journal* **11**: 42–76.
- Singh, H., Nivsarkar, A.E., and Suman, C. 1991. Growth curve analyses and genetic parameters of body weight in indigenous guineafowl. *Indian J. Poult. Sci.* **26**(1): 20–25.
- Soler, J.J., Neve, L. de, Pérez-Contreras, T., Soler, M., and Sorci, G. 2003. Trade-off between immunocompetence and growth in magpies: an experimental study. *Proc. R. Soc. London B Biol. Sci.* **270**(1512): 241–248.

- Sprague, R.S., and Breuner, C.W. 2010. Timing of fledging is influenced by glucocorticoid physiology in Laysan Albatross chicks. *Horm. Behav.* **58**(2): 297–305.
- Szép, T.P., and Møller, A.P. 1999. Cost of parasitism and host immune defence in the sand martin *Riparia riparia*: a role for parent-offspring conflict? *Oecologia* **119**(1): 9–15.
- Tremblay, I., Thomas, D.W., Lambrechts, M.M., Blondel, J., and Perret, P. 2003. Variation in blue tit breeding performance across gradients in habitat richness. *Ecology*. **84**(11): 3033–3043.
- Tripet, F., and Richner, A. 1997. The coevolutionary potential of a “generalist” parasite, the hen flea *Ceratophyllus gallinae*. *Parasitology*. **115**(4): 419–427.
- Tschirren, B., Bischoff, L.L., Saladin, V., and Richner, H. 2007. Host condition and host immunity affect parasite fitness in a bird-ectoparasite system. *Funct. Ecol.* **21**(2): 372–378.
- Venables, W. N., and Ripley, B. D. 2002. Modern applied statistics with s. fourth edition. Springer, New York.
- Wagner, R.H., Davidar, P., Ali, S., Schug, M.D., and Morton, E.S. 1997. Do blood parasites affect paternity, provisioning and mate-guarding in purple martins? *Condor*. **99**(2): 520–523.
- WHO 1990a. Permethrin. Environmental Health Criteria no. 94. World Health Organization, Geneva, Switzerland.
- Zuur, A., Ieno, E.N., Walker, N., Saveliev, A.A., and Smith, G.M. 2009. Mixed effects models and extensions in ecology with R. Springer Science & Business Media.

Chapter 4: Thesis Conclusion

Despite the fact that numerous studies have been conducted on the ecomorphology and development of the avian wing, there is still much that is unclear. My thesis covers some of these knowledge gaps, furthering our understanding of avian wing morphology. The importance of wing morphology in migration has been outlined in numerous theoretical studies based on optimal migration theory but, as I have demonstrated (Chapter 2), wing morphological parameters had a weaker influence on migration performance than departure timing in a long-distance migratory songbird. Additionally, I show that temperature influenced stopover duration on spring migration, implying that stopover decisions can be impacted by environmental conditions. Ongoing global climate change is expected to continue (Intergovernmental Panel on Climate Change 2014), which is expected to advance spring phenology, forcing birds to adjust their migration timing to match arrival to capitalize on peak food abundance (Jonzén *et al.* 2006, Møller *et al.* 2008, Schmaljohann *et al.* 2017). If birds are unable to adjust their timing, they may not be able to arrive and breed under optimal conditions, leading to reduced reproductive fitness. My results (Chapter 2) imply that late-departing spring migrants follow a time-selected migration strategy, which may allow them to avoid arriving in suboptimal conditions, but whether this trend is consistent from year-to-year is unknown. Further research towards the mechanisms controlling timing of migration events in birds is required to better understand the impact of climate change on migration.

Prior to my study (Chapter 3), changes in wing morphology over time in nestlings could only be inferred through changes in wing length, which only explains changes in allometric size. I show for the first time that changes in wingtip pointedness increase over time, while aspect ratio decreased. The differences in morphometry among nestlings may have been the result of some

nestlings allocating more energy towards structural wing and feather growth, causing faster growth rates. However, the amount of energy that can be used for growth and development ultimately depends on the amount of food they receive from the parents, and energy may also be allocated to other functions, such as thermoregulation or immunocompetence (Saino *et al.* 1998), reducing growth rates.

Overall, I have shown that changes in wing morphology throughout the nestling growth period can differ between nests of the same colony (*i.e.*, at the same site), but the resulting morphology among all nestlings may be similar upon fledging, which may lead to low morphometric variation as adults. If different populations of the same species have similar wing morphometric values, then their performance on spring migration (relative to conspecifics of the same population) may be better predicted by other factors, such as migration timing or environmental factors. Evolutionary forces are thought to have driven the development of wings to become adapted for travelling long-distance in a short amount of time in migratory birds. As such, selection may force growth and development of the wings to conform to a shape and size that is adapted for high-speed flight resulting in low morphometric variation within species. Interspecific comparisons of wing morphology across multiple migratory species may reveal whether endogenous and/or exogenous factors still exert a greater influence over wing morphology or if morphometric parameters are the dominant predictors of migration performance.

References

Intergovernmental Panel on Climate Change, 2014. Climate Change 2014—impacts, adaptation and vulnerability: regional aspects. Cambridge University Press.

Jonzén, N., Lindén, A., Ergon, T., Knudsen, E., Vik, J.O., Rubolini, D., Piacentini, D., Brinch, C., Spina, F., Karlsson, L., Stervander, M., Andersson, A., Waldenströ, J., Lehikoinen, A., Edvardsen, E., Solvang, R., and Stenseth, N.C. 2006. Rapid advance of spring arrival dates in long-distance migratory birds. *Science*. **312**(5782): 1959–1961.

Møller, A.P., Rubolini, D., and Lehikoinen, E. 2008. Populations of migratory bird species that did not show a phenological response to climate change are declining. *Proc. Natl. Acad. Sci.* **105**(42): 16195–16200.

Saino, N., Calza, S., and Møller, A.P. 1998. Effects of a dipteran ectoparasite on immune response and growth trade-offs in barn swallow, *Hirundo rustica*, nestlings. *Oikos* **81**(2): 217–228.

Schmaljohann, H., Lisovski, S., and Bairlein, F. 2017. Flexible reaction norms to environmental variables along the migration route and the significance of stopover duration for total speed of migration in a songbird migrant. *Front. Zool.* **14**(17): 1–16.

Appendix A

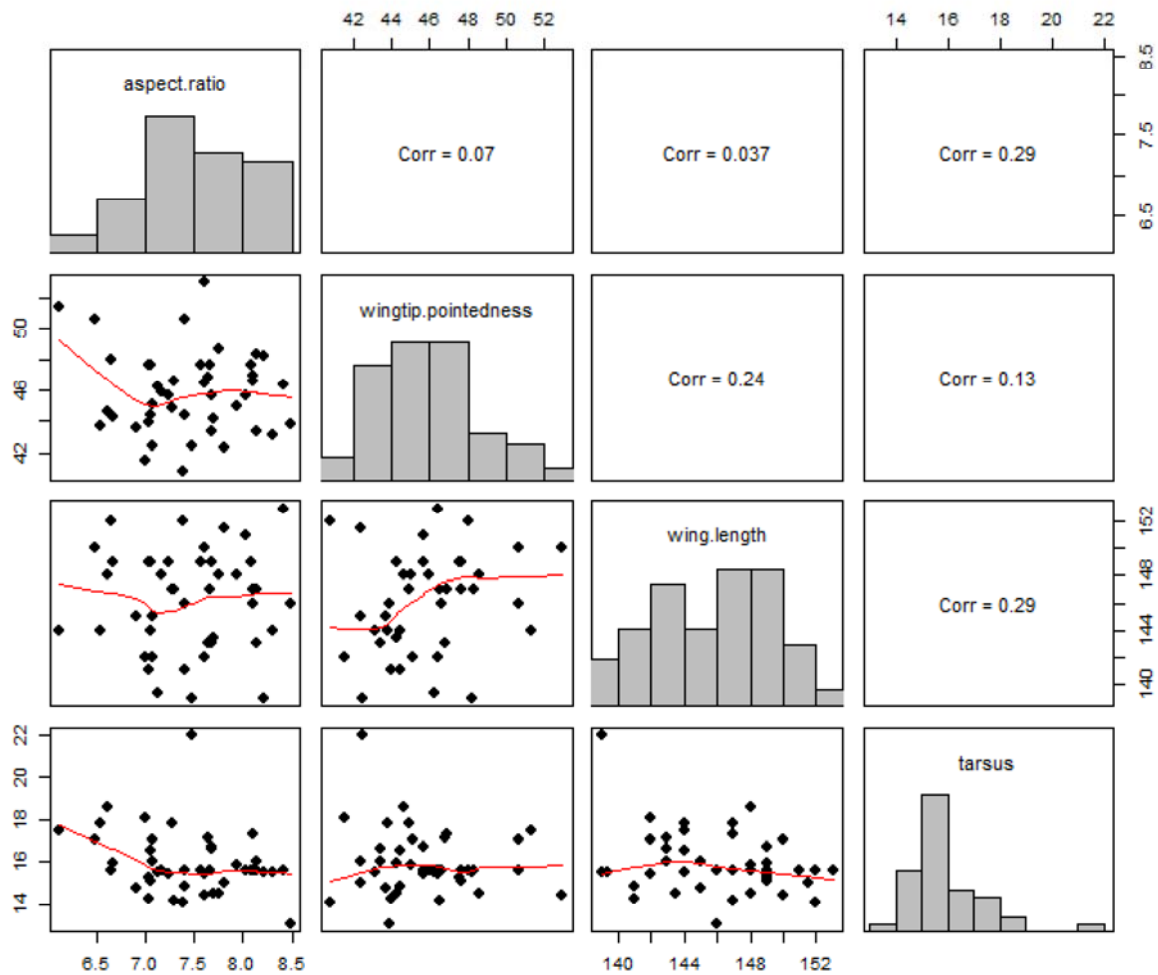


Figure A1. Scatterplot matrix of the data used to examine wing morphometric differences among populations and sexes (Chapter 2). The diagonal plots depict the distribution of the variables in the data (from top-left to bottom-right: aspect ratio, wingtip pointedness, wing length (mm), and tarsus length (mm)). The lower, off-diagonal plots and the solid red line in these plots (loess smoother) depict the relationship between the different variables on the diagonal. The upper, off-diagonal boxes show the Pearson correlation coefficient between the two variables.

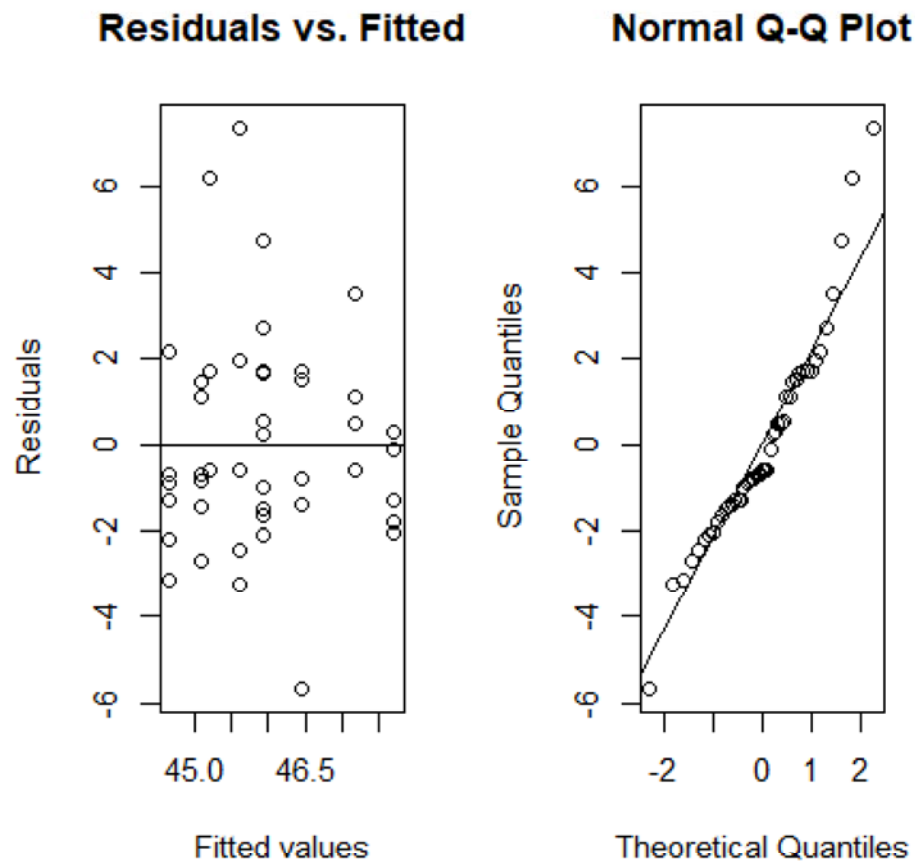


Figure A2. Diagnostic plot for linear model comparing wingtip pointedness between populations and sexes. The residuals versus fitted values plot (left) is used to assess for homogeneity of variance, and the q-q plot (right) is used to assess for normality in the residuals. Left: The random pattern in the residuals indicates that the model has met the assumption of homogeneity of variance. Right: as most of the observations fall onto a straight line, the model has met the assumption that the data is normally distributed.

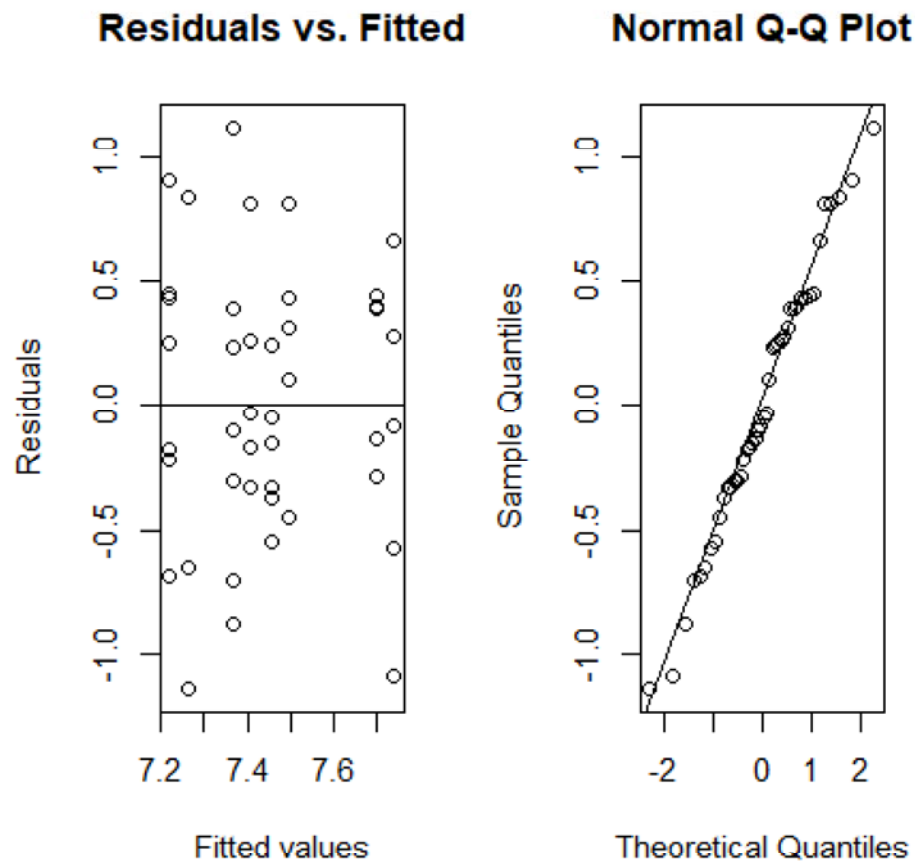


Figure A3. Diagnostic plot for linear model comparing aspect ratio between populations and sexes. The residuals versus fitted values plot (left) is used to assess for homogeneity of variance, and the q-q plot (right) is used to assess for normality in the residuals. Left: The random pattern in the residuals indicates that the model has met the assumption of homogeneity of variance. Right: as most of the observations fall onto a straight line, the model has met the assumption that the data is normally distributed.

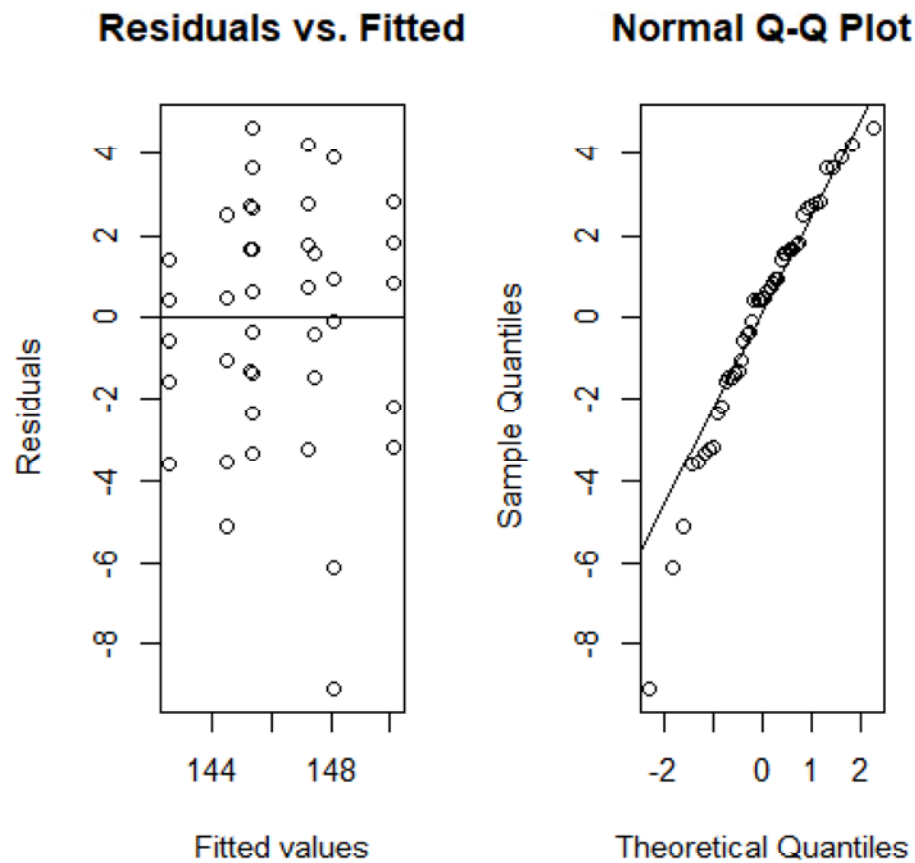


Figure A4. Diagnostic plot for linear model comparing wing length between populations and sexes. The residuals versus fitted values plot (left) is used to assess for homogeneity of variance, and the q-q plot (right) is used to assess for normality in the residuals. Left: The random pattern in the residuals indicates that the model has met the assumption of homogeneity of variance. Right: as most of the observations fall onto a straight line, the model has met the assumption that the data is normally distributed.

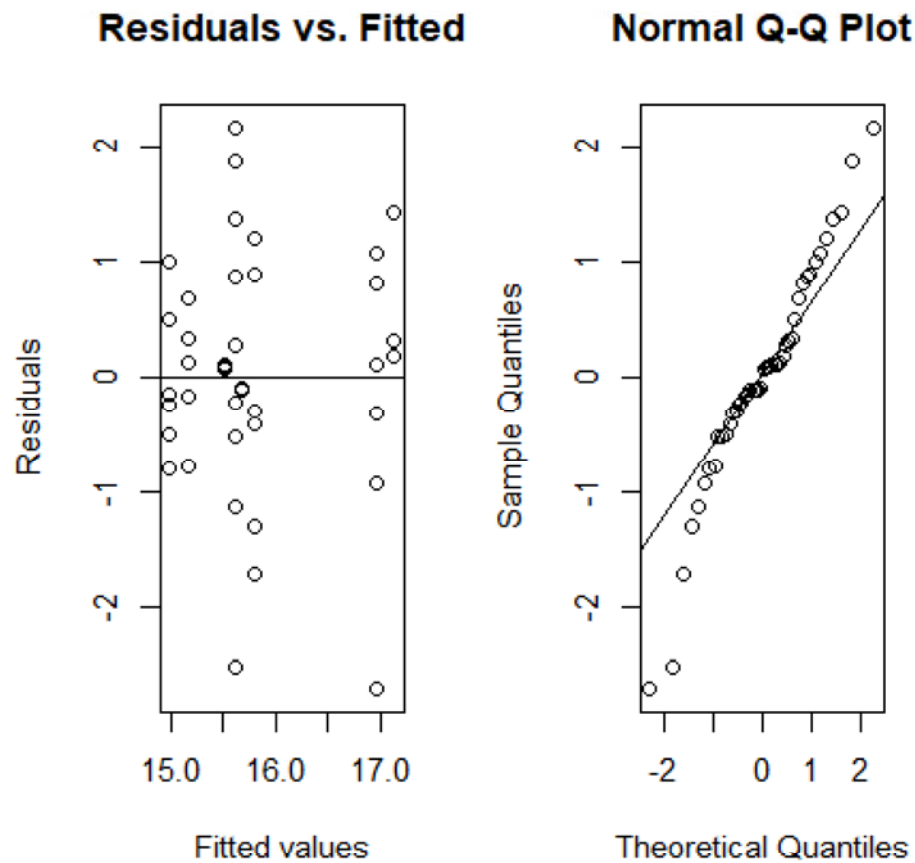


Figure A5. Diagnostic plot for linear model comparing tarsus length between populations and sexes. The residuals versus fitted values plot (left) is used to assess for homogeneity of variance, and the q-q plot (right) is used to assess for normality in the residuals. Left: The random pattern in the residuals indicates that the model has met the assumption of homogeneity of variance. Right: as most of the observations fall onto a straight line, the model has met the assumption that the data is normally distributed.

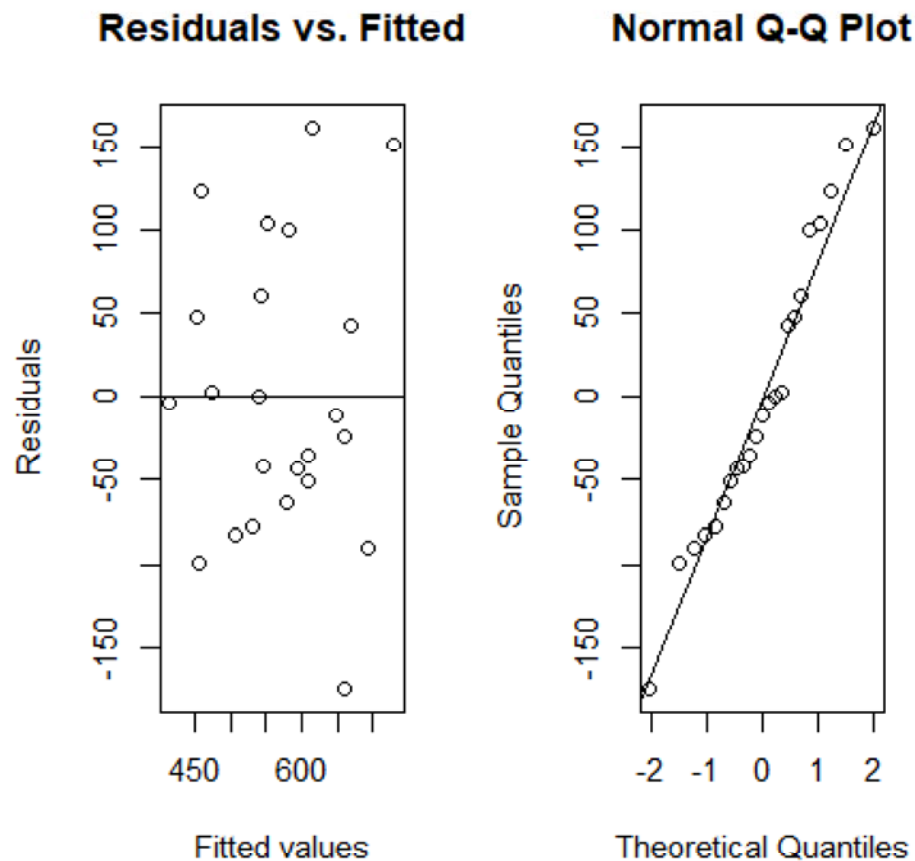


Figure A6. Diagnostic plot for linear model for total spring migration speed. The residuals versus fitted values plot (left) is used to assess for homogeneity of variance, and the q-q plot (right) is used to assess for normality in the residuals. Left: The random pattern in the residuals indicates that the model has met the assumption of homogeneity of variance. Right: as most of the observations fall onto a straight line, the model has met the assumption that the data is normally distributed.

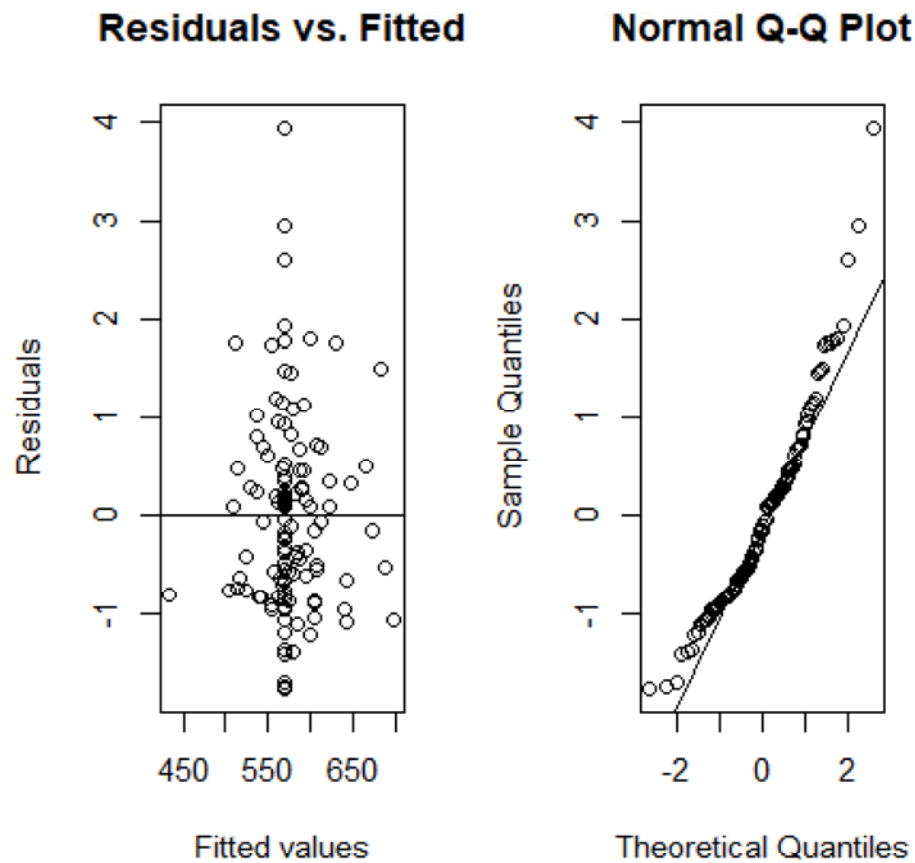


Figure A7. Diagnostic plot for linear mixed effects model for spring migration speed between stopovers. The residuals versus fitted values plot (left) is used to assess for homogeneity of variance, and the q-q plot (right) is used to assess for normality in the residuals. Left: The random pattern in the residuals indicates that the model has met the assumption of homogeneity of variance. Right: as most of the observations fall onto a straight line, the model has met the assumption that the data is normally distributed.

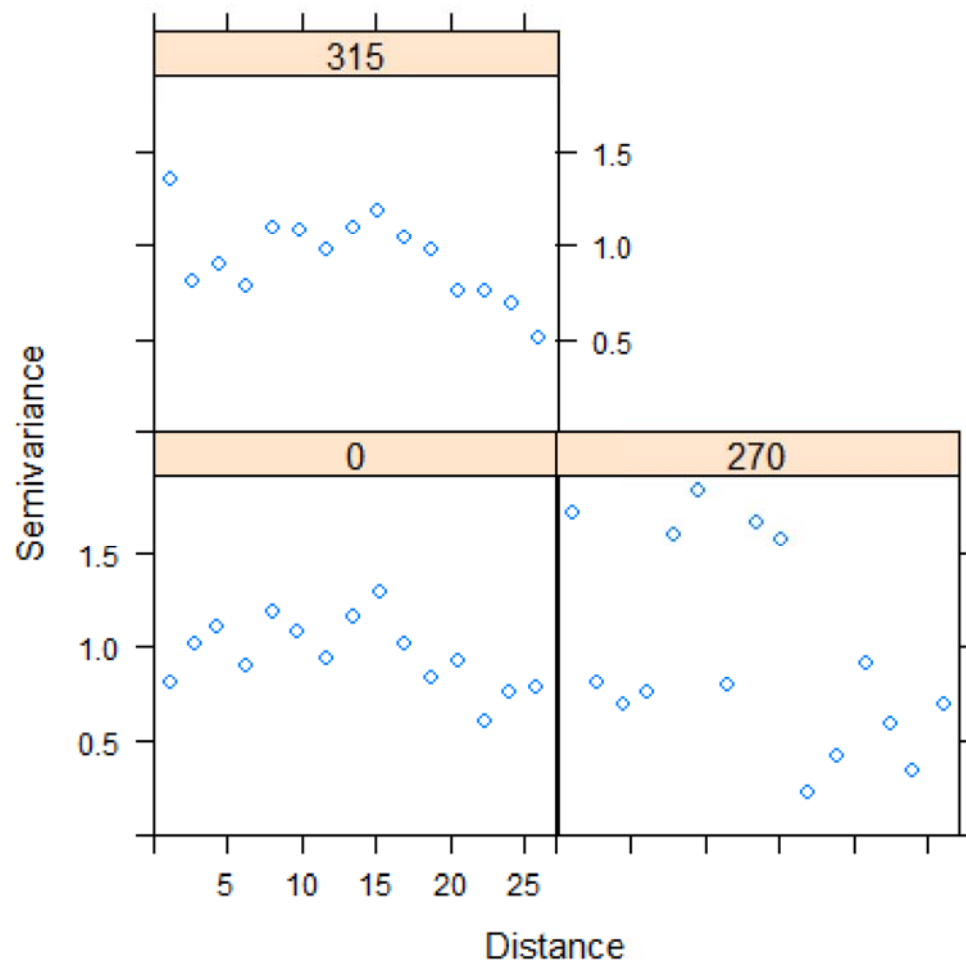


Figure A8. Semi-variogram of the standardized residuals from the linear mixed model for migration speed used to detect spatial autocorrelation. This figure displays the average distance between residual points plotted against the estimated values of the variogram. As birds migrate west, northwest, and north on spring migration, a variogram for each of these direction is shown (north = 0, west = 270, northwest = 315). The random patterns in the residuals in all three directions indicate that there is weak or no spatial autocorrelation present in the data.

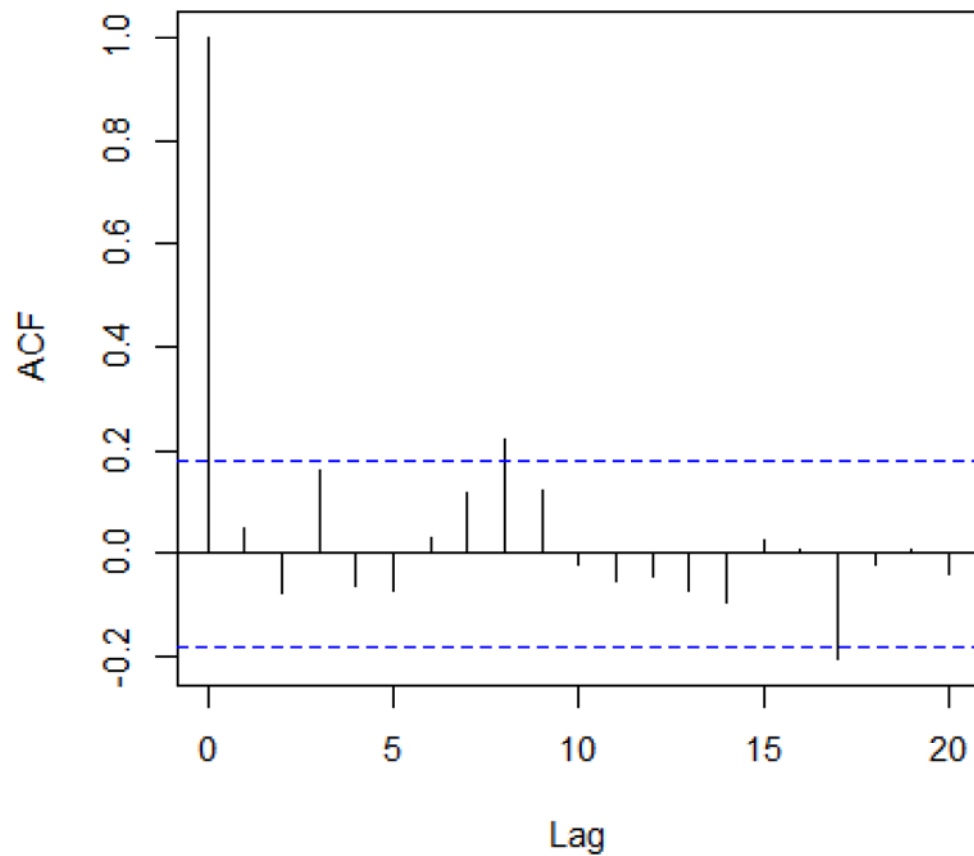


Figure A9. Autocorrelation plot of the residuals from the migration speed linear mixed effects model, with departure date as a time component in the model. The correlations between residual points (y-axis) at lag intervals (x-axis) is used to detect temporal autocorrelation in the data. With the exception of two points (at lag interval 8 and 17, excluding lag 0), all the points do not show any significant correlations; there is weak or no temporal autocorrelation of the residuals present in the data.

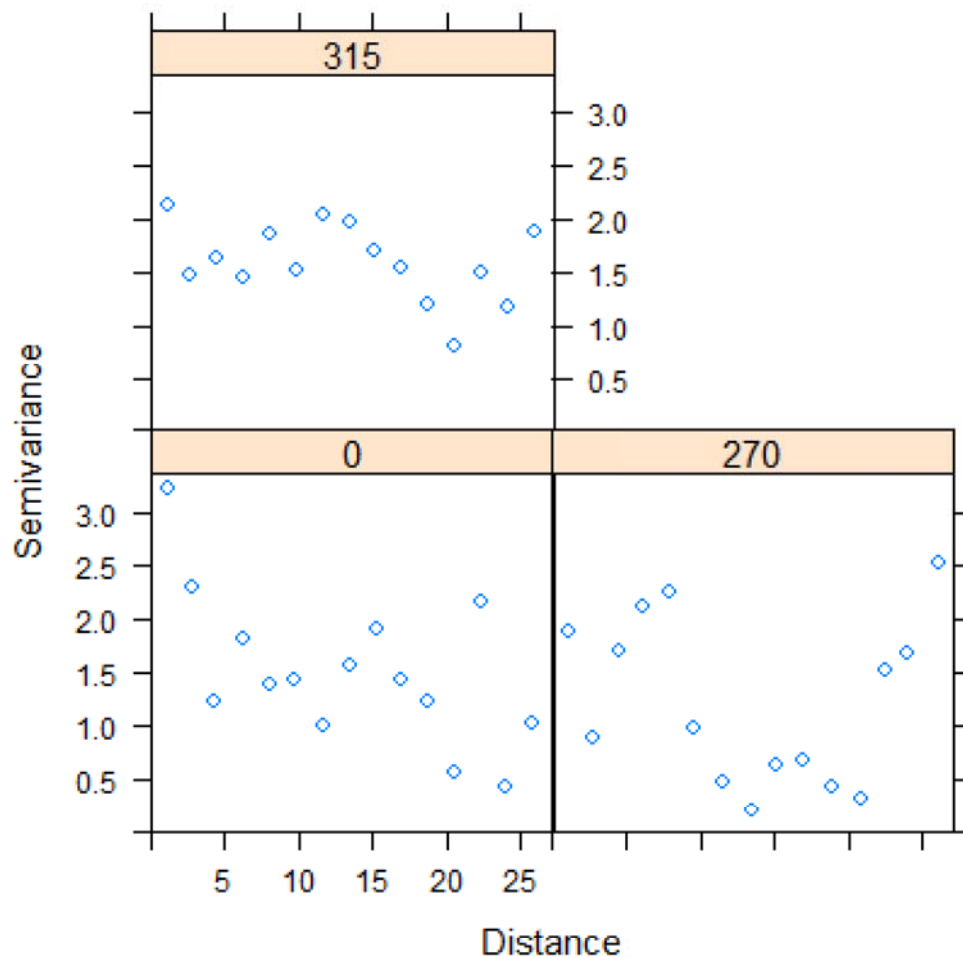


Figure A10. Semi-variogram of the standardized residuals from the generalized linear mixed model for stopover duration used to detect spatial autocorrelation. This figure displays the average distance between residual points plotted against the estimated values of the variogram. As birds migrate west, northwest, and north on spring migration, a variogram for each of these directions is shown (north = 0, west = 270, northwest = 315). The random patterns in the residuals in all three directions indicate that there is weak or no spatial autocorrelation present in the data.

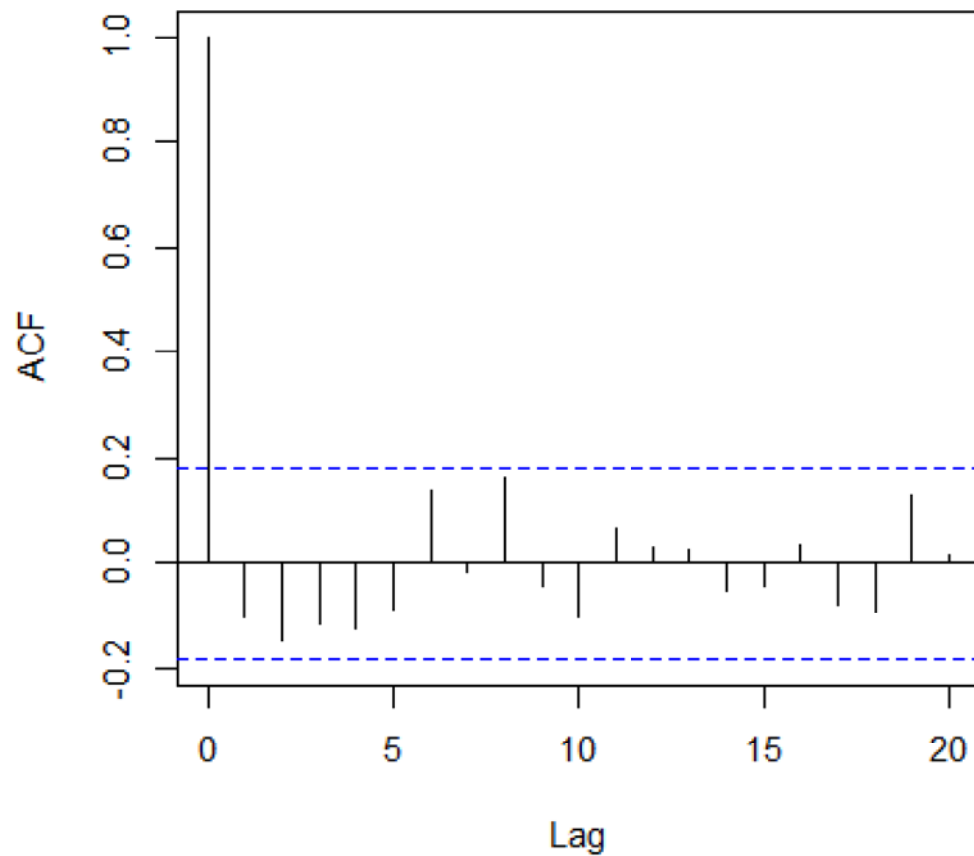


Figure A11. Autocorrelation plot of the residuals from the stopover duration generalized linear mixed effects model, with departure date as a time component in the model. The correlations between residual points (y-axis) at lag intervals (x-axis) is used to detect temporal autocorrelation in the data. All the points (excluding lag 0) do not show any significant correlations; there is weak or no temporal autocorrelation of the residuals present in the data.

Appendix B

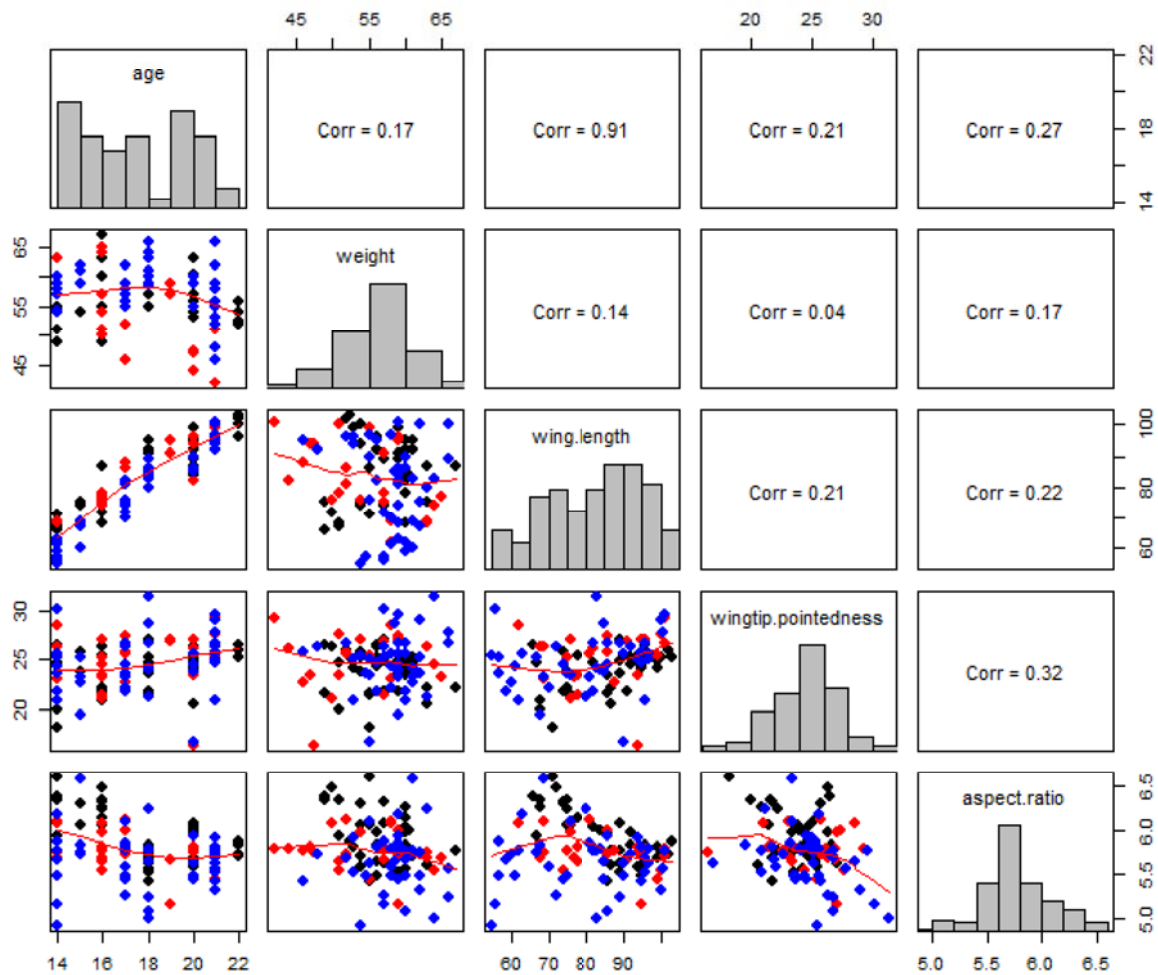


Figure B1. Scatterplot matrix of the data used to examine growth rates of purple martin nestlings (Chapter 3). The diagonal plots depict the distribution of the variables in the data (from top-left to bottom-right: nestling age (days), body weight (g), wing length (mm), wingtip pointedness, and aspect ratio). The colour of the points in the plots correspond to the 3 different groups in the study (control (black), sham-treated (red), and insecticide-treated (blue)). The lower, off-diagonal plots and the solid red line in these plots (loess smoother) depict the relationship between the

different variables on the diagonal. The upper, off-diagonal boxes show the Pearson correlation coefficient between the two variables.

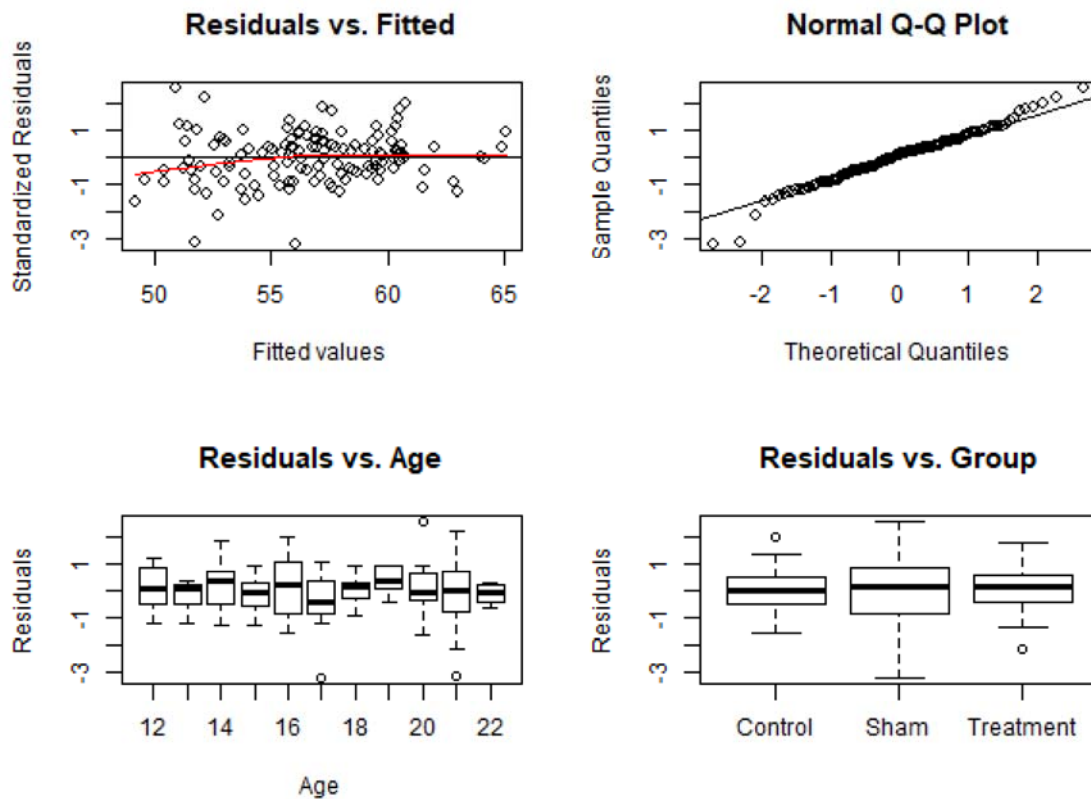


Figure B2. Diagnostic plots of the linear mixed model for changes in weight over time between the three treatment groups. The residuals versus fitted values plot (top left) is used to assess for homogeneity of variance, and the q-q plot (top right) is used to assess for normality in the residuals. The residuals vs. age (bottom left) and residuals vs. group (bottom right) depict variance in the residuals between ages and groups, respectively.

Temporal Autocorrelation of Weight

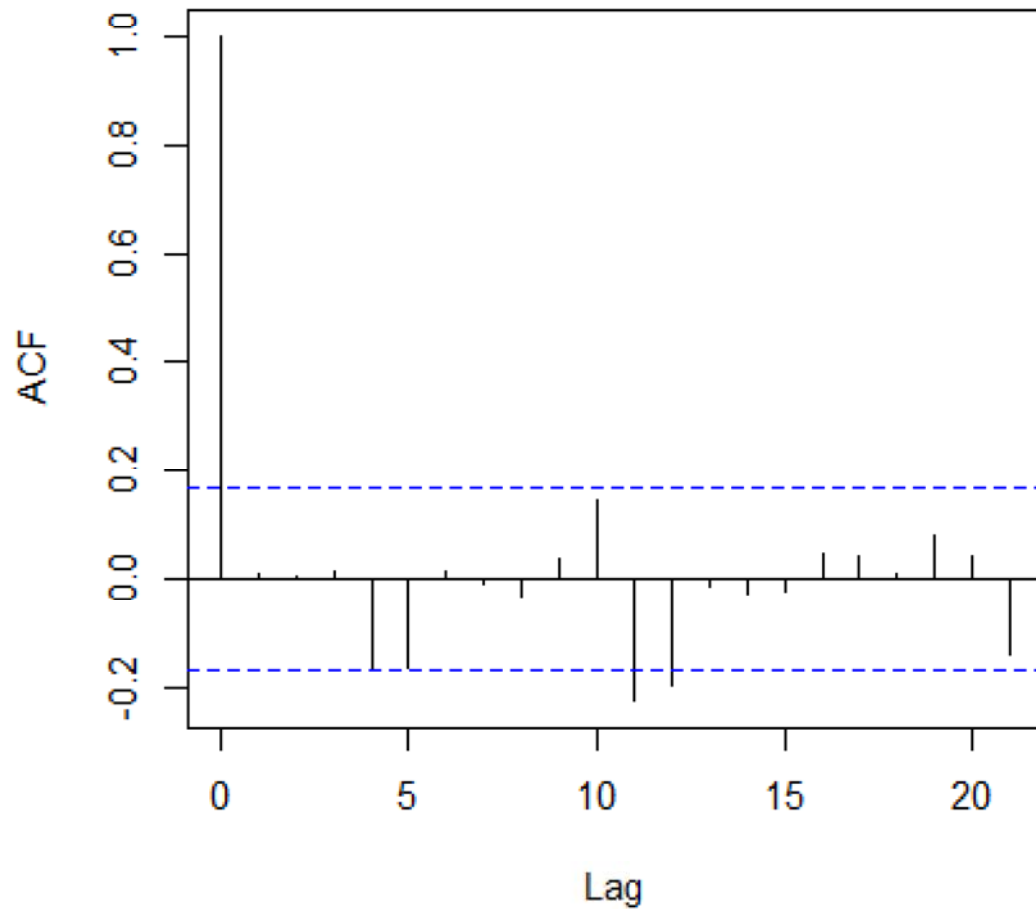


Figure B3. Autocorrelation plot of the residuals from the body weight linear mixed effects model, with age as the time component in the model. The correlations between residual points (y-axis) at lag intervals (x-axis) is used to detect temporal autocorrelation in the data. With the exception of two points (at lag intervals 11 and 12, excluding lag 0), all the points do not show any significant correlations; there is weak or no temporal autocorrelation of the residuals present in the data.

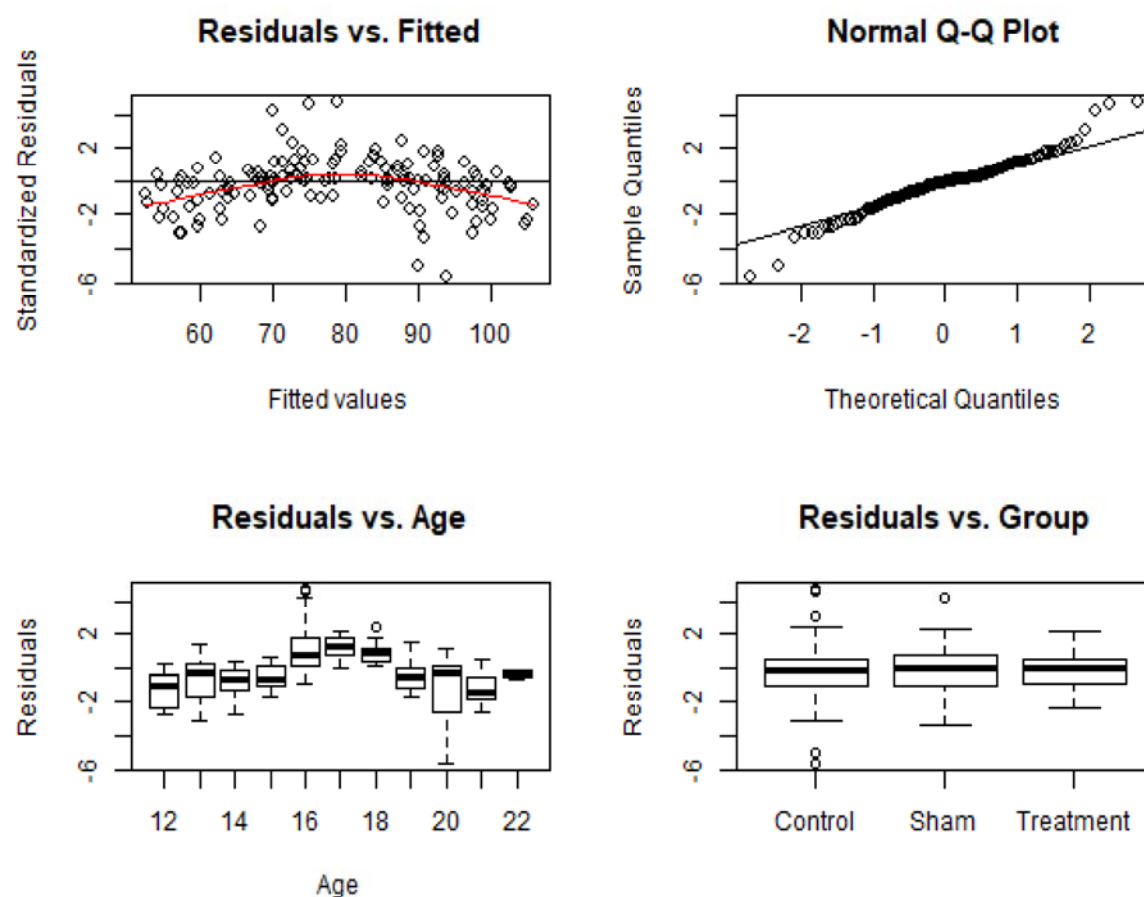


Figure B4. Diagnostic plots of the wing length linear mixed-effects model. The residuals versus fitted values plot (top left) is used to assess for homogeneity of variance, and the q-q plot (top right) is used to assess for normality in the residuals. The residuals vs. age (bottom left) and residuals vs. group (bottom right) depict variance in the residuals between ages and groups, respectively. A power variance structure and first-order autoregressive correlation structure were included in the model when calculating the residuals, to correct for unequal variance between ages and temporal autocorrelation, respectively.

Temporal Autocorrelation of Wing Length

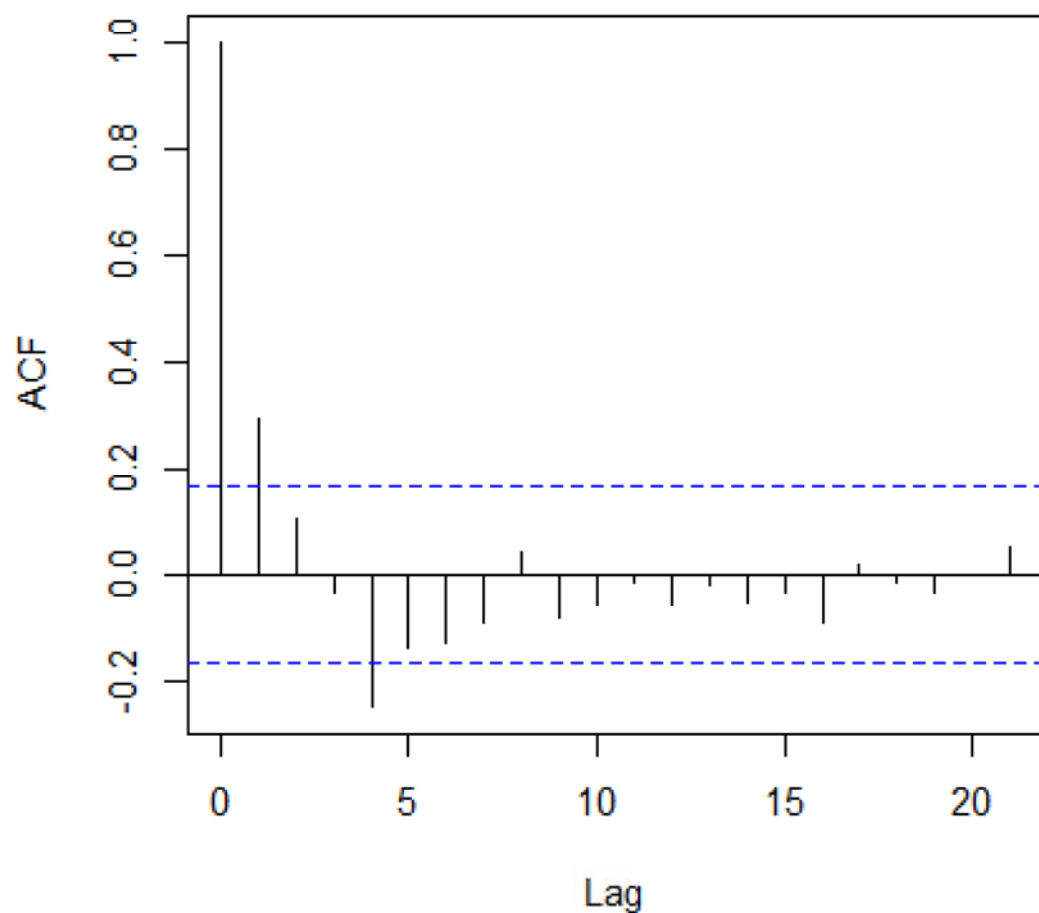


Figure B5. Autocorrelation plot of the residuals from the wing length linear mixed effects model, with age as the time component in the model, used to detect temporal autocorrelation. The correlations between residual points (y-axis) at lag intervals (x-axis) is used to detect temporal autocorrelation in the data. With the exception of two points (at lag intervals 1 and 4, excluding lag 0), all the points do not show any significant correlations; there is weak or no temporal autocorrelation of the residuals present in the data.

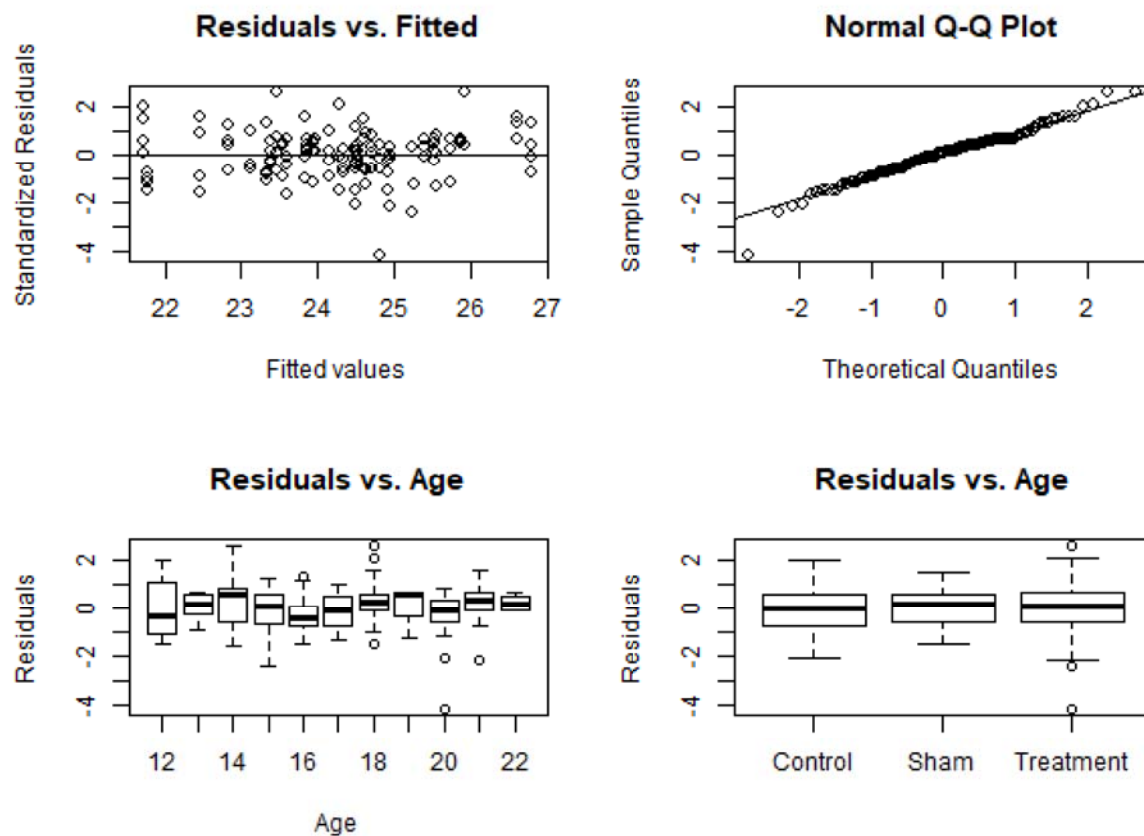


Figure B6. Diagnostic plots of the wingtip pointedness linear mixed-effects model. The residuals versus fitted values plot (top left) is used to assess for homogeneity of variance, and the q-q plot (top right) is used to assess for normality in the residuals. The residuals vs. age (bottom left) and residuals vs. group (bottom right) depict variance in the residuals between ages and groups, respectively. A power variance structure was included in the model when calculating the residuals, to correct for unequal variance between ages.

Temporal Autocorrelation of Wingtip Pointedness

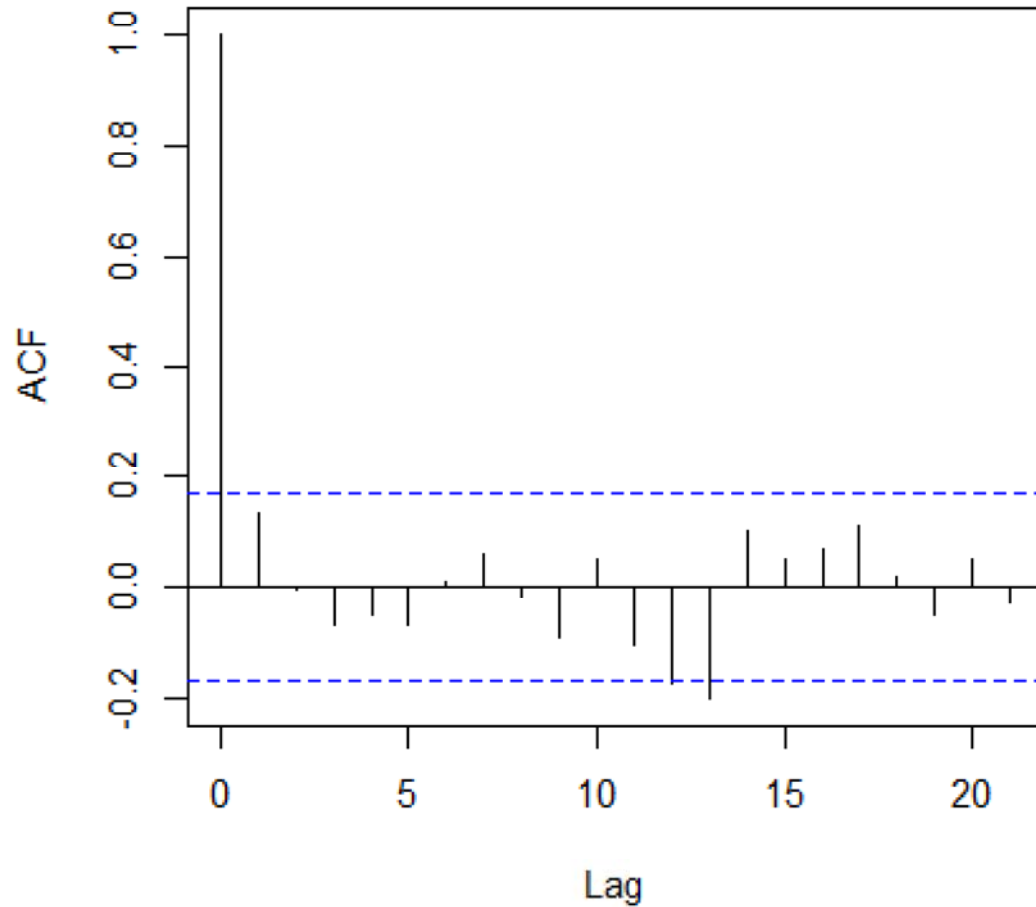


Figure B7. Autocorrelation plot of the residuals from the wingtip pointedness linear mixed effects model, with age as the time component in the model, used to detect temporal autocorrelation. The correlations between residual points (y-axis) at lag intervals (x-axis) is used to detect temporal autocorrelation in the data. With the exception of two points (at lag intervals 12 and 13, excluding lag 0), all the points do not show any significant correlations; there is weak or no temporal autocorrelation of the residuals present in the data.

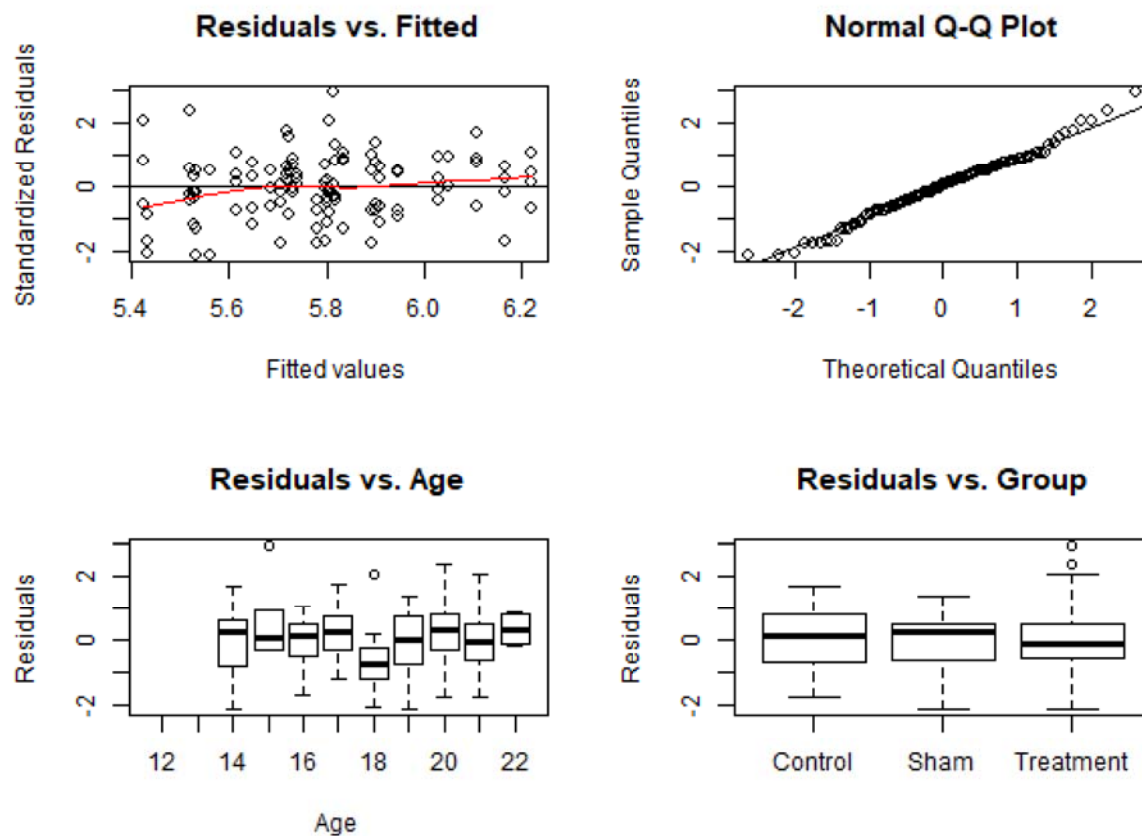


Figure B8. Diagnostic plots of the aspect ratio linear mixed-effects model. The residuals versus fitted values plot (top left) is used to assess for homogeneity of variance, and the q-q plot (top right) is used to assess for normality in the residuals. The residuals vs. age (bottom left) and residuals vs. group (bottom right) depict variance in the residuals between ages and groups, respectively. A power variance structure was included in the model when calculating the residuals, to correct for unequal variance between ages.

Temporal Autocorrelation of Aspect Ratio

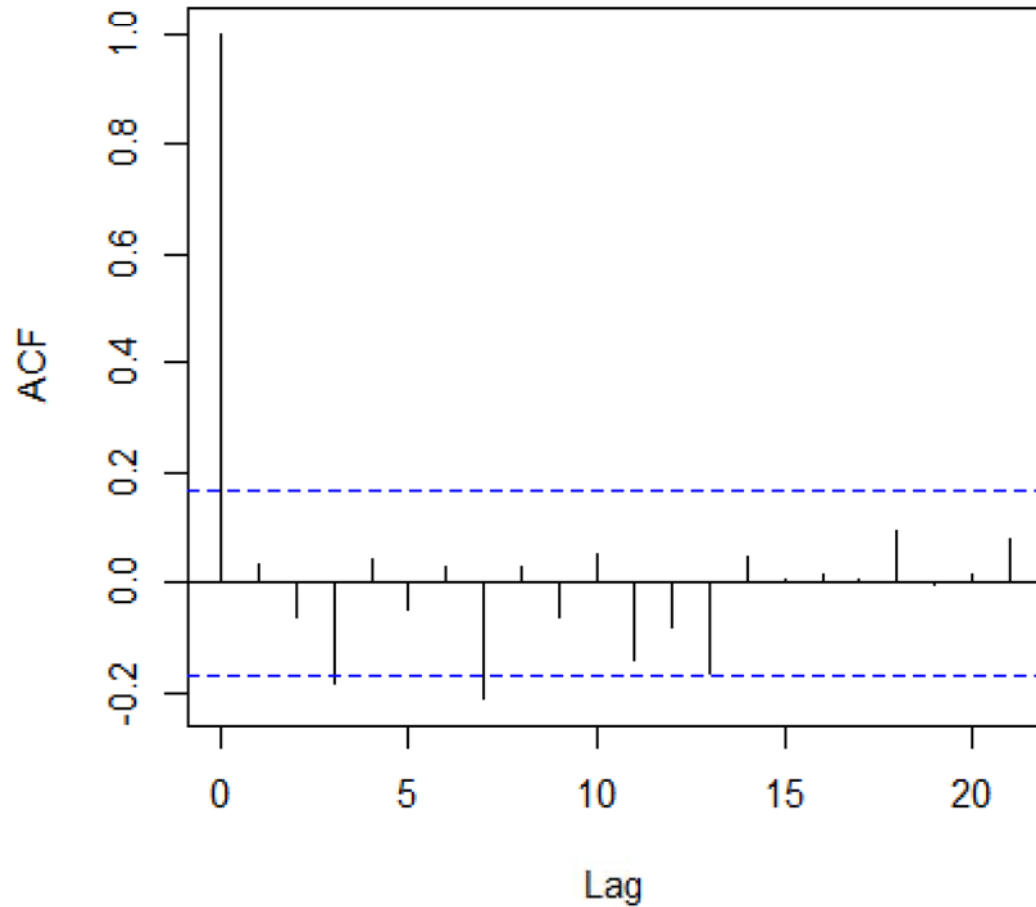


Figure B9. Autocorrelation plot of the residuals from the aspect ratio linear mixed effects model, with age as the time component in the model, used to detect temporal autocorrelation. The correlations between residual points (y-axis) at lag intervals (x-axis) is used to detect temporal autocorrelation in the data. With the exception of two points (at lag intervals 3 and 7, excluding lag 0), all the points do not show any significant correlations; there is weak or no temporal autocorrelation of the residuals present in the data.